FALCon

Formation flight for in-**A**ir **L**auncher 1st stage

Capturing dem**on**stration

Technical Report on different RLV return modes' Performances

Deliverable D2.1

EC project number 821953
Research and Innovation action
Space Research Topic: SPACE-16-TEC-2018 – Access to space

FALCon
Formation flight for in-Air Launcher 1st stage Capturing demonstration

Technical Report on different RLV return modes' Performances

Deliverable Reference Number: D2.1

Due date of deliverable: 30th November 2019

Actual submission date (draft): 15th December 2019

Actual submission date (final version): 19th October 2020

Start date of FALCon project: 1st of March 2019

Duration: 36 months

Organisation name of lead contractor for this deliverable: DLR

Revision #: 2

Dissemination Level		
PU	Public	**X**
PP	Restricted to other programme participants (including the Commission Services)	
RE	Restricted to a group specified by the consortium (including the Commission Services)	
CO	Confidential, only for members of the consortium (including the Commission Services)	

APPROVAL

Title	**issue**	revision
Technical Report on different RLV return modes' performances	2	1

Author(s)	**date**
Sven Stappert	19.10.2020
Madalin Simioana	21.07.2020
Martin Sippel	

Approved by	**Date**
Sven Stappert	19.10.2020
Martin Sippel	

Contents

List of Tables

List of Figures

Nomenclature

a	acceleration	m/s^2
C_D	Drag coefficient	-
C_L	Lift coefficient	-
F	Thrust	N
H	Altitude	km
I_{Sp}	Specific impulse	s
m	Mass	kg
$\dot{m}$	Mass flow	kg/s
m_T	Propellant mass	kg
n_x	Load factor along the main axis of the vehicle	-
n_z	Load factor normal to the main axis of the vehicle	-
t	Time	s
α	Angle of attack	°
γ	Flight path angle	°

Abbreviations

3STO	Three Stage To Orbit
AoA	Angle of Attack
CFD	Computational Fluid Dynamics
CH4	Methane
DRL	Downrange Landing
ELV	Expendable Launch Vehicle
FEM	Finite Element Method
GG	Gas Generator
GLOM	Gross Liftoff Mass
HL	Horizontal Landing
IMR	Inert Mass Ratio
L/D	Lift/drag ratio
LC3H8	Liquid Propane
LCH4	Liquid Methane
LFBB	Liquid Fly-Back Booster
LH2	Liquid Hydrogen
LOX	Liquid Oxygen
MECO	Main Engine Cut-off
MoM	Minutes of Meeting
RANS	Reynolds-Averaged Navier-Stokes Equations
RLV	Reusable Launch Vehicle
RP	Rocket Propellant
RP-1	Rocket Propellant 1
SC	Staged Combustion
SI	Structural Index
TN	Technical Note
TRL	Technology Readiness Level
TSTO	Two Stage To Orbit
UAV	Unmanned Aerial Vehicle
VL	Vertical Landing

VTHL	Vertical Takeoff, Horizontal Landing
VTVL	Vertical Takeoff, Vertical Landing
WP	Workpackage

1 Executive Summary

1.1 Scope of the deliverable

According to the FALCon GA [1] the WP 2.1 is about “Critical Analyses of different RLV return modes”. It consists of a focused systematic research on different reusability options of space transportation systems to address and identify key aspects of reusable launch vehicles (RLVs). The impact of reusability on performance and costs shall be evaluated by multidisciplinary pre-design of reusable launchers. In this context, different return methods are under investigation. The goal is to allow for a comparison of different return options including options using In-Air-Capturing. Thus, a feasible RLV reference design has been derived which should serve as baseline for the full-scale In-Air-Capturing scenario.

Within the WP 2.1 the subordinate WP 2.1.1 focuses on the trajectory optimization of feasible RLV stages to further optimize trajectories of the In-Air-Capturing baseline derived in WP 2.1. This should allow a higher fidelity and accuracy of the RLV baseline stage and also allows for the optimization of other concepts to enhance the level of comparison between difference return options.

According to [1], the WP 2.1 was started with the kick-off of the project in March 2019 and ended in August 2019. The WP went according to plan with a prolongation of around 1 month.

According to the project plan, this deliverable is not supposed to include economic analysis of return modes and In-Air-Capturing procedures yet. However, due to the high urgency of this task, the respective WP 2.3 “Economic interest analyses” was already started and this report D2.1 includes results from this ongoing task. However, the final results from WP 2.3 shall be included in another deliverable D2.4 to close this work package.

1.2 Results

This deliverable includes the results of the finished tasks WP 2.1 and WP 2.1.1. This includes a comparison of different return options which is presented in section 3. Those selected for closer assessment are vertical landing with the two options of either a downrange landing (DRL) or a landing back at the launch site (RTLS), if equipped with wings the horizontal landing in two different options are considered: the LFBB method (Liquid Flyback Booster) using turboengines for a propelled flyback and the In-Air-Capturing (IAC) method using a capturing and towing aircraft.

The comparison is performed considering performance and masses, re-entry trajectories and loads and preliminary economics for recovery and total launch costs. From a performance perspective, the IAC mode is highly attractive. Figure 1-1 presents a comparison of the inert mass ratio for generic TSTO-launchers and different return modes of the reusable first stage. All launchers have been sized for 7.5 tons GTO payload with a variation in separation Mach-number of the RLV. As mission and stage number are identical, the inert mass ratio can be presented as function of the total ascent propellant loading. RTLS for GTO results in excessively high stage size and inert mass ratio and has hence been excluded from further studies with GTO-mission.

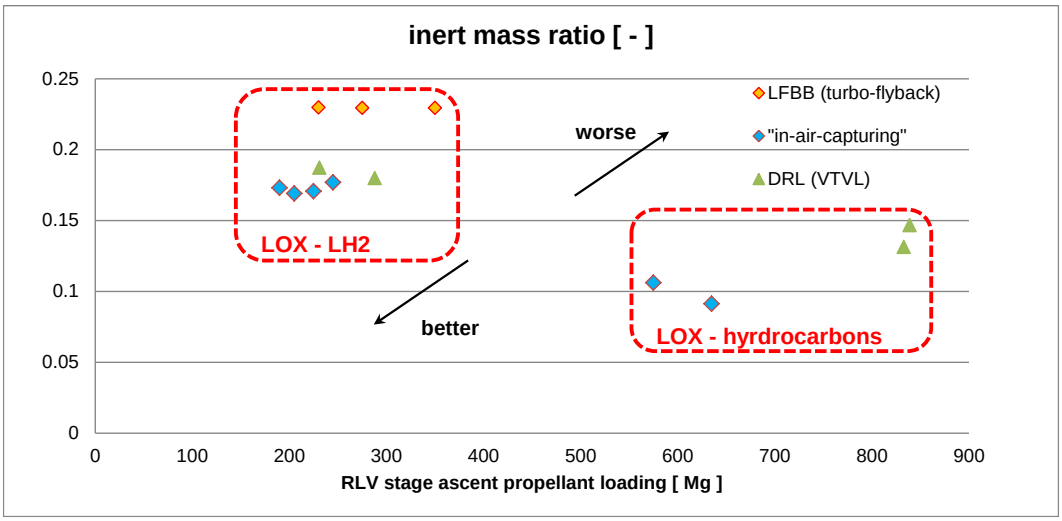

Figure 1-1: Inert mass ratios of different RLV-return modes (all same GTO mission)

In all of the investigated cases the IAC-mode RLV stages have a performance advantage not only when compared to the LFBB with turbojet flyback but also in comparison to the DRL-mode used by SpaceX for GTO-missions.

Beyond looking into launcher performance, the mechanical and thermal loads acting on the RLV-stage during atmospheric reentry are considered by performing extensive trajectory and aero-thermo-dynamic calculations. Considering all these results the In-Air-Capturing strategy seems to be a viable and efficient option compared to the vertical landing SpaceX method. The masses and performance losses are low, the size is comparably compact and the re-entry loads are manageable.

Attractive performance is not the only criterion for choosing the RLV-return mode. In the end operating costs are the drivers. In section 5 and extensive bottom-up cost model is established for the reusable stage's recovery. IAC of VTHL cost is found close to the VTVL DRL-mode and in the range of approximately 500 k€ per flight. Autonomous return as with the LFBB and RTLS modes is cheaper in recovery cost, but is linked to strongly reduced performance and hence significantly increased launch costs which are considerably above the potential savings in recovery. It is important to note that all sections including economic analyses are based on results from the WP 2.3 which is still ongoing at the time of publication of this deliverable. Hence, those results are preliminary outcomes which will be updated with the progress of WP 2.3.

The section 6 focuses on the reference stage for the In-Air-Capturing full-scale scenario including the results from the ASTOS trajectory optimization WP 2.1.1. The convergent preliminary design of a variable-wing first stage is shown in Figure 1-2 which can serve as the reference for the full-scale IAC-simulations. Figure 1-2 also shows the difference between the re-entry configuration with the movable part of the wings retracted (right) and the transonic and subsonic flight configuration with wings extended (left). The trimmed subsonic L/D is around 6 and to be towed mass is around 70 tons which is compatible with existing large four-engine airliners as towing vehicle.

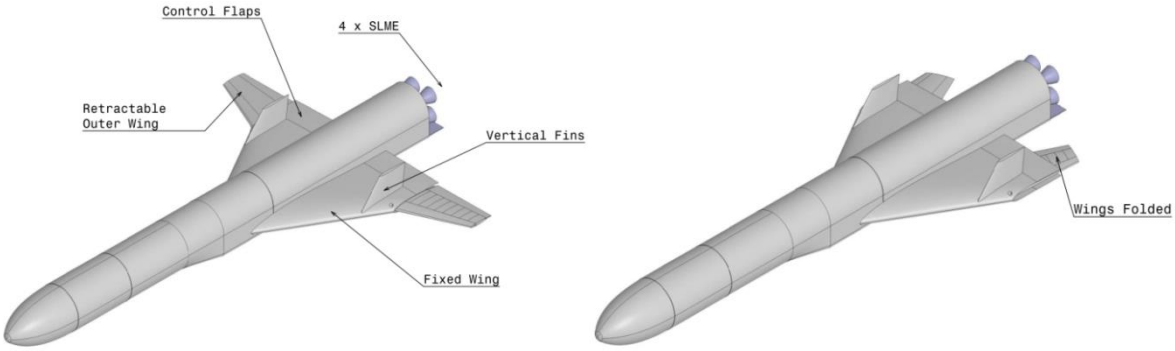

Figure 1-2: Conceptual design of variable wing reference RLV stage with wings extended (left) and wings stored (right)

1.3 Specific highlights

-

1.4 Forms of integration within the work package and with other WPs

The results of the WP 2.1 considering RLV modes comparison are independent of other work packages. The results considering the RLV baseline for In-Air-Capturing are valid for the WP 2.3, 7.1, 7.3, 7.4, 7.5 and 7.6.

1.5 Problems

-

2 Introduction

Complex, high-performance, high-cost rocket stages and rocket engines are disposed today after a short operating time. Used components fall back to Earth, crashing on ground or into the Oceans. Returning these stages back to their launch site could be attractive - both from an economical as well as an ecological perspective. However, early reusability experience obtained by the Space Shuttle and Buran vehicles demonstrated the challenges of finding a viable operational and business case.

Recently, the emerging private companies SpaceX and Blue Origin have successfully demonstrated the landing, recovery and reuse of a first booster stage. Blue Origin launched their suborbital launcher New Shephard, which shall transport paying customers to the edge of space, several times with a reused first booster stage (see Figure 2-1). SpaceX has successfully landed around 40 stages and has flown 19 missions with reused stages of the Falcon 9 launch vehicle as of November 2019. Their successes have proved the possibility to develop, produce and operate low-cost reusable launch vehicles. Hence, the interest in reusable launch vehicles has experienced a recent boost. However, different methods of reusing first stages are known and each method comes with its unique advantages, drawbacks and technical challenges. It is of crucial importance to understand these differences to identify a return method that is suitable for a European application.

Figure 2-1: SpaceX Falcon Heavy side boosters landing in Cape Canaveral (left) and Blue Origin's New Shephard booster stage landing (right)

The technical approach of SpaceX and Blue Origin is the so-called “Vertical Take-Off, Vertical Landing” (VTVL) method. As can be seen in Figure 2-1 the stages are landed vertically by means of retropropulsion. Therefore, following separation of the first stage from the rest of the launcher several correctional maneuvers are performed which make it necessary to reignite the rocket engines. This approach however is not the only method for landing and recovering reusable booster stages. A further possibility is to launch the stages vertically but land them horizontally (VTHL – Vertical Takeoff, horizontal landing). Prominent representatives of this strategy are the popular Space Shuttle with its horizontally landing Orbiter (see Figure 2-2) and the Liquid Fly-Back Booster concept which was studied extensively at DLR in the 2000s.

Figure 2-2: Liquid Fly-Back Booster study (left) and Space Shuttle Orbiter during landing (right)

These two approaches can be further divided into subcategories. For both landing approaches the landing can occur at a landing site downrange of the launch site or the vehicle can return to the launch site (RTLS). In case of vertical landing the former method is employed by SpaceX by landing their Falcon9 on their droneships. Generally, landing downrange requires less propellant for the return maneuvers and subsequently leads to less performance losses. Hence, this method is used for high-energy orbits such as GTO whereas the RTLS method is used for low-energy mission (LEO, SSO).

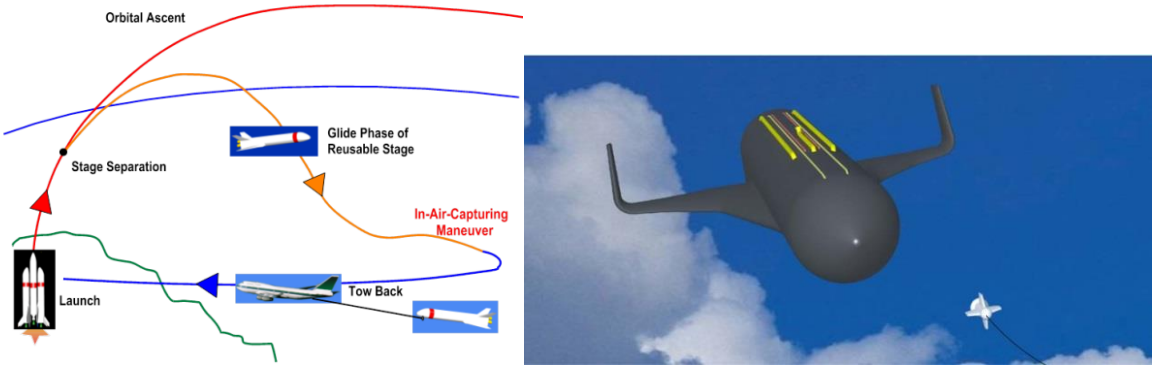

Figure 2-3: In-Air-Capturing Mission profile (left) and capturing procedure (right, artist's impression)

For horizontally landing stages, the landing can also occur downrange or at the launch site. The latter possibility based on the idea to horizontally land a RLV stage by using an on-board propulsion system, respectively a conventional air breathing jet engine. This engine would be ignited once the stage is cruising at subsonic velocities and would require a certain amount of propellant to be reserved to fly the stage to its landing site. This procedure was envisioned to be used for the LFBB as seen in Figure 2-2.

Landing downrange requires an airfield downrange or any device similar to the droneships of SpaceX that is used as a sea-going landing platform. Since landing rather big RLV stages on an aircraft carrier is impossible, a further possibility can be thought of: capturing the returning RLV stage in the air. This so called “In-Air-Capturing” method, which is the core of the FALCon project, is set around the idea to employ a towing aircraft with an aerodynamically controlled capturing device to catch the returning RLV stage. After successful capture, the RLV stage can then be towed to its respective landing site.

All these different return methods are considered nowadays most viable and feasible methods to actually introduce reusability to launchers. There exist further possibilities to land and reuse stages including parachutes, partial recovery of only parts of the stages and further more. However, in the current context of launcher development they are deemed less viable then the aforementioned four major methods of recovering stages.

For a viable application of one of those methods to a possible future launch vehicle, it is important to understand the differences between these return methods and to identify the challenges, drawbacks

and advantages and disadvantages of the described methods. This shall help in identifying a suitable method for a future European RLV. In the context of the project FALCon this shall also highlight especially the In-Air-Capturing procedure and its positioning with respect to other return strategies. Finally, the reference RLV stage for the full-scale IAC procedure will be designed and presented based on these results.

2.1 Study/investigation logic

The comparison of the different return options is performed on different levels, respectively technical, operational and economic. The preliminary design of different launcher options was performed using equal mission requirements and design assumptions that were as uniformly as possible. The reference RLV stage is then designed based on the results from this comparison.

2.2 Tools used

For the design of RLV stages, the technical comparison and the economic comparison, the following computation tools have been used:

- stsm (Stage Transportation System Mass Estimation) – calculation of stage and launcher masses
- cac (Calculation of Aerodynamic Coefficients) – calculation of aerodynamic coefficients for RLV stages
- hotsose – calculation of aerodynamic coefficients and aerothermodynamic behavior during re-entry in hypersonics
- tosca (Trajectory Optimization and Simulation of Conventional and Advanced Spacecraft) – trajectory calculation and simulation of spacecraft
- ASTOS – trajectory calculation and simulation of spacecraft
- CATIA – CAD software for preliminary stage design

3 RLV Return Modes Comparison

This section focuses on the comparison of the considered RLV return options. First, the considered options are presented in section 3.1. The logic of the study and the design assumptions will be explained in that section as well. The results of the comparison will be presented in section 4 to 5, focusing on different factors in each level.

3.1 Return Options and Methods

The investigated RLV first stage configuration types are much different in their aerodynamic and mechanical lay-out as well as in their return and landing modes. One common element is the conventional vertical lift-off, offering significant advantages for rocket-powered vehicles.

The potential RLV stage return modes strongly vary from pure ballistic to using aerodynamic lift-forces, gliding flight or captured towing. In case of propelled return, the options stretch from using the rocket engines or separate air-breathing turbo-fan or even propeller for efficient low-speed flight. A schematic of the available options is presented in Figure 3-1 which considers also the possibility of returning only some key-components of the first stage while discarding other elements. Recovery of merely the propulsion bay with the main rocket engines has been proposed for ULA Vulcan and another concept from Airbus which is called Adeline.

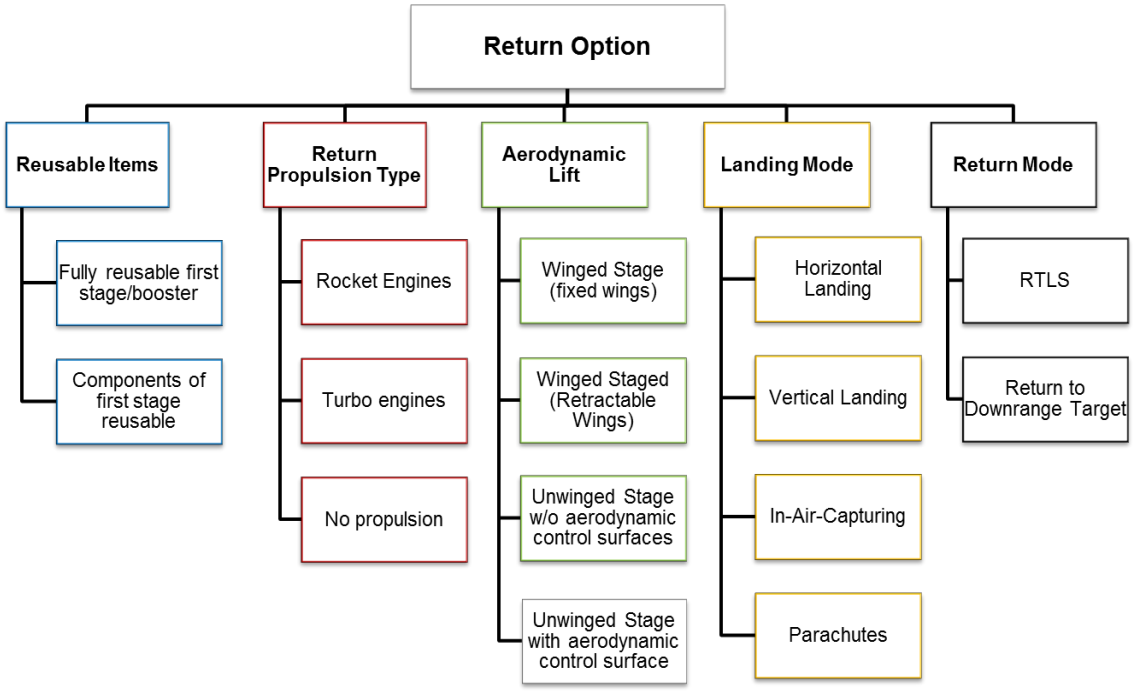

Figure 3-1: Potential RLV stage return modes

It is important to note that not every combination of the different modes presented in Figure 3-1 is possible. The reusable stage's aerodynamic shape is influencing the landing as well as the return options. A wing attached to the fuselage or tank structure has to generate lift force as its main purpose. Aerodynamic control devices as found on a ballistic reusable stage like the Falcon 9 are understood as similar to control flaps but with minimum lift contribution. While the non-winged type has no capability of soft horizontal aerodynamic landing, the winged RLV-stages in most cases are designed for a conventional horizontal runway touch-down. However, a specific type with relatively small wing area used in high-speed reentry might switch to vertical powered landing afterwards (e.g. New Glenn landing strategy).

Figure 3-2 shows the return modes considered for full first stage recovery within this report. A first stage equipped with no wings has to do a vertical landing with the two options of either a downrange landing (DRL) or a landing at the launch site (RTLS). A first stage equipped with wings or wing-like devices creating sufficient lift can either land horizontally like a conventional aircraft or land vertically using its own engines. In the case of a horizontal landing, two different options are considered herein: the LFBB method (Liquid Flyback Booster) using turboengines for a propelled flyback and the In-Air-Capturing (IAC) method using a capturing and towing aircraft.

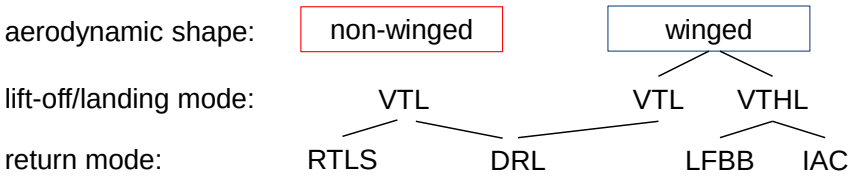

Figure 3-2: Investigated RLV full first stage return modes

Further recovery methods exist which focus on the partial recovery of first stage elements. Ideas that have been promoted in the past were the ADELINE concept of Airbus or the ULA SMART technology (see Figure 3-3 and Figure 3-4). In both concepts, the engine and avionics bay as most expensive part of the first stage is separated from the rest of the stage after MECO and stage separation. In case of the Adeline concept which is comparable to a winged fly back approach the reused hardware would decelerate aerodynamically and would then fly to the landing site by using its own propeller engines. The SMART approach decelerates aerodynamically with an inflatable heat shield and once reaching subsonic velocity would deploy a parachute system to slow down the recovered hardware. Similar to the In-Air-Capturing method, the recovered hardware would be captured by Mid-Air-Retrieval (MAR) with the use of a helicopter.

As of November 2019, both ideas are not followed anymore in the respective companies. The partial recovery is of minor interest for full-scale first stages of RLVs and is thus not considered in detail in this report.

Figure 3-3: Airbus' ADELINE concept (left) and ULA SMART concept with inflatable heat shield (right)

3.1.1 VTVL with return-to-launch-site (RTLS)

Vertical Landing (VL) is based on the idea to land a rocket stage vertically by using the rocket engine for deceleration (see Figure 3-4). SpaceX succeeded for the first time in bringing the booster stage back in December 2015, even before successful touchdown on a droneship. A dedicated landing zone called LZ-1 has been constructed for this purpose in Cape Canaveral, Florida (Figure 3-4). A typical RTLS mission consists of the ascent phase with the first stage accelerating the complete stack. Following MECO and stage separation the stage points the engines in the direction it is travelling to and reignites one to several engines to revert the horizontal velocity. The stage coasts then along a

ballistic trajectory which is interrupted by a re-entry burn to decrease the re-entry loads and is then landed on land (see Figure 3-4).

This approach is usually used for low-performance LEO or SSO missions of Falcon 9, e.g. the CRS-flights for NASA to the ISS. In general, this return mode is more suitable in case of lower separation Mach numbers and in moderate distance to the launch site because of the otherwise excessive amount of fuel needed by the rocket engines to reverse the horizontal velocity.

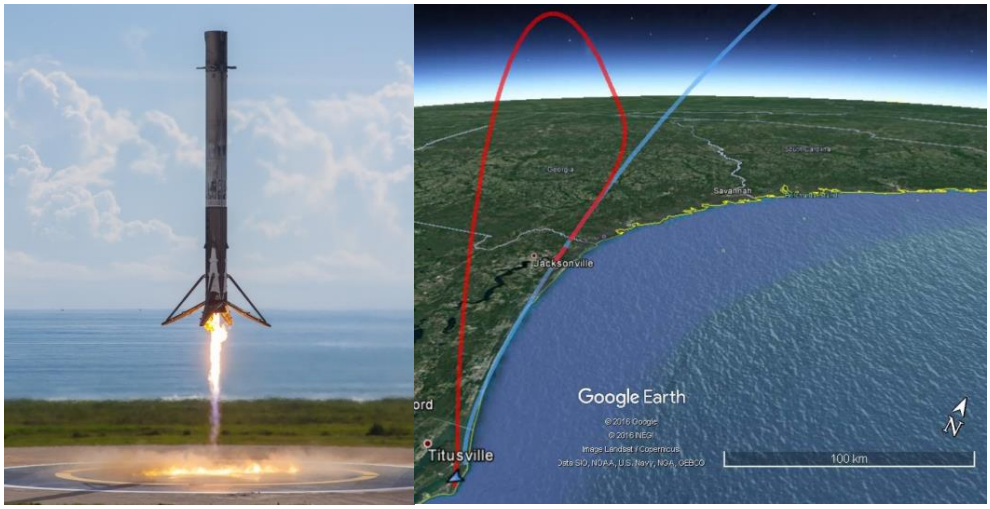

Figure 3-4: Landing of F9 FT first stage on LZ-1, X-37B mission, September, 7th 2017 (left, Courtesy https://www.flickr.com/photos/spacex) and typical trajectory profile for a RTLS mission

3.1.2 VTVL with Down-range landing (DRL)

Landing a used stage down-range of its launch site is probably the most straight-forward idea and thus has been proposed several times already in the past. However, the particular challenge is related to the fact that suitable natural down-range sites are very scarce if existing at all. An artificial sea-going platform or ship is offering significantly more flexibility to the missions and has been adopted by SpaceX for the Falcon 9 high performance missions (Figure 3-5). The performance loss of a launch vehicle applying the DRL-method is reduced compared to one using the RTLS mode.

Figure 3-5: Sea-going platform (“barge” or “droneship”) of company SpaceX (left, Courtesy https://www.flickr.com/photos/spacex) and landing of the Falcon 9 first stage on the droneship

The sea-going platform should be capable of delivering the landed stage back to a sea-port close to the launch site and, therefore, needs to be a sea-going ship. The approximate size of the SpaceX’ droneship is not small: 91 m by 52 m. The SpaceX platform needs additional tugboats towing it back typically within 4 to 5 days to the Cape Canaveral port. Further, depending on the port location, substantial ground transportation equipment is required for moving the stage to the refurbishment site.

Overall, the better performance of DRL compared to RTLS is paid for by additional infrastructure investment and operations cost.

Theoretically, the DRL-mode is independent of vertical or horizontal landing. In practice even large (and expensive) aircraft carriers are probably too short and too narrow to allow landing of a winged RLV. Therefore, in this investigation DRL is linked to VTVL-configurations.

3.1.3 Horizontally Landing Autonomous airbreathing-powered fly-back (LFBB)

The classical method of bringing reusable first stages back to their launch site in autonomous flight is using a separate airbreathing cruise propulsion system. The approach was popular in the 1980s up to the early 2000s. Famous examples are studies on a second generation Soviet Energia Buran [7], the derived Baikal or in late 1990s studies on potential Space Shuttle upgrades intending the replacement of the SRB [8]. In Germany the ASTRA study investigated such LFBB [2] as shown in Figure 3-6 as an Ariane 5 modernization option. All concepts have two things in common: horizontal landing (HL) which requires wings and aerodynamic surfaces to generate sufficient aerodynamic forces and the use of airbreathing engines to return to the landing site. Contrary to the vertical landing stages, a reignition of the rocket engines is not necessary during re-entry. Instead, the stage is decelerated by aerodynamic forces only which are created by a sufficiently large wing.

Figure 3-6: LFBB of ASTRA-study in artists' impression at separation from expendable core

The interest in the LFBB approach originates from the fact that turbofans in subsonic cruise flight are at least ten times more efficient than rocket engines using the same fuel. Thus, the fly-back propellant and inert mass during ascent should be significantly reduced.

In the ASTRA concept, typical for LFBB, three turbo engines without afterburner using hydrogen have been foreseen for the stages' fly-back. The feasibility of replacing kerosene by hydrogen in an existing military turbofan (EJ-200) investigated within the ASTRA-study shows the engine is capable of continuous operation with hydrogen fuel under all LFBB attitudes and manoeuvre [9], [10]. Such an additional propulsion system is adding some complexity to the RLV while components accommodation – at least for the ASTRA LFBB – is not an issue (Figure 3-7).

On the downside, the LFBB-mode in any case adds the secondary propulsion system mass and is not feasible without a sufficiently large wing allowing cruise flight at acceptable L/D.

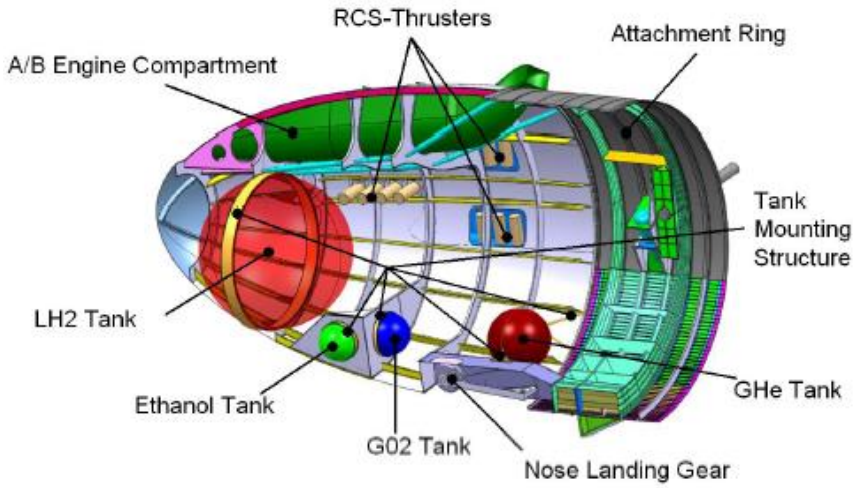

Figure 3-7: Integration of turbofan engine and auxiliary tank in nose of ASTRA LFBB [10]

3.1.4 "In-Air-Capturing" (IAC)

Techniques of powered return flight like LFBB obligate an additional propulsion system and its fuel, which raises the stage's inert mass. The patented "In-air-capturing" [6] offers a different approach with better performance: The winged reusable stages are to be caught in the air, and towed back to their launch site without any necessity of an own propulsion system [11]. The idea has similarities with the DRL-mode, however, initially not landing on ground but "landing" in the air. Thus, additional infra-structure is required, a relatively large-size capturing aircraft. For this task used, refurbished and modified airliners should be sufficient.

After DLR had patented the "in-air-capturing"-method (IAC) for future RLVs, two similar approaches have been proposed. However, those named *mid-air retrieval* or *mid-air capturing* are relying on parachute or parafoil as lifting devices for the reusable parts and helicopters as capturing aircraft. The first proposal was made by the Russian launcher company Khrunichev [12] and the most recent one by the American company ULA for its newly proposed Vulcan launcher. A parachute and helicopter-based system is obviously less flexible and significantly less robust than the in-air-capturing based on winged RLV and winged aircraft. Consequently, the ULA proposal intends recovering not more than the first stage's engine bay instead of a full stage.

A schematic of the reusable stage's full operational circle is shown in Figure 3-8. At the launcher's lift-off the capturing aircraft is waiting at a downrange rendezvous area. After its MECO the reusable winged stage is separated from the rest of the launch vehicle and afterwards performs a ballistic trajectory, soon reaching denser atmospheric layers. At around 20 km altitude it decelerates to subsonic velocity and rapidly loses altitude in a gliding flight path. At this point a reusable returning stage usually has to initiate the final landing approach or has to ignite its secondary propulsion system.

Differently, within the "In-Air-Capturing" method, the reusable stage is awaited by an adequately equipped large capturing aircraft (most likely fully automatic and unmanned), offering sufficient thrust capability to tow a winged launcher stage with restrained lift to drag ratio. Both vehicles have the same heading still on different flight levels. The reusable unpowered stage is approaching the airliner from above with a higher initial velocity and a steeper flight path, actively controlled by aerodynamic braking. The time window to successfully perform the capturing process is dependent on the performed flight strategy of both vehicles, but can be extended up to about two minutes. The entire maneuver is fully subsonic in an altitude range from around 8000 m to 2000 m [4]. After successfully connecting both vehicles, the winged reusable stage is towed by the large carrier aircraft back to the launch site. Close to the airfield, the stage is released, and autonomously glides like a sailplane to Earth.

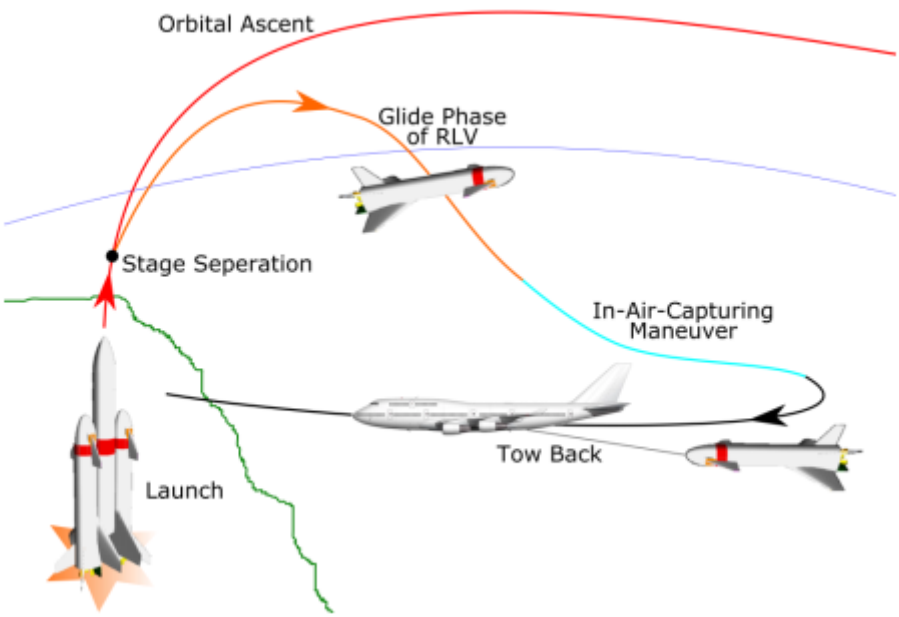

Figure 3-8: Schematic of the proposed in-air-capturing

The selected flight strategy and the applied control algorithms show in simulations a robust behavior of the reusable stage to reach the capturing aircraft. In the nominal case the approach maneuver of both vehicles requires active control only by the gliding stage. Simulations (3DOF) regarding reasonable assumptions in mass and aerodynamic quality proof that a minimum distance below 200 m between RLV and aircraft can be maintained for up to two minutes [13]. The most promising capturing technique is using an aerodynamically controlled capturing device (ACCD), showing the best performance and lowest risk.

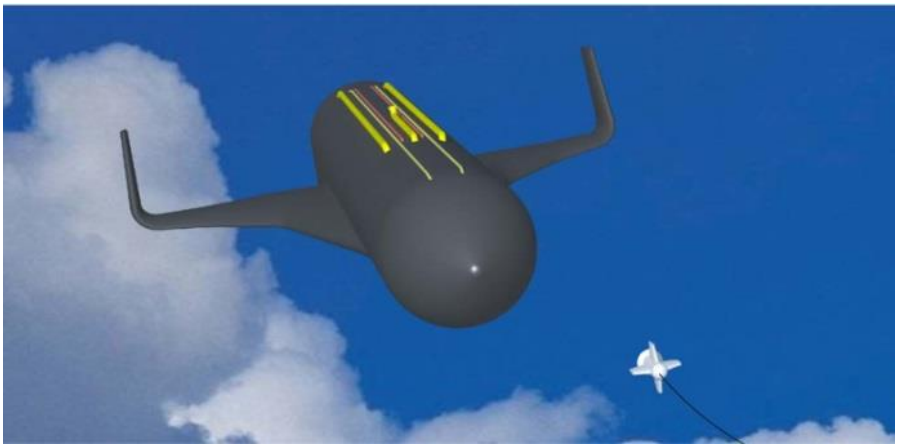

Figure 3-9: Artist's Impression of the SpaceLiner Booster during In-Air-Capturing

The In-Air-Capturing method is the centerpiece of the FALCon project. The maneuver of capturing the RLV stage will be reproduced on a subscale level with UAVs but will also be calculated and simulated on a fullscale level. Therefore, understanding this method and putting it into context with the other return methods is of high importance in this report. It is important to note that the IAC method in this report is used for the capturing of first stages of reusable launch vehicles.

3.2 Comparison and Design Logic

The different return methods lead to completely different stage and RLV designs if applied to any launch vehicle. Comparing those methods is best possible if similar design assumptions and mission requirements are used. Furthermore, considering several propellant combinations or engine cycles

should guarantee that all common launcher designs are considered. The design assumptions are the following:

- 7000 kg + 500 kg margin payload to GTO of 250 km x 35786 km x 6° (standard Ariane 5 GTO) via a LEO parking orbit of 140 km x 330 km x 6°
- Launch from CSG, Kourou
- TSTO: Two Stage to Orbit
- Engine Cycles: Gas Generator (GG) and Staged Combustion (SC)
- 2nd stage Δv of 6.6 km/s, 7.0 km/s
- Propellant Combinations: LOX/LH2, LOX/LCH4, LOX/RP-1. LOX/LC3H8 (propane)

Several RLVs with reusable first stages based on vertical landing design with either DRL or RTLS or based on horizontal landing with either LFBB or IAC technology were designed and investigated. Those preliminary designs are performed using the DLR in-house tools developed at the department of Space Launcher Systems Analysis. The detailed description of the design process and the different assumptions used would go beyond the scope of this report. However, more detailed information can be found in several publicly available DLR papers [16], [17].

4 Performance, Mass and Re-entry Analysis

The performance of launch vehicles can be measured by different means. Usually, launch vehicles of different providers are compared with respect to payload mass into several orbits. Since in our case the payload mass was given as a design input, choosing this parameter for comparison doesn't make much sense. Instead, using the same design payload mass to design RLVs requires to compare total system masses and dry masses. The lighter a system for equal payload mass, the more performant it is since the mission can be achieved with less total mass. Furthermore, comparing indices such as the structural index or the inert mass ration are good indicators for performance. The section 4.1 will be focusing on the comparison from this perspective.

Additionally, for an RLV re-entry loads are of high importance since they determine the amount of refurbishment that has to be invested into the vehicle to overhaul it and getting it ready for the next flight. Logically, it is expected that lower re-entry loads shall decrease the amount of refurbishment needed between flights and prolong the lifetime of the parts that experience the most stress during re-entry. Nevertheless, it is difficult to determine the precise impact of those loads on the stage since it depends on stage design and requires actual tests at re-entry conditions. However, at this preliminary stage the re-entry loads are a reasonably well indicator of loads and stresses on the stage.

In the following, all vertical landing methods will be referred to as VL and all horizontal landing methods as HL. Further, the abbreviation ***IAC*** is used for ***In-Air-Capturing***, ***FB*** for ***Flyback Booster***, ***DRL*** for ***downrange landing*** and ***RTLS*** for ***return-to-launch-site***. The propellant combinations considered and presented include ***LOX/LH2, LOX/liquid methane (LCH4), LOX/kerosene (RP-1)*** and ***LOX/propane (LOX/LC3H8)***. ***GG*** stands for engines using the ***gas generator*** cycle and ***SC*** for ***staged combustion cycle***. If not specified otherwise, the gas generator cycle is the standard.

4.1 Size, Performance & Mass

In this section different RLVs using the four major return modes as described in section 3.2 are compared with respect to lift-off masses, dry mass and structural index (SI), system design and impact on payload performance.

The size, layout and internal geometry of those launchers are shown in Figure 4-1. Considering the internal layout, the launchers with VL stages consist of (from bottom to top) a rear skirt with a baseplate where the engines are attached to and parts of the propellant supply are covered by. Further, the landing legs are located there. In all first stages the fuel tank is positioned beneath the oxygen tank with a common bulkhead separating both stages. The interstage connects the first with the second stage and stays attached to the first stage after separation. The grid fins are connected to the interstage which also acts as a protection of the second stage engine and nozzle during ascent. The second stage tank order is reversed compared to the first stage. On top of the upper fuel tank a front skirt is attached which houses avionics and GNC of the 2nd stage and also acts as a connection to the fairing and the payload adapter.

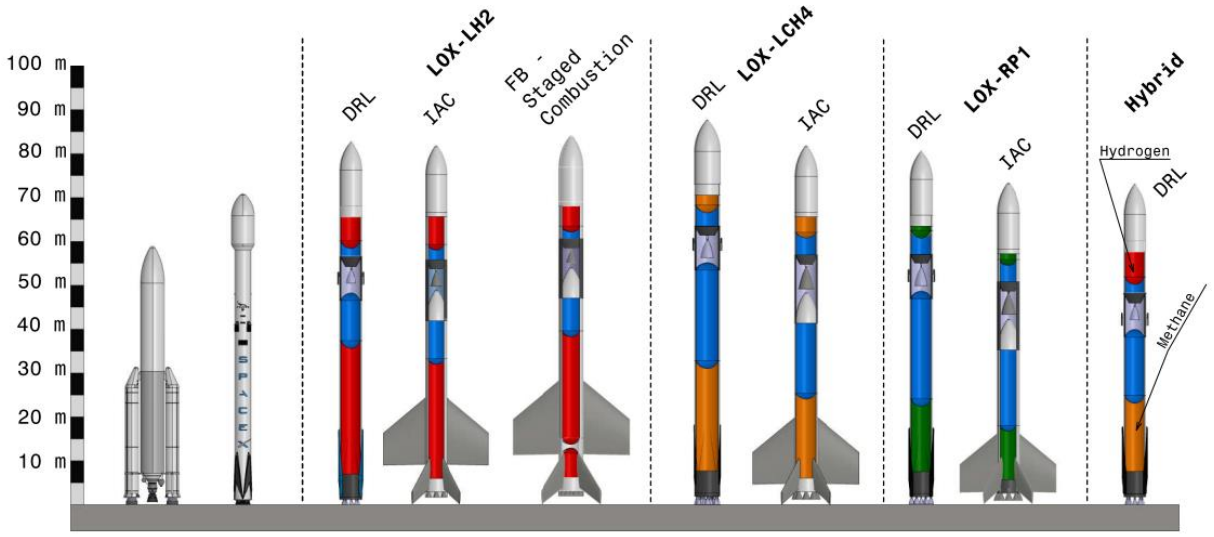

Figure 4-1: Geometry and Layout of conceptual RLVs compared to Falcon 9 and Ariane 5

The HL launchers follow the same principle except for the difference in first stage layout resulting from the wings and aerodynamic control surfaces. Also, the HL launchers re-enter nose first which requires the HL stage to be equipped with an ogival nose which is covered by the interstage during ascent. In that case, the interstage is not recovered and reused. Further, in case of flyback HL stages an additional fuel tank to drive the turbine engines is required. The IAC conceptual launchers don't require additional propellant and all propellant is used during ascent to accelerate the launcher.

Another aspect worth mentioning is the fact that a hybrid launcher is presented as well. Hybrid in this case refers to a stage design with different propellant combinations in both stages. This hybrid VL stage uses LOX/LCH4 in the first stage and LOX/LH2 in the upper stage, thus combining the high Isp upper stage propellant combination with a lower stage that is more in line with current engine development in Europe (e.g. Prometheus engine).

In general, the conceptual RLV stages are all bigger than the Ariane 5 or Falcon 9. This can be explained by the fact that the launchers are designed as RLVs with a different payload capability compared to Ariane 5 (13 t as ELV to GTO) or the Falcon 9 (5.5 tons to GTO as RLV). The relatively high volume of the LOX/LH2 launchers is due to the low bulk density of that propellant combination, for the hydrocarbons the low Isp leads to more propellant required. The total size is smallest for the hybrid vertical landing concept due to the combination of upper LOX/LH2-driven stage with high efficiency and the LOX/LCH4 lower stage with less performant but denser propellants.

For all other concepts the IAC method leads to comparable smaller sizes compared to the vertical landing method. This is due to the fact that vertical landing requires propellant for the engine firings so that the tanks have to accommodate more propellant. The IAC requires no additional propellants so the tanks are dimensioned smaller. However, the additional hardware, respectively wings, landing gear, aerodynamic control surfaces, environmental and IAC hardware and TPS lead to a usually higher dry mass than it is the case for VL stages.

These results are further highlighted in Figure 4-2. This mass breakdown shows the empty masses and propellant masses of both stages. It is clearly visible that the LOX/LH2 launchers are lighter than their hydrocarbon counterparts for any upper stage Δv. The lowest GLOM, the HL launcher with LOX/LH2, In-Air-Capturing and stage combustion engines, is around 350 tons. This shows that IAC offers the possibility to build the comparably lightest reusable stages, especially in combination with a high-performant propellant combination such as LOX/LH2. Hence, the IAC offers a competitive alternative to the SpaceX vertical landing strategy considering launcher size and mass.

The reason for the higher stage mass of the hydrocarbons, although generally having a better structural index, is lying in the lower Isp of that combination. The dependence of first stage GLOM on Isp is shown in. A low Isp has even more impact for vertical landings, since propellant is needed for

the engine firings during descent. This descent propellant has to be accelerated during ascent, thus acting as “dead” or payload mass during ascent. According to the Tsiolkowski equation, the total propellant mass has to be increased in order to deliver the required Δv. In general, switching from hydrogen to hydrocarbons leads to a doubling in GLOM for HL systems and almost tripling in GLOM for VL systems.

$$SI = \frac{m_{dry}}{m_{propellant}} \tag{4-1}$$

$$Inert\ Mass\ Ratio = \frac{m_{inert}}{m_{GLOM,Stage}} \tag{4-2}$$

These effects get clearer when taking a look at Figure 4-3 to Figure 4-5 where the structural index and the inert mass ratio are plotted versus a range of other parameters. Here, the structural index and the inert mass ratio (IMR) are presented as defined according to equations (4-1) and (4-2). Inert mass is the mass of all components that are not contributing to accelerating the system during ascent. Hence, the IMR is, together with the Isp, a direct indicator of performance since it can be directly related to the mass fraction within the logarithm of the Tsiolkowski equation.

Figure 4-3 shows a comparison of all SIs and inert mass ratios for all considered return methods. Generally, the SI of LOX/LH2 stages is higher compared to the hydrocarbons as it was expected. However, the figures also show the impact of equipping the HL stages with wings and further equipment in a pronounced increase of dry mass, respectively SI. The SI is highest for flyback stages due to the added mass of engines and return propellant tanks. However, taking also inert mass ratio into account this effect diminishes in significance. Whereas VL stages have a lower dry mass, they carry a considerable amount of descent propellant with them, leading to a higher ratio of accelerated total “useless” mass. In general, the higher the required Δv for the return maneuvers, the higher the inert mass ratio and thus the decrease in performance.

The structural index is also highly dependent on propellant loading. Generally, the more propellant a stage carries the lower the structural index gets. Figure 4-3 shows this dependence for the range of return methods considered herein. Additionally, there is a clear dependence of propellant choice on the structural index as well. LOX/LH2 as propellant choice leads to higher SIs due to the low bulk density of the propellant combination and the voluminous tanks. Furthermore, the extremely low temperature of liquid hydrogen demands a good insulation system, thus adding mass. Considering only structural index, the IAC stages seem to be worse than the vertical landing options. Nevertheless, whereas structural index is a good indicator for dry mass weight with respect to propellant loaded, the inert mass ratio is a better indicator for overall performance.

The inert mass ratio indicates how high the ratio of “dead” or inert mass is during ascent. The lower this value the more performance is available from the same amount and type of propellant. In Figure 4-6 the inert mass ratio versus the amount of ascent propellant is shown. It is clearly visible that the IAC with hydrogen have slightly lower inert mass ratios than the other return methods. The lowest inert mass ratios are observed for the LOX/RP-1 RLV with In-Air-Capturing. From a performance perspective the use of hydrocarbons leads to less inert mass ratio and hence less performance losses compared to conventional RLVs. However, due to the fact that the stage and propellant mass is the lowest for hydrogen and the inert mass ratio of the In-Air-Capturing method is among the lowest of all hydrogen systems, the In-Air-Capturing method once again demonstrates its capability to compete with the vertical landing method of SpaceX. One has to also keep in mind that the costs of a launcher scale with its dry mass. Hence lighter launchers by using hydrogen are expected to result in lower total launch costs. This topic will be elaborated in more detail in section 5.2.

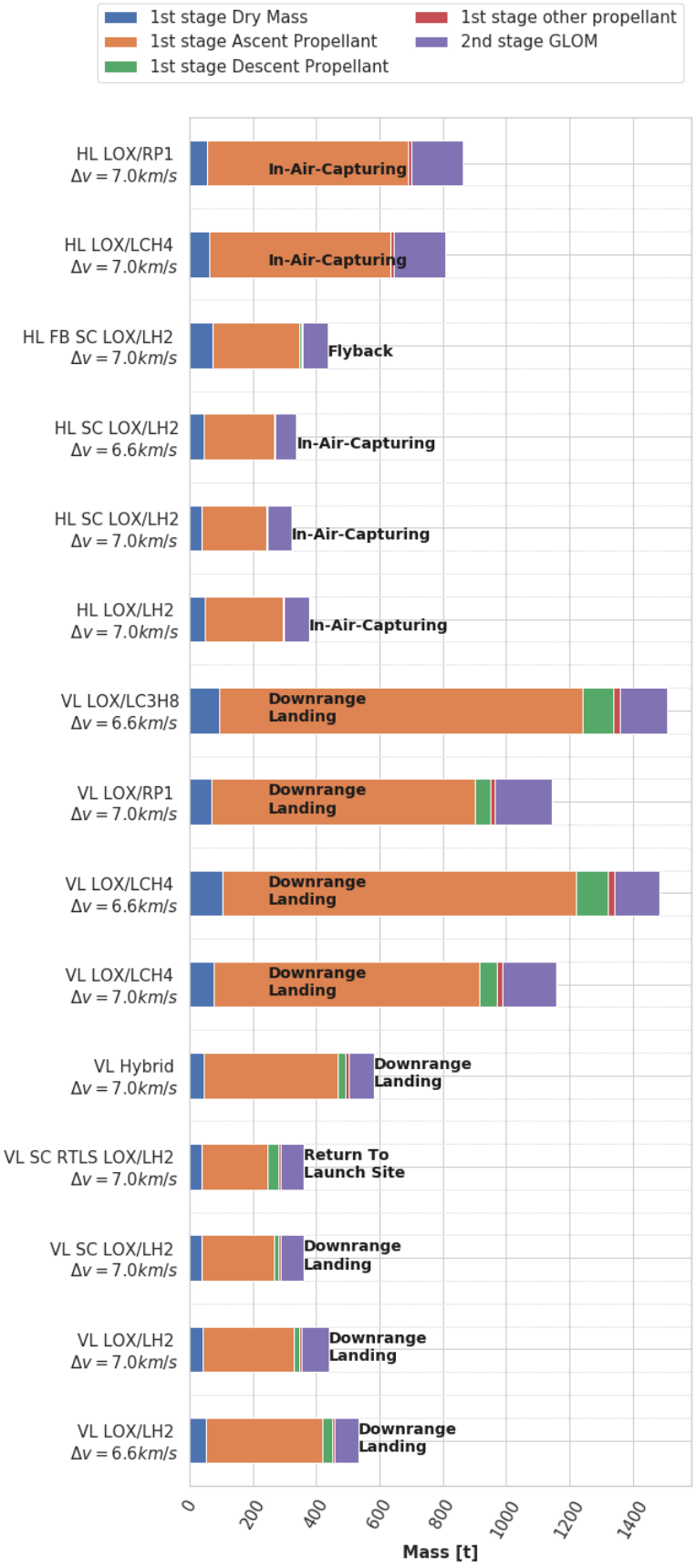

Figure 4-2: Mass Breakdown of the RLVs with vertical downrange landing, vertical RTLS, horizontal landing with In-Air-Capturing and horizontal landing with flyback engines

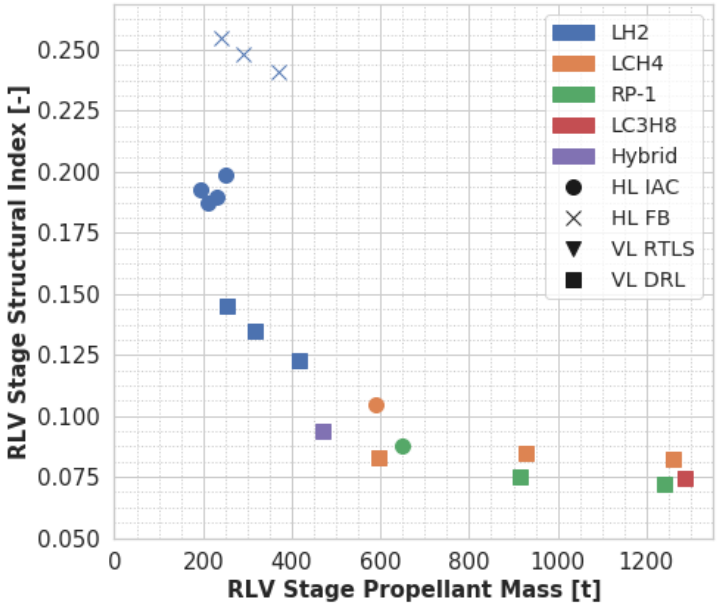

Figure 4-3: Structural Indices of the RLVs with different return modes with respect to propellant loading

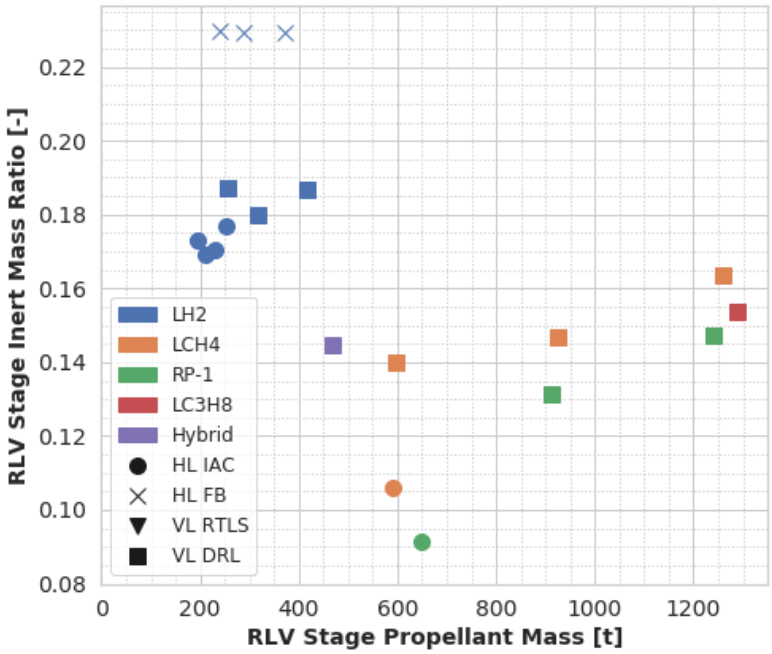

Figure 4-4: Inert Mass Ratios of the RLVs with different return modes with respect to propellant loading

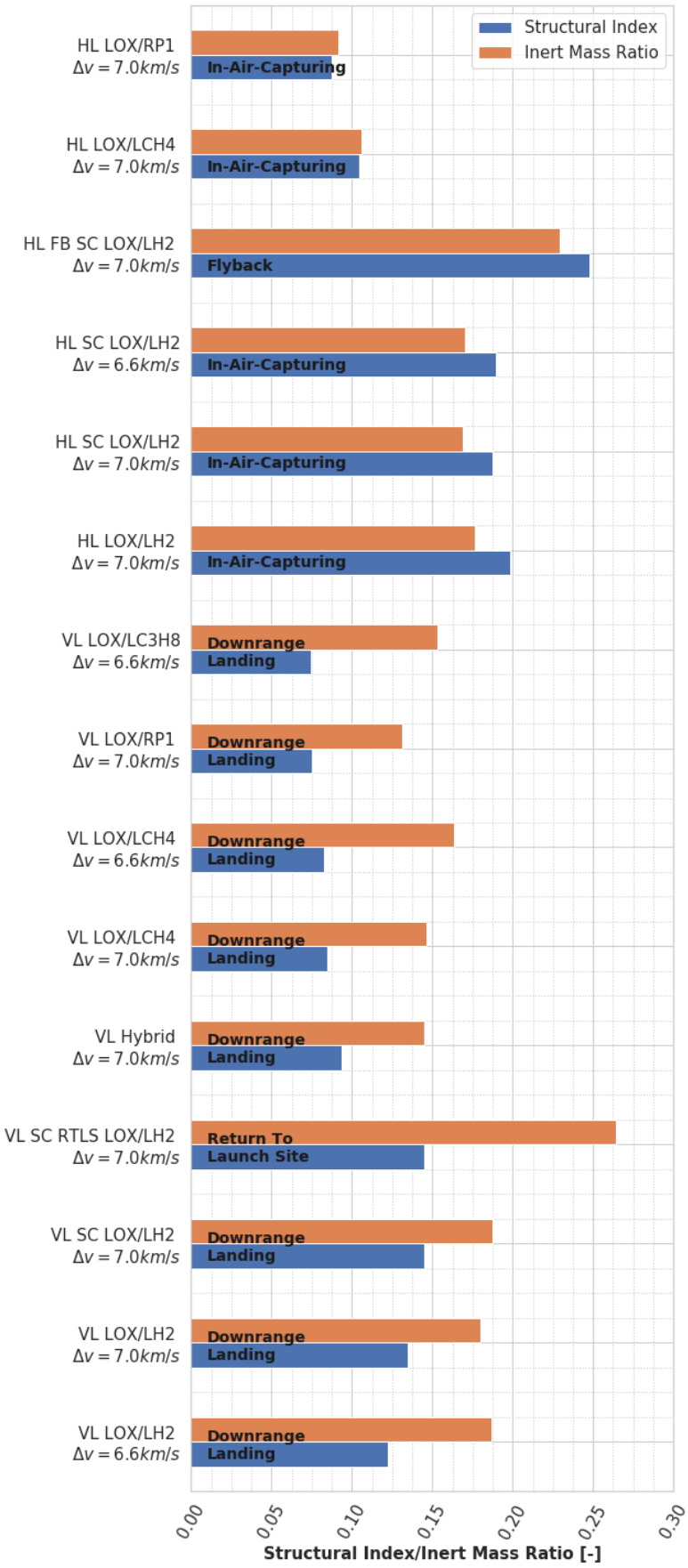

Figure 4-5: Structural Indices and Inert Mass Ratio of the RLVs with vertical downrange landing, vertical RTLS, horizontal landing with In-Air-Capturing and horizontal landing with flyback engines

The choice of hydrogen as a propellant combination for the In-Air-Captured winged stages is further highlighted when considering the correlation between first stage GLOM and first stage vacuum Isp shown in Figure 4-6. The high vacuum Isp from 405 s - ~435 s the Isp of the LOX/LH2 stages with the two highest Isp values referring to a staged combustion cycle. The hydrocarbons are less efficient and Isp values range from 310 s to 320 s for RP-1 and 320 s – 330 s for methane. The higher Isp of the VTHL stages is due to the greater expansion ratio of the engines which renders higher specific Impulse in vacuum. The figure also shown that for the VL versions a higher Isp does not necessarily lead to lower stage mass (compare mass of RP-1 vs LCH4 VL). Contrary, the GLOM for winged stages decreases in any case.

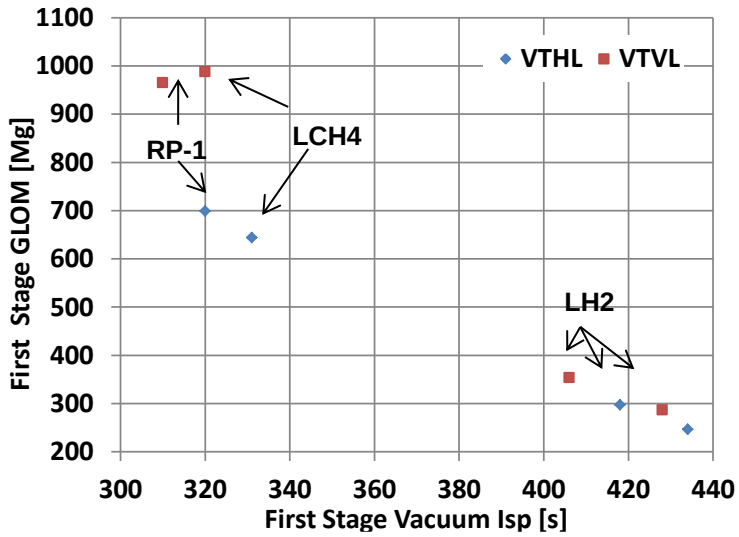

Figure 4-6: First Stage GLOM over vacuum Isp for VTHL and VTVL RLVs

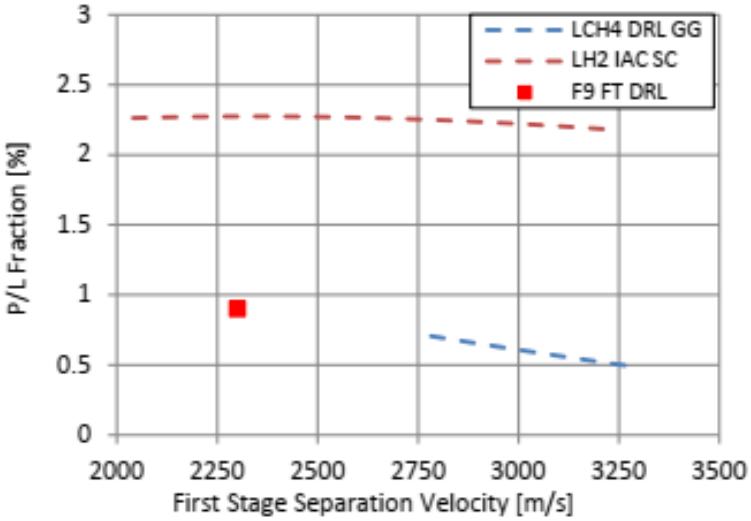

Figure 4-7: Payload Fraction over first stage separation velocity for the downrange landing method with LOX/LCH4 and the In-Air-Capturing method with LOX/LH2

Finally, it is important to note that the upper stage Δv also has a considerable impact on the resulting lift off mass and performance. Figure 4-7 shows the payload fraction as payload mass divided by launcher GLOM over separation velocity. A higher payload fraction implicates higher efficiency and more performance. Once again, the performance of the hydrogen combination is highlighted. Also the advantage of the combination of winged stages with IAC and hydrogen is shown by the almost constant trend of the respective curve. Contrary, the payload fraction for vertical landing stages decreases with high stage separation. This arises from the fact that a higher separation velocity leads

to more propellant demand for the re-entry and deceleration burns. Hence, efficiency and thus payload fraction decrease.

4.2 Re-entry Analysis

An RLV has a further major difference to a conventional expendable launch system: the re-entry and landing has to happen in a controlled manner to keep loads low and control the trajectory. The trajectory and re-entry parameters have a major influence on the re-entry loads experienced. To put it simply these loads in combination with the stage design can be used as an indicator for the refurbishment and maintenance effort required between flights of the same stage. Generally, higher loads lead to either a more sophisticated and expensive stage design or to more refurbishment. Comparing re-entry loads with respect to temperature, heat flux, dynamic pressure and aerodynamic forces, body accelerations and maneuvers and control required allows for a better understanding and comparison of the different return options.

The re-entry trajectories and loads of the conceptual RLVs are shown in Figure 21. The trajectory of the SpaceX Falcon 9 mission SES 10, which was launched in 2017, is added for comparison with an operational RLV. It is important to note that this trajectory was derived based on reverse-engineering the SpaceX mission and using in-house tools to reproduce a trajectory close to the actual one. Isolines for heatflux and dynamic pressure are shown in the graph. The heatflux is calculated based on a modified Chapman equation as shown in equation (7). Here, ρ is the local density at the respective altitude according to the US standard atmosphere 1976, ρR is a reference density value of 1.225 kg/m³, RN,r is reference nose radius (here 1 m), RN is the vehicle nose radius (here 0.5 m for all vehicles), v is the vehicle's velocity and vR is a reference velocity of 10000 m/s.

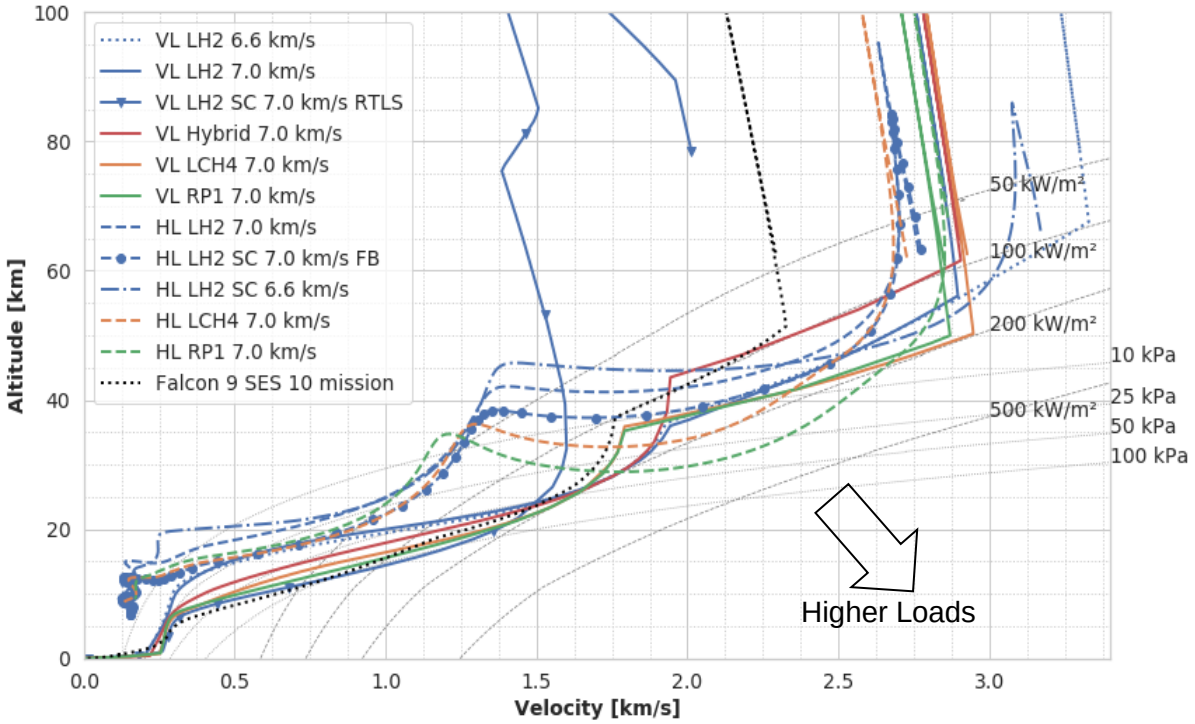

Figure 4-8: Re-entry Trajectories of the RLVs with different return methods

$$\dot{q} = 20254.4\ W/cm^2 \cdot \sqrt{\frac{\rho}{\rho_R}\frac{R_{N,r}}{R_{,N}}}\left(\frac{v}{v_r}\right)^{3.05} \tag{4-3}$$

The altitude vs. velocity diagram shows the difference in re-entry strategy and load handling. The VL launchers are unable to control the heat flux via lift as the winged vehicles can do. Hence, a re-entry burn is required that occurs between 50 km and 67 km in altitude, marked by a sudden change in the velocity gradient. The VL launchers are limited to a maximum heat flux of 200 kW/m² which is based on the heat flux that was prevalent during the SES-10 mission. Due to this boundary, all VL launchers follow a similar re-entry profile. The ballistic coefficient, defined as the ratio between mass and drag as shown in equation (4-4), is of considerable importance for the aerodynamic phase of the VL's re-entry. The light, but voluminous LOX/LH2 launchers have a low ballistic coefficient and can thus reduce the burn time of the re-entry burn since more velocity can be shed by aerodynamic deceleration. The heat flux is the main driver of the re-entry burn since all other parameters, such as dynamic pressure, lateral and longitudinal loads and forces are well within reasonable limits.

$$BC = \frac{m}{C_d S} \tag{4-4}$$

Contrary to the VLs, the HL stages have a more gradual deceleration profile characterized by the generation of aerodynamic forces. In the upper layers of the atmosphere the air is too thin to decelerate the vehicle. Once the stage drops into the denser parts of the atmosphere significant aerodynamic forces are created, resulting in a deceleration of the vehicle. On the other hand, the lift generated by the wings and fuselage is used to maintain a certain altitude to reduce the maximum heat flux. Furthermore, the re-entry velocity and flight path angle such as the ballistic coefficient are the other main drivers of the HLs' re-entry loads. A shallow re-entry with a low flight path angle is advantageous since the gradient of aerodynamic forces is not as pronounced as with a steep re-entry. Figure 4-9 shows this dependence for the winged HL stages. Here, the re-entry flight path angle is defined as the maximum angle that occurs before the stage flattens the trajectory due to the increase in lift force. The differences between hydrogen and hydrocarbon stages are quite visible: the hydrogen stages are light and have a low ballistic coefficient and separate at slightly lower flight path angles. Hence, the heat flux during re-entry can be reduced which in turn results in a lighter TPS (see Figure 4-9). This is also highlighted in Figure 4-11 where the maximum temperatures for one LOX/LH2 winged stage and one LOX/RP1 winged stage are compared. The TPS mass is driven by re-entry heat flux and vehicle area. The fact that hydrogen as propellant leads to light launchers with low surface area and advantageous re-entry conditions explains the superiority of hydrogen to the hydrocarbons.

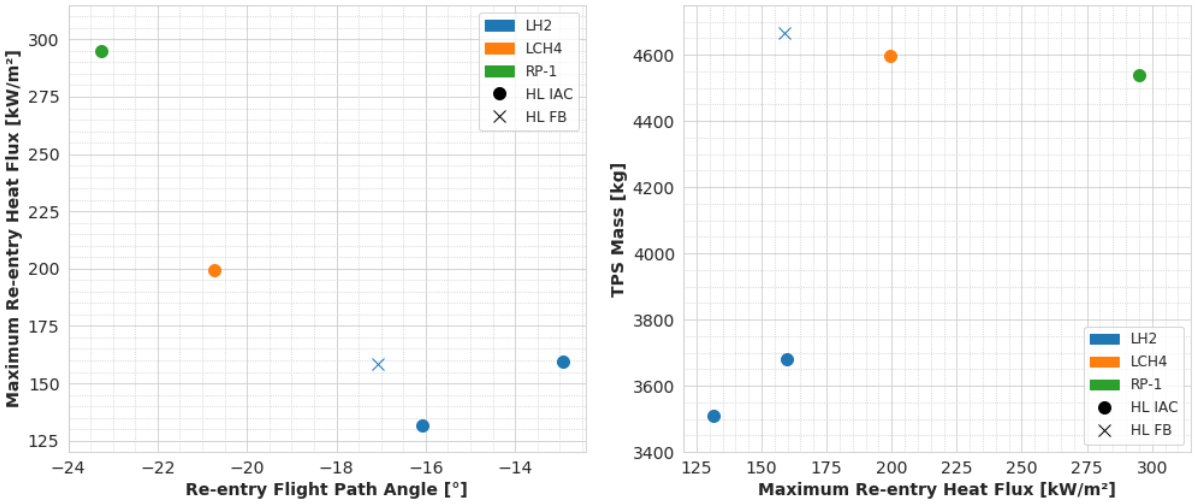

Figure 4-9: Maximum re-entry stagnation point heatflux over re-entry flight path angle (left) and TPS mass over maximum heat flux (left) of the winged HL stages

In case of the VL stages the re-entry loads can be directly influenced by engine ignition. Instead, the maximum heat flux value of 200 kW/m² was set for all stages leading to burn timing and duration as a result of that boundary. The parameter of comparison in that case is the re-entry propellant, since more re-entry propellant diminishes performance. Figure 4-10 shows the re-entry propellant of some of

the VL stages with respect to separation velocity and ballistic coefficient. As already mentioned, a higher separation velocity naturally leads to more propellant required. Additionally, the effect of aerodynamic shape and mass is also of high importance even for the VL stages as can be seen by the dependence of re-entry propellant on ballistic coefficient. The light but voluminous hydrogen stages have quite low ballistic coefficients, which in combination with the highly efficient propellant combination reduce the required propellant and thus increase efficiency.

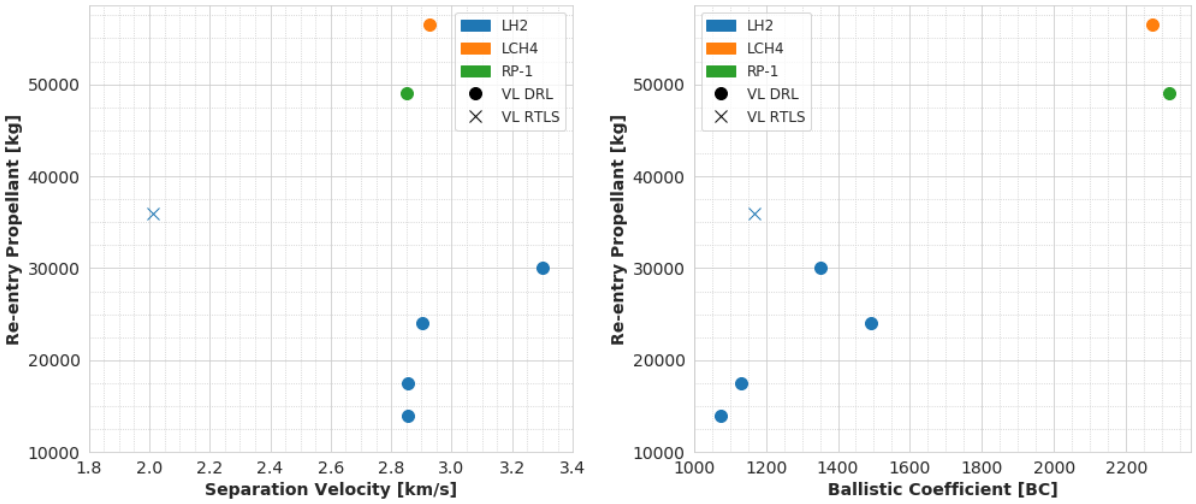

Figure 4-10: Re-entry propellant versus stage separation velocity (left) and re-entry propellant versus ballistic coefficient (right) of the VL stages

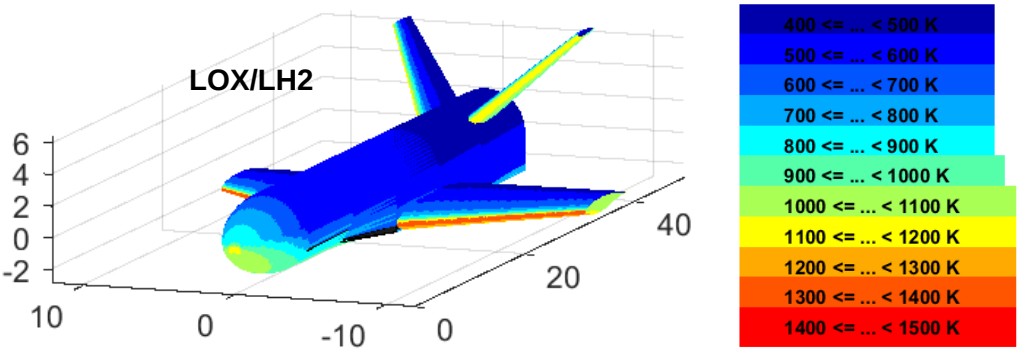

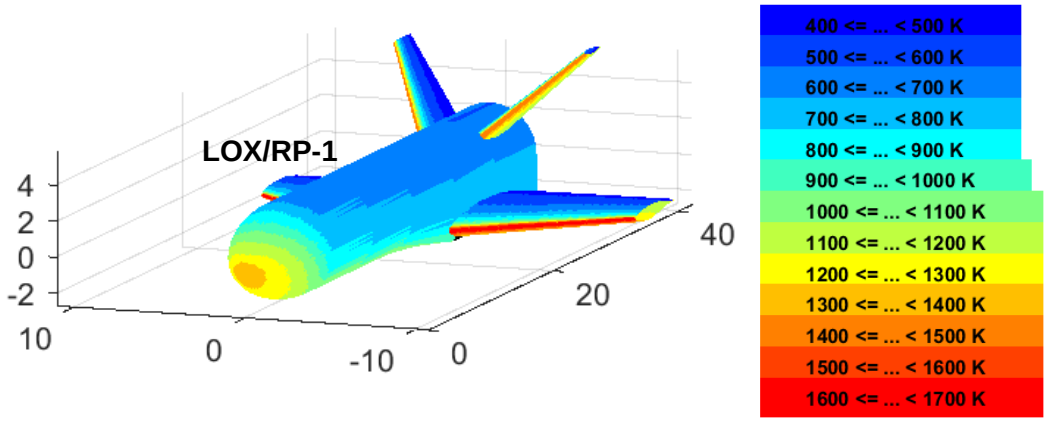

Figure 4-11: Maximum Temperatures during re-entry for a LOX/LH2 winged stage and a LOX/RP1 winged stage

The Δv breakdown for the re-entry trajectories is shown in Figure 4-12. The Δv budget is made up of Δv reduction by engine burns (for VL and HL with turbine engines), Δv reduction by aerodynamic forces and the Δv added by gravitational acceleration. Positive values indicate an increase in velocity (mostly by gravity) and a negative sign value indicates that the stage is decelerated. Summing up all Δv for one stage roughly gives the separation velocity.

The Δv breakup clearly shows the difference between the winged and the vertical landing stages; whereas the deceleration of the winged stages is only performed by aerodynamic means the VL stages have to compensate the lower aerodynamic performance with reignition of the engines. Interestingly, the LOX/LH2 launchers, as mentioned before, can shed more velocity by aerodynamic forces. Acceleration by gravity is driven by a combination the trajectory shape (the flatter, the better) and flight time.

In summary, for VL and HL stages there are solutions where the re-entry loads stay in a range that is manageable. Comparing the heat flux with the value from the SES 10 SpaceX mission shows that the loads are close to the ones seen by that Falcon 9 stage. Generally, for HL and VL stages hydrogen is the better option considering re-entry since, it offers low re-entry loads due to a combination of high performance propellant, favorable aerodynamic performance and low system masses. Paying special interest to the IAC procedure reveals some advantages but also disadvantages compared to the SpaceX vertical landing method: first, the deceleration of the re-entering RLV stage occurs only by aerodynamic means only. Hence, no additional propellant is needed to decelerate the stage, making it the most efficient return strategy from a performance perspective. Nevertheless, the cost of this method is the higher dependency on separation conditions (flight path angle, velocity) on the maximum loads experienced during re-entry.

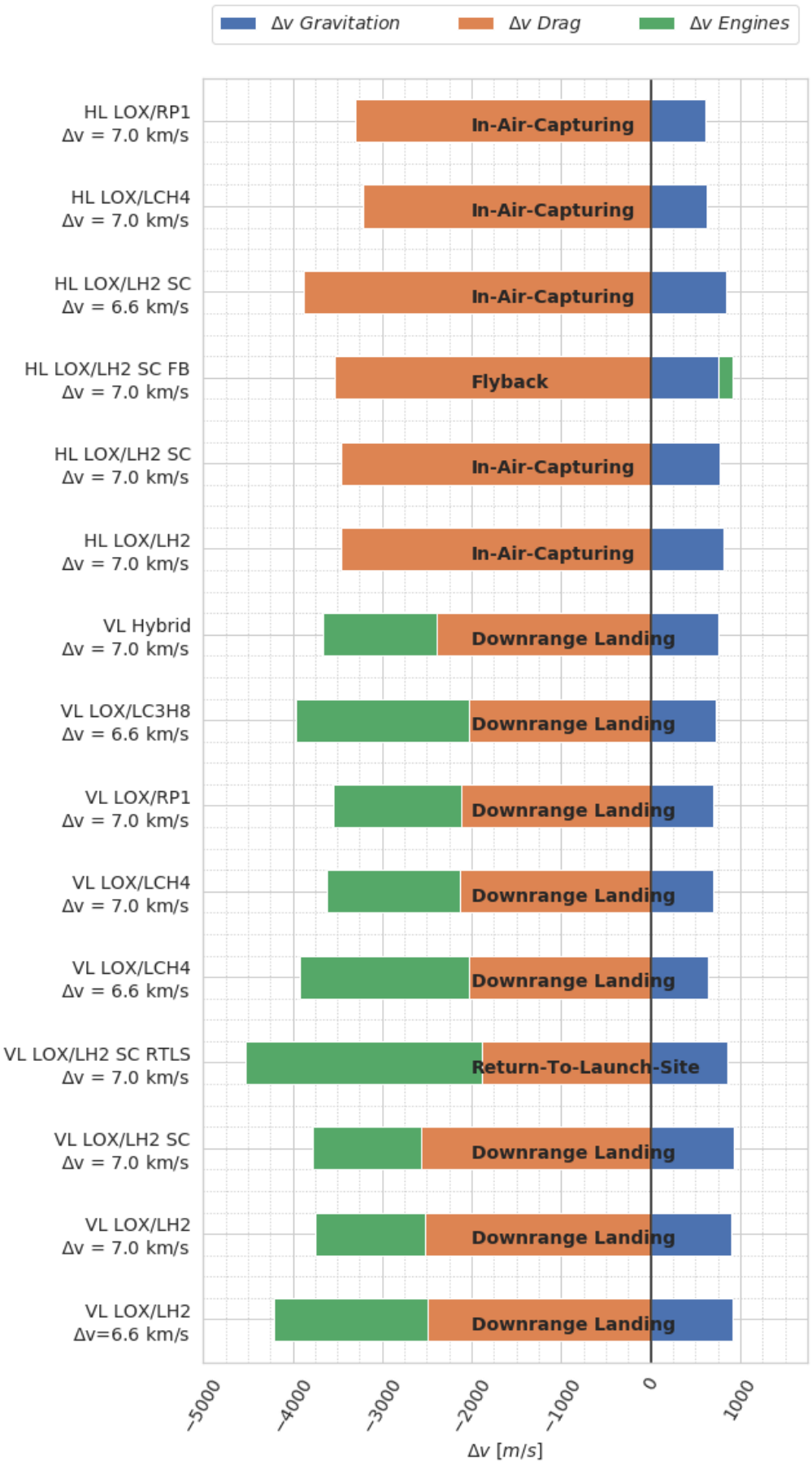

Figure 4-12: Δv Breakdown for re-entry for different return methods

4.3 Summary

In the previous sections the technical differences of the four return methods In-Air-Capturing (HL), Flyback Booster (HL), Downrange Landing (VL) and Return-to-Launch-Site (VL) were presented and discussed. The major key points of this comparison with a highlight on the IAC with respect to the other return methods will be summed up in the following:

- **System Design and Size:**
  - The size of RLVs using In-Air-Capturing is comparable and even slightly lower than the size of RLVs using the vertical landing method when comparing launchers with the same propellant combination and payload capability
  - Winged RLVs require more added hardware compared to the VL method, respectively wings, aerodynamic control surfaces, landing gear and capturing hardware
  - LOX/LH2 as propellant in combination with IAC leads to the lowest-sized vehicles
- **Mass and Performance:**
  - Lowest Masses for LOX/LH2 launchers with IAC followed by VL launchers with downrange landing
  - Masses as RLV with IAC and LOX/LH2 even lower than Ariane 5 (GTO: up to 10.8 t) and Falcon 9 (GTO as RLV: up to 5.5 t) masses
  - Higher structural indices and dry mass weight of HL IAC compared to conventional ELV or VL stages due to more hardware for re-entry and controlled flight
  - Lowest performance losses of all return strategies observed when using IAC and LOX/LH2
- **Re-entry and Loads:**
  - Re-entry Loads are low for IAC and LOX/LH2 but get high when using hydrocarbons
  - Loads are highly dependent on separation conditions (velocity, flight path angle) and determine the size of the TPS

Considering these results the In-Air-Capturing strategy seems to be a viable and efficient option compared to conventional ELVs and even the VL SpaceX method. This can be deduced due to the low masses and performance losses, the comparably compact size and the manageable re-entry loads during its flight back to the earth. Since a winged reusable stage was already operational in the past and expertise and know-how was already gained in returning such stages, the focus clearly has to be set on investigating the In-Air-Capturing method and developing the technology that will enable its use for a future possible European launch vehicle.

5 Economic Analysis

Economic viability and the possibility to decrease the launch costs is the main rational behind reusability. Hence, the consideration of these costs is of great importance to determine feasible and economically viable RLV designs. However, determining these costs is difficult due to a lot of uncertainties and the unavailability of reliable cost data.

The costs of a launch vehicle can be expressed in two different cost types: *recurring* and *non-recurring costs.* In launcher development, the *non-recurring costs* include the **development costs** of the launch vehicle. This includes the costs for the system development and all tests and experiments including prototypes and the first flight unit (theoretical first unit = TFU). *Recurring costs* include **production and manufacturing costs** and **operational costs** including ground operations, mission control, preflight operations and post-flight operations. For a reusable launch vehicle **recovery** and **refurbishment costs** are added.

Figure 5-1 shows the cost breakdown for a typical launch vehicle according to the TransCost model which was used to determine costs within this project [18]. The costs added by reusability are considered as well. The operations costs can be further divided into direct operational costs (DOCs), indirect operations cost (IOC) and refurbishment and spares cost (RSC). The direct costs include all costs linked directly to the operation of the vehicle such as materials, propellant, labor and fees. Indirect costs which include so-called overhead costs refer to the costs that are not directly related to the operation of the vehicle such as facility and management costs, administration and all support activities.

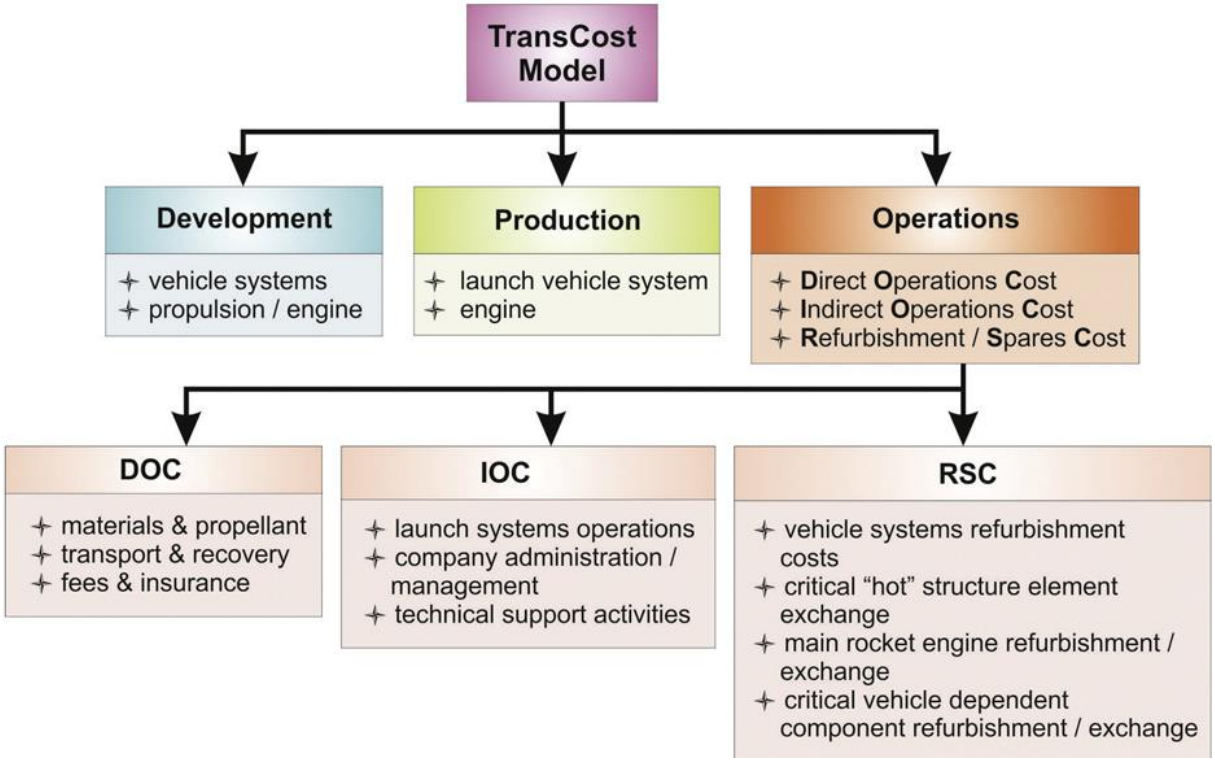

Figure 5-1: Launch Vehicle Cost Breakdown according to the TransCost model [18]

The TransCost model uses a so-called "top-down" approach to estimate the respective costs as depicted in Figure 5-1. This means that the costs are evaluated on a very high system level based on cost estimation relationships (CERs) which are statistically derived values based on actual cost data of historical or operational launchers. Estimating the cost of expendable launchers is a sufficiently validated with this cost model. However, using this model to determine reusable vehicles' launch costs is difficult and unreliable since the model requires a sufficiently large database of RLV's cost data. Up to date there are only two reusable launch vehicles that are or were used to deliver payload to orbit: the Space Shuttle or STS and the Falcon 9 of SpaceX. Whereas the cost data of the Space Shuttle is

available it doesn't serve as a good database for the estimation of the cost of winged vehicles due to the fact that the Space Shuttle program turned out to be costlier than hoped for. On the other hand, the Falcon 9 launcher is a rather cheap launch vehicle but cost data is unavailable to the public.

Hence, in this report an alternative model to determine all cost related to recovery is presented in the section 5.1. Instead of a "top-down" approach, a "bottom-up" approach was chosen to determine these costs. This approach will be explained in the following section and results for all considered recovery methods will be presented. The estimation of total launch costs was performed using the in-house derived cost model from section 5.1 and an adapted form of the TransCost model which will be explained in section 5.2. However, this report does not include the final results of this analysis which shall be added in a later report.

It is important to note that this report includes a very generic and, at the time being, very academic approach to model the launch costs of any vehicles. The reference mission of the fullscale IAC maneuver, which features an A 340-600 and the reference stage presented in chapter 6, will be briefly described and costs will be presented. However, more reliable costs should be presented in a subsequent report including more detailed cost models.

This report is divided into two parts: first, the costs for a heavy-launch vehicle (Ariane 5/6 class) are evaluated in section 5.1 and section 5.2. Originally, the In-Air-Capturing technology was planned for such launchers. In the recent years however, the smallsat market has experienced quite a boom and a lot of private companies are now en route to develop small-sat launch vehicles. The most popular companies are Rocketlab with their Electron launch vehicle, Virgin Orbit with the Launcher 1 launch vehicle, Bloostar and Firefly. For smaller launch vehicles, reusability usually requires the refurbishment costs to be very low since the production and manufacturing costs compared to the overhead costs are much lower [18]. Furthermore, the small-sat launch vehicle market is expected to be saturated once two or three competitors enter the market with an operational vehicle. Hence, the focus in Europe of the public space agencies should be to focus on a heavy lift launch vehicle.

Nevertheless, a preliminary analysis of the costs of such a small-sat launch system with IAC are included in this report to at least show some of the challenges and to determine if it would be economically viable at all. This analysis is shown in section 5.3.

5.1 Recovery Costs

Contrary to an expendable launch vehicle, any reusable launch vehicle requires hardware and additional personnel to recover or land the stage. The acquisition, maintenance and operation of the hardware and the additional personnel lead to additional costs which are added by the recovery strategy itself. In the following sections, the main differences between the four recovery methods, RTLS, DRL, LFBB and IAC shall be explained and the cost model to calculate the IAC costs is described in detail. This model used for the calculation of the respective costs was established in-house and the in-depth explanation of all and assumptions can be found in [19]. Details about the cost modelling of the remaining methods (Downrange Landing, LFBB, RTLS) can be also found in that report.

For all labor-related costs the values provided in Table 5-1 and Table 5-2 were used. *It is important to note that all costs for all presented calculations and models refer to the economic conditions in 2018 if not specified otherwise.*

Table 5-1: Wages for different professions in USA, 2017. $/h are based on 2080 workhours per year. From U.S. Department of Labor Bureau of Labor Statistic, www.bls.gov

Profession	$/h	$/yr
Aerospace Engineers	55.02	114450
Aerospace Engineering and Operations Technicians	32.66	67940
Aircraft Mechanics and Service Technicians	30.57	63590
Aircraft structure, surfaces, rigging, and systems assemblers	26.96	56070
Aircraft Cargo Handling Supervisors	27.66	57530
Airline Pilots Copilots and Flight Engineers	69.24	144010
Aircraft Pilots and Flight Engineers	54.56	113480
Captains, Mates and Pilots of Water Vessels	26.45	55010
Tank Car, Truck and Ship Loaders	20.82	43300

Table 5-2: Labour Costs (LC) for professions considered in FY2018, based on Table 5-1.

Profession	Wages $/wh	Cost $/wh	Workyear Cost $/wyr
Aerospace Engineers	56.37	174.04	362001
Aircraft Maintenance and Cargo Handling	30.18	93.19	193824
Launcher Maintenance	35.42	109.36	227468
Captains, Mates and Pilots of Water Vessels	27.09	54.19	112707
Transport Loadings and Trailer	21.33	42.65	88715

5.1.1 In-Air-Capturing Cost Model and Assumptions

This section analyses the costs associated to the IAC recovery mode. First, the aircraft mission is defined and the performance analyzed to calculate duration and fuel during a typical IAC mission. The performance results are the input to the cost model in terms of flying time and fuel consumption.

5.1.1.1 Aircraft and Flight Performance

The objective of the flight performance model is to provide values of the IAC operation factors affecting the cost model by a preliminary approximation of the total aircraft mission and towing performance. Large passenger aircrafts are considered due to their availability, flexibility and large propulsion capabilities, suitable for towing a first stage. The following sections describe in detail the models used. The aircrafts analyzed are the B747-400 (as the acquired model by Virgin Orbit for air-launches), the B747-8F, A330-800NEO, the A380-800 and the A 340. The aircraft and engine characteristics are obtained from the manufacturer websites [19] . These are given in Table 5-3.

Figure 5-2: Commercial Aircraft that could be used for In-Air-Capturing: B747-400 (top left) and A340-600 (top right)

Table 5-3: Aircraft Characteristics

Aircrafts	B747-400	B747-8F	A330-800	A380-800
$Maximum\ Takeoff\ Weight$	396.89	447.7	251	575
$Operational\ Empty\ Weight$	163.7	197.13	176	277
$m_{MFW}(t)$	163.48	180.89	111.27	258.84
$S_{ac}\ (m^2)$	525	554	362	845
CD_0	0.025	0.028	0.026	0.012
K	0.0435	0.0408	0.0344	0.0456
M_{crit}	0.83	0.83	0.83	0.83
$\left(\frac{L}{D}\right)_{max}$	17.2	17.2	16.7	19.36
$\left(\frac{L}{D}\right)_{cr}$	14.9	14.9	14.5	16.8

The flight mission for the aircraft for the stage retrieval operation can be considered similar to a classical military drop and go mission but in reverse. Figure 5-3 shows the typical mission profile for a considered IAC mission with all phases that were considered. To analyze the fuel consumed during the mission, some predefined mass fractions based on typical large aircraft values as mentioned in [19] are used. The same is performed for the total time for each flying phase. The mass fraction is defined as the fraction of the stage weight before (m_i) and after (m_{i+1}) a given phase, as

$$\lambda_{i+1,i} = \frac{m_i}{m_{i+1}} \tag{5-1}$$

For this flight, the large aircrafts considered have enough fuel capacity to complete the mission. Therefore, it is assumed that the aircraft is not fully loaded (to realistically increase its performance capabilities).

The calculation of the fuel consumption for standard phases such as taxi and takeoff are calculated using standard parameters (compare Table 5-4). The first cruising phase to the IAC site is computed with the assumed reference aircraft cruise speed and L/D in cruise. In addition, a nominal distance from the take-off site to the IAC site of R is considered (in reality, the distance traveled during cruise would be lower as a consequence of the ascent phase). The mass fraction is then computed using the Breguet range equation as follows from equation (5-2

$$\lambda_{3,2} = e^{-\frac{R*SFC(h_{cr},V_{cr})}{V_{cr}*\left(\frac{L}{D}\right)_{cr}}} \tag{5-2}$$

The loiter phase is computed with a modified Breguet equation, and assuming that the aircraft would loiter at approximately 600 km/h and at an altitude of 8 km for a predefined time window E_{window} as

$$\lambda_{4,3} = e^{-\frac{E_{window} * SFC(h_{lo}, V_{lo})}{\left(\frac{L}{D}\right)_{max}}} \tag{5-3}$$

Note that in reality, the maximum endurance condition would also depend on the SFC consumption, and therefore it would not correspond to the maximum L/D condition. The returning cruise phase, in the towing configuration, is calculated by using the adapted performance of the towing aircraft in combination with the RLV stage. Once the stage is released, additional phases are considered to account for the reserve fuel:

- Mission phase 8-9: A loiter wait of possibly 45 minutes to account for any probable runway issue with the stage. Same altitude and speed as during the launch window loiter
- Mission phase 10-11: A trip to an alternative landing site at a distance of 300 km (to be conservative, although Cayenne airport is at around 80 km). This is assumed already after descent, with a non-optimal polar with a $\frac{L}{D} = 9$ at a speed of 360 km/h

In addition, 5% of unused trapped fuel is considered. The total consumed fuel, reserve fuel, and trapped fuel are computed as

$$m_f^{cons} = m_f^{01} + m_f^{12} + m_f^{23} + m_f^{34} + m_f^{45} + m_f^{56} + m_f^{89} + m_f^{1011} \tag{5-4}$$

$$m_f^{res} = m_f^{67} + m_f^{910} \tag{5-5}$$

$$m_f^{trap} = 0.05 * m_f^{load} \tag{5-6}$$

$$m^{total} = m_f^{cons} + m_f^{res} + m_f^{trap} \tag{5-7}$$

Table 5-4: Mission profile computation summary

Mission Phase	Identifier	Time	Fuel Fraction λ
Start-up, Taxi and Take-Off	0-1	30 mins	0.97
Ascent	1-2	10 mins	0.985
Cruise to IAC Site	2-3	R/V_{cr}	Breguet
Launch Window Loiter	3-4	3 hours	Breguet
IAC Maneuver*	4-5	~2 mins max.	0
Cruise to Recovery Site*	5-6	Calculated with performance model	
Release Maneuver*	6-7	0	0
Loiter Wait**	7-8	45 mins	Breguet
Aircraft Descent	8-9	10 mins	0.995
Trip to Alternative Landing Site**	9-10	50 mins	Breguet
Aircraft Landing	10-11	5 mins	0.995
Stage Glide	sg	Depending on stage L/D	-

Stage Landing	sland	1 min	-
Additional			+5% trapped fuel

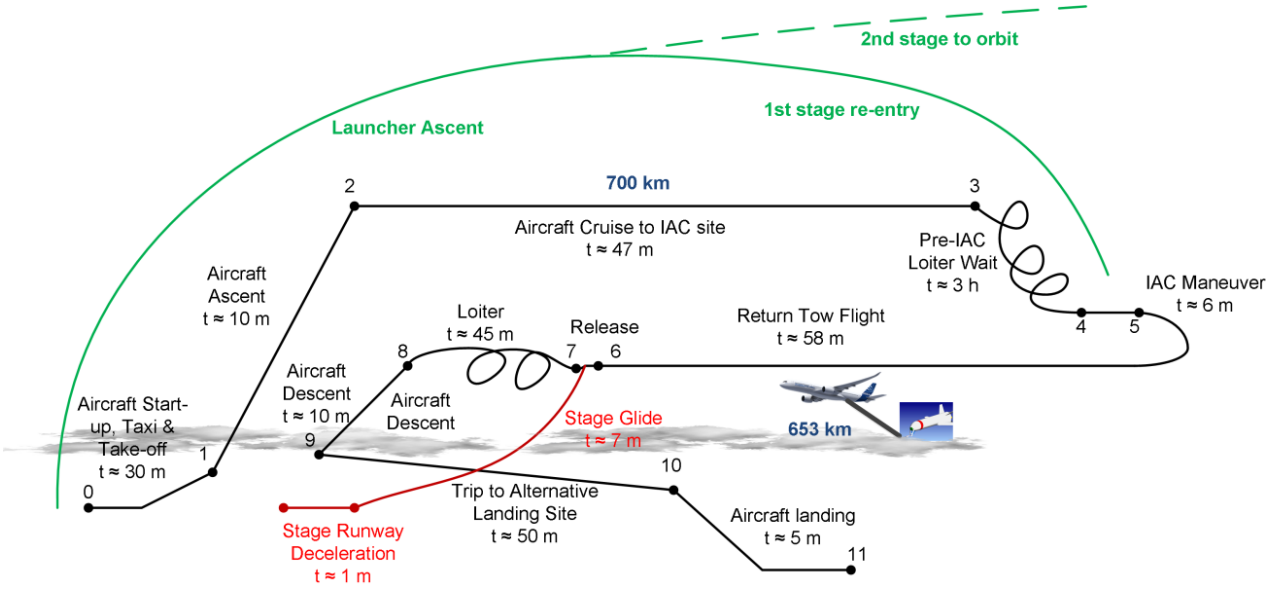

Figure 5-3: IAC Mission Profile

The towing performance is computed using the in-house established performance calculation routine. A stable equilibrium flight is assumed throughout the computation, with negligible angle of attack for the aircraft and thrust angle to separate the lift and drag equations. In addition, it is assumed that the stage and aircraft balance their own weight, respectively.

First, the maximum ceiling altitude is computed. The towing altitude is selected by assuming a 5% lower altitude than the maximum, and selecting the available Flight Level immediately bellow it. The cruising speed is then selected by computing the maximum range cruise (MRC) speed V_{MRC}, by taking into account both the stage and aircraft drag.

Given the towing altitude, also the range the stage flies once released is estimated by assuming it flies near its maximum range (maximum lift to drag) configuration (although this is not necessarily the optimum profile if the stage is released at a different speed). Then, assuming no dependency of the stage maximum lift to drag on altitude (it does change as a consequence of the Mach dependency) and small flight path angles, the maximum range flown can be obtained and based on the Breguet equation the fuel consumption for the towback flight can be calculated.

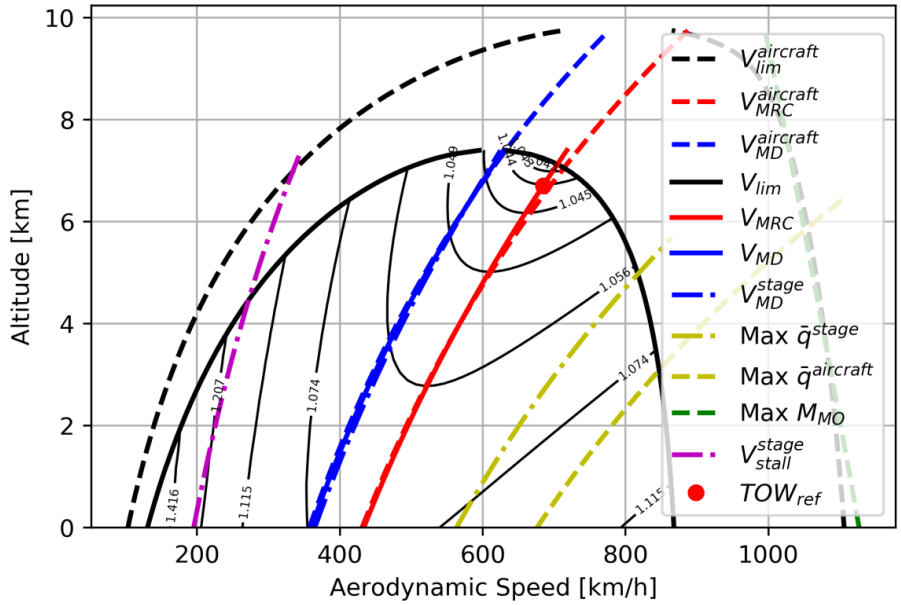

Figure 5-4: Exemplary Towing Performance Estimation for the B747-400

5.1.1.2 Aircraft Costs Estimation

Aircraft Direct Operating Costs (DOC) are directly related the flying costs of a particular aircraft mission and type. Aircraft costs are data sensitive and usually confidential for aircraft operators, but there exist some estimation methods which could be used to provide rough orders of magnitude. Also, commercially published data such as the Aircraft Cost & Performance Reports CAB reports could be consulted (used by Aviation Week in their annual reports) [19].

This section will describe the cost models available to estimate aircraft Direct Operating Costs (DOC) and the adaptations implemented for this analysis. First, a discussion on acquisition costs and listed prices is presented. Then, the modeling of other ownership costs and cash costs is explained in the following sections and finally a discussion on the cost model limitations is presented.

Direct Operating Cost (DOC) estimation varies considerably per airline. Factors affecting it include the airline financial model, crew salaries, and aircraft operating conditions. Maintenance costs, for example, are heavily dependent on historical data, which could be dependent on specific airline operations and are thus confidential. Nevertheless, a first-order-of-magnitude estimation is important for preliminary aircraft design studies to quantify the effects of some design decision on the final costs and evaluate the attractiveness of different models. Therefore, the literature contains some DOC models based on parametric Cost Estimating Relationships (CERs) for fast analysis.

One of the first DOC model available for turbine powered airplanes was the Air Transport Association (ATA) method based on statistical data [19]. This model included, depreciation, insurance, crew, fuel and maintenance costs as DOCs, but does not consider navigation and landing fees and interest rates due to the different industry conditions at the time. In a NASA contractor report interest rates were included, as well as navigation and landing fees, which are based on the operating costs of McDoneell Douglas and Boeing Commercial Airplane Group aircrafts in service until 1993. Roskam adapted the ATA method for applicability to any aircraft type. The method used is based on the Liebeck method, adapted with some specific corrections. For further details the reader can consult the DLR report on modeling recovery costs [19].

5.1.1.2.1 Acquisition and Listed Prices

The IAC method requires a commercial aircraft to be bought and modified so it is able to perform the tasks according to the requirements. Hence, a second-hand or used commercial aircraft should be used for this task since only a few flights per year are necessary and acquiring a new-constructed

aircraft would lead to high costs. Aircraft delivery price can vary considerably depending on the state of the aircraft, the market situation of second-hand aircraft of that type and the age and launch year of the respective aircraft type. It has to be noted that, although old aircraft will have a lower acquisition cost, their maintenance costs could increase considerably and they could suffer from performance degradations.

The listed prices for newly build aircraft differ highly from the second-hand prices. Table 5-5 shows some acquisition values for different aircraft comparing the prices of newly build aircraft with some second-hand selling values found in some broker websites. For the Boeing B747 there is a huge second-hand market due to the fact that the first B747 was produced in 1969 and over 1500 aircraft were produced since then. This leads to quite low prices on the second-hand market starting from 16 M US$ (as of 2018 economic conditions). The A340 acquisition prices range from 9 M$ to 110 M$ thus making it also a viable option for the towing aircraft. The A380 prices are too high to consider it for In-Air-Capturing.

Table 5-5: Aircraft acquisition costs in FY2018 $

Aircrafts	Listed Price*	Secondhand Selling Price**
B747-400	306 M$	16 M$ for a 27 year old B747-400 with 66000 flying hours[1] 28 M$ for a 11 year old B747-400 in 2010. Now would be around 32 M$
B747-8F	403 M$	
A330-800	260 M$	27 $M for a 17 year old A330 with 58000 flying hours[2]
A380-800	446 M$	205 M$
A340-600	307 M$	9 M$ for a 22 year old A340-600 with 46000 flying hours[3]. 35 M$, unknown conditions[4] 110 M$ for a 13 year old A340-500 with VIP Package and 42000 flying hours[5]

5.1.1.2.2 Aircraft Upgrades and Modifications

As of the beginning of the FALCon project, in March 2020, the reference IAC mission featured an unmanned, remote-controlled aircraft. Since there is no comparably scaled aircraft currently operated as such a system on the world, the costs and the administrative effort to convert a manned to a remote-controlled unmanned aircraft is a major uncertainty within the project. Nevertheless, at the current status of the project a contact to Airbus was established to discuss the changes that would be

[1] 1992 BOEING 747-400 For Sale In Monterey, California. Controller. [Available at www.controller.com, 12.03.2019]
[2] 2002 AIRBUS A330 For Sale In Monterey, California. Controller. [Available at www.controller.com, 12.03.2019]
[3] 1997 AIRBUS A340 For Sale In Monterey, California. Controller. [Available at www.controller.com, 12.03.2019]
[4] AIRBUS A340. Trade-A-Plane. [Available at www.trade-a-plane.com, 12.03.2019]
[5] 2006 AIRBUS A340 For Sale In BOURNEMOUTH, DORSET United Kingdom. Controller. [Available at www.controller.com, 12.03.2019]

necessary to the current reference aircraft, the A340-600 [26]. In this discussion, the Airbus representative recommended to only fly the aircraft manned, since anything else would require major modifications to the aircraft.

In the case of the aircraft being manned, the IAC procedure still would be performed automatically by switching from guided/piloted flight to IAC autopilot during the actual IAC maneuver. This would require systems similar to any standard autopilot system where the additional effort would have to be spent towards adapting the sophisticated control algorithms for the IAC maneuver and integrating the necessary hardware which would be:

- Communication hardware (LiDAR, GNSS, Radar…)
- ACCD
- Towing Rope
- Optional: Additional drag surfaces

To estimate the cost of including the aerodynamically controlled capturing device, the cost to upgrade an aircraft to be able to do In-Air Refueling was used. The ACCD could be analogous to Multi-Port Refueling Systems (MPRS) used for aerial refueling operations, although it would require a stronger rope device to be able to tow the stage. In this report it is estimated that the cost to adapt a KC-135 aircraft to accept an MPRS could be of roughly 5.1 M$ in FY2004, or 6.8 M$ in FY2018 according to the values found in [19]. The ACCD could be housed in the central landing gear shaft of the A340-600 aircraft. Airbus recommended to remove the central landing gear for the IAC aircraft in FALCon since the GLOM of the aircraft would be well below its design limits.

In addition to the ACCD system, the aircraft would require specific structural reinforcements to be able to cope with the additional forces at the ACCD attachment point. There is another case in the literature of an airplane which required heavy structural modifications. The SOFIA flying observatory was incorporated in a Boeing 747SP by modifying the structure. A hole was cut in the fuselage and a pressure bulkhead was added to accommodate the telescope. No cost estimate was found in the literature, although DLR participated in the mission and could be consulted. Nevertheless, this modification is considered to be excessive. A closer analogy could be the costs associated to converting a passenger B747 aircraft to a cargo aircraft. In [19], it was estimated that this could cost 14.3 M$ in FY1982, or 37.1 M$ in FY2018. These costs are summarized in Table 5-6. Additionally, it looks like for the A340-600, the structural reinforcement could be marginally due to the fact that the rope would be attached close to the CoG position where the structure is rather strong anyways. However, any definitive answer would require more precise analysis. The contact with Airbus will hopefully give more answers as the project continues.

Table 5-6: Aircraft upgrade and modification cost analogies

Upgrade	Purpose and Reasoning	Cost
MPRS modification	To adapt a KC-135 for refueling operations. Similar to adding the ACCD system. The costs associated to stricter rope reinforcements for towing are assumed to be factored out by not requiring an internal piping system for fuel	Based on 5.1 M$ (2004) or 6.8 M$ in 2018
Passenger to Cargo Structural Modifications	Structural reinforcements to convert a B747 from passenger aircraft to cargo aircraft	Based on 14.3 M$ (1982) or 37.1 M$ in 2018
Total Considered		43.9 M$ in FY2018

5.1.1.2.3 Aircraft Ownership Costs/Indirect Costs

These costs are not directly linked to the aircraft flight, but to an overhead on the flight. They are estimated as the sum of the depreciation costs, the interest costs and the insurance costs as shown in

$$C_{OWN} = C_{DEP} + C_{INT} + C_{INS} \tag{5-8}$$

The depreciation of the physical asset can be estimated with the total aircraft value C_{VAL}, computed by adding the acquisition costs C_{ACQ} with the upgrades/modifications C_{UP} as in

$$C_{VAL} = C_{ACQ} + C_{UP} \tag{5-9}$$

In addition to this total value, some spares have to be accounted for in the model, both for the engine and the airframe. The costs C_S for this spares is assumed as a percentage of the total airframe and engine costs as follows

$$C_S = k_{S,AF} C_{AF} + k_{S,ENG} C_{ENG} \tag{5-10}$$

For the percentages, the values used in Liebeck/NASA [20] are used, of $k_{S,AF} = 6\%$ and $k_{S,ENG} = 23\%$. The total asset values can then be computed as

$$C_{TOT} = C_{VAL} + C_S \tag{5-11}$$

A useful life (n_{DEP}) of 15 years is assumed which is the average useful life of some B747s in the American airline industry. Since the number of flights for an IAC aircraft is much lower than for a commercial airliner this is considered an adequate starting point. The aircraft residual value (R_{DEP}) is assumed as 10% as is generally done in aircraft studies.

$$C_{DEP}^{yr} = \frac{C_{VAL}(1 - R_{DEP}) + C_S}{n_{DEP}} \tag{5-12}$$

Interest rates are strongly dependent on the world economic climate, local exchange rates, credit standing, off-set agreements and other difficult to quantify factors. Therefore, these factors are ignored by many models although it's a big contributor to costs. In Liebeck/NASA [20], a 15 year loan period with two payments per month was assumed, with an 8% interest rate. It also assumes 100% financing from external sources. Nevertheless, it was impossible to validate this with their case studies (results were over predicting by more than 60%), and it is unknown which interest rate model they were using in the study. Therefore, the model explained in [19] is used, assuming no relative residual value of outside capital remaining in the company. The adapted equation is then given as:

$$C_{DEP}^{yr} = k_{AVR} * k_{FINANCED} * C_{TOT} \tag{5-13}$$

With k_{AVR}given as

$$k_{AVR} = \frac{\frac{((1 + k_{INT})^{n_{DEP} * n_{PPY}} * k_{INT} * n_{DEP} * n_{PPY})}{(1 + k_{INT})^{n_{DEP} * n_{PPY}} - 1} - 1}{n_{DEP}} \tag{5-14}$$

Here, k_{INT} is the interest rate considered and n_{PPY} being the number of payments per year (the higher, the higher the average interest rates). It is recommended to use the national interest rate for these computations. Checking the European Central Bank interest rate, a value of zero is observed (recent effort to revive the economy). Nevertheless, the highest interest rate was of 4.75%, which was used in this analysis as a conservative estimate.

Insurance rates are directly proportional to the involved risks and potential claims given an aircraft loss. For the case of an IAC aircraft, although the failure probability could be considerably high as compared to commercial aircraft operations, the loss potential is much lower, as there are no passengers on-board and the operations is mainly performed in open seas. Different methods specify different insurance rates as shown in [19]. The low insurance rate of 0.35% from [19] is used in the following equation

$$C_{INS}^{yr} = k_{INS} * C_{ACQ} \quad (5\text{-}15)$$

where k_{INS} is the insurance rate. However, insurance for such aircraft is as of today uncharted terrain and it is difficult to predict how any insurance offer and finance plan would look like.

5.1.1.2.4 Direct Cash Costs

Cash costs, or trip costs, are those that depend directly on the operating mode of the aircraft. These operations are defined by the towing phase and the launching interface, by accounting for holding patterns due to launch window delays, and other possible issues. This mission profile is discussed in the previous section 0. These costs are obtained as shown in equation (5-16) where C_{FUEL} are the fuel costs, C_{CREW} are crew costs, C_{MAN} are maintenance costs, C_{NAV} are navigational costs and C_{LAND} are landing fees.

$$C_{CASH} = C_{FUEL} + C_{CREW} + C_{MAN} + C_{NAV} + C_{LAND} \quad (5\text{-}16)$$

Fuel costs account for the majority of the DOCs in commercial applications, explaining the huge dependency of the aircraft industry on the oil market. This market has shown excessive variations in the past 20 years (50-350%) and is now expected to increase as a consequence of carbon pricing forecasts making it difficult to obtain a reasonable estimate. Rates of 2 $/gallon could apply in this future carbon pricing framework of 200 $ per equivalent CO2 emitted, doubling current jet fuel prices unless biofuels are used. Nevertheless, for the low launch rates considered, fuel accounts for a small part (around 5%) of the total DOCs, and therefore its variations become less important for the analysis. For the reference mission, a value of 707.59 $/t is considered, based on the average jet fuel price of 90$/barrel in 2018[6] and a kerosene density of 800 kg/m^3. The cost is then computed with the total aircraft fuel loaded $m_{f,load}$, in metric tons, for the mission.

$$C_{FUEL}^{l} = 707.59 \frac{\$}{\text{t}} * m_{f,load} \quad (5\text{-}17)$$

In this analysis, no crew was considered. The whole operation should be semi-autonomous/remote to increase the safety and reduce crew requirements and costs. Therefore, remote operators in the mission control center would oversee the operation, directly controlling the combined flight of both vehicles. Aerospace labor rates as shown in Table 5-1 and Table 5-2 based on TRANSCOSTS work-year costs are assumed applicable. Although a single operator could control a fleet of Unmanned Autonomous Vehicles (UAV) it is considered that a team of 6 aerospace engineers (in mission control and for support) would be responsible for the operations. When the towing phase is taking place, it is assumed that 14 additional engineers in mission control are also working in the operation. This is based on the FESTIP studies [25]. Therefore, based on 2018 labor cost values, the following equation is used

$$C_{CREW}^{l} = 174 \frac{\$}{wh} * t_B * n_{OPERATORS} \quad (5\text{-}18)$$

An extra (or more) back-up pilot might also be necessary in case of a necessary switch to manual remote control. This is currently not considered in the model, although it could be easily included, although it is would be necessary to know if the pilot would be fully dedicated to this task through the year or would be hired occasionally when launches are required.

Maintenance costs typically account for 10-20% of the DOCs of an aircraft under business as usual airline operations. These costs are divided traditionally in scheduled and unscheduled maintenance costs, with the later one being the highest as a consequence of the unexpected appearance, resulting aircraft downtime, facility and spare costs, etc. In addition, it is highly dependent on ageing. Scheduled maintenance costs, on the other hand, are divided into different work packages which are the A-Checks, B-Checks, C-Checks and D-Checks. The first one involves daily visual inspections of different

[6] [Available at www.iata.org, 13.03.2019]

aircraft subsystems such as fluid levels and tires, whereas the later one is performed every 6 to 12 years, with duration of approximately a month, and involves a major aircraft overhaul with detailed structural and hydraulic inspections. Considering the low number of flights per year and the cost of a D-Check it should be discussed if an IAC aircraft should not just be dispensed and replaced by a new (second-hand) aircraft once a D-Check is about to take place.

In this preliminary model, the total maintenance costs per launch are estimated based on [19] as follows, where AF stands for airframe and E for engines.

$$C_{MAN} = C_{MAN,AF} + C_{MAN,E} \tag{5-19}$$

These airframe and engine components have a direct cost of labor (C_{LC}), material (C_{MAT}) and overhead/burden (C_{BRD}) components, estimated as follows

$$C_{MAN} = C_{LC} + C_{MAT} + C_{BRD} \tag{5-20}$$

The labor costs are based on direct labor costs/wages (LC^{wages}) for the aircraft maintenance and cargo handling workers, without overhead. In the Liebeck/NASA [20] methodology, the overhead costs are assumed to be two times the direct labor costs. This is similar to the value of 3 used to estimate the labor costs for the aerospace industry based on average labor wages, as shown in Table 5-1.

In addition, the airframe labor costs have a per flight hour $C_{MAN,AF,LC/FH}$ and per flight cycle $C_{MAN,AF,LC/FC}$ components. These are estimated as follows

$$C_{AF,\frac{LC}{FH}} = LC^{wages} * C_{AF,\frac{WH}{FH}} \tag{5-21}$$

$$C_{AF,\frac{LC}{FC}} = LC^{wages} * C_{AF,\frac{WH}{FC}} \tag{5-22}$$

$$C_{AF,LC} = C_{AF,\frac{LC}{FH}} * t_b + C_{AF,\frac{LC}{FC}} \tag{5-23}$$

With

$$C_{AF,\frac{WH}{FH}} = 1.26 + 1.774 * \left(m_{AF} * \frac{f_{kg}^{pm}}{10^5}\right) - 0.1071 * \left(m_{AF} * \frac{f_{kg}^{pm}}{10^5}\right)^2 \tag{5-24}$$

$$C_{AF,\frac{WH}{FC}} = 1.614 + 0.7227 * \left(m_{AF} * \frac{f_{kg}^{pm}}{10^5}\right) + 0.1024 * \left(m_{AF} * \frac{f_{kg}^{pm}}{10^5}\right)^2 \tag{5-25}$$

The same applies for the material costs, estimated directly in FY1993 dollars as follows

$$C_{AF,MAT} = C_{AF,\frac{MAT}{FH}} * t_b + C_{AF,\frac{MAT}{FC}} \tag{5-26}$$

$$C_{AF,\frac{MAT}{FH}} = \left(12.39 + 29.8 * \left(m_{AF} * \frac{f_{kg}^{pm}}{10^5}\right) + 0.1806 * \left(m_{AF} * \frac{f_{kg}^{pm}}{10^5}\right)^2\right) * D_{1993}^{2018} \tag{5-27}$$

$$C_{AF,\frac{MAT}{FC}} = \left(15.2 + 97.33 * \left(m_{AF} * \frac{f_{kg}^{pm}}{10^5}\right) - 2.862 * \left(m_{AF} * \frac{f_{kg}^{pm}}{10^5}\right)^2\right) * D_{1993}^{2018} \tag{5-28}$$

The airframe mass is estimated in a similar way to its cost, using the aircraft OEW as

$$m_{AF} = m_{OEW} - n_{ENG} * m_{ENG} \tag{5-29}$$

The engine maintenance costs in the Liebeck/NASA model [20] have only a per flight hour component. Nevertheless, for detailed estimations, workhour values from the engine manufacturer could be used. For this preliminary analysis, these costs can be estimated from historical figures in the airline industry as follows [19]

$$C_{ENG,LC} = C_{ENG,\frac{WH}{FH}} * L^{wages} * t_b * n_{ENG} \quad (5\text{-}30)$$

$$C_{ENG,\frac{WH}{FH}} = \left(0.645 + 0.05 * T_{ENG} * \frac{f_N^{pf}}{10^4}\right) * \left(0.566 + \frac{0.434}{t_B}\right) \quad (5\text{-}31)$$

The engine material costs are also based on the aircraft flight hours and are computed with the following equation

$$C_{ENG,MAT} = \left(25 + 0.05 * T_{ENG} * \frac{f_N^{pf}}{10^4}\right) * \left(0.62 + \frac{0.38}{t_B}\right) * t_b * n_{ENG} * D_{1993}^{2018} \quad (5\text{-}32)$$

Nevertheless, it is unclear if the unscheduled maintenance costs are also included in the engine and airframe maintenance relationships. Nevertheless, it is assumed that it is, as the costs were based on historical data of airline year expenditure on maintenance tasks.

In Liebeck/NASA methodology, the navigation fee only applies for international flights, although it is unknown if this also applies currently to national flights. Nevertheless, as the flight could enter international waters, it is assumed that it also applies in this case. The estimation is based on the MTOW and on the first 500 nautical miles. The CER is given as follows

$$C_{NAV} = 0.136 * 500 * \sqrt{\left(m_{MTOW} * \frac{f_{kg}^{pm}}{10^3}\right)} \quad (5\text{-}33)$$

Landing fees are also modeled with the following CER from [19] for international flights.

$$C_{LAND} = 4.25 * m_{MTOW} * \frac{f_{kg}^{pm}}{10^3} \quad (5\text{-}34)$$

It is assumed that the landing and ground handling costs apply also if the airport is operated by the same launch provider, as an effort for aircraft ground handling operations and landing site maintenance per launch.

5.1.1.2.5 Limitations Cost Model

There are some factors that are not accounted by the cost model, such as aircraft availability, maintenance hour's dependency on aircraft age or cumulated flight hours, and maintenance dependency on operation conditions

The first factor is not considered to be limiting for this analysis as a consequence of the low launch rates compared with airline operations, providing the possibility to schedule maintenance accordingly with launch planning. Nevertheless, some maintenance intensive aircraft could have availability values of 70%. Combining this with the risks of unscheduled maintenance operations (which account for about 50-70% of the total direct maintenance costs, and can take between 10-25% of the total time spent on maintenance[7]) could put an additional requirement on 1 or 2 extra aircrafts for redundancy, increasing ownership costs.

The second factor would penalize older aircraft. Nevertheless, maintenance costs predicted are around 15% of the cash costs which in turn are a lower fraction of the direct operation costs, which are highly driven by the ownership costs as a consequence of low aircraft utilization. Therefore, this factor

[7] Brian Whitehead, Quora. [Available at https://www.quora.com/What-would-be-the-portion-of-unscheduled-maintenance-cost-in-the-overall-maintenance-cost-of-aircraft,08.04.2019]

is not considered significant for the analysis. Nonetheless, when acquiring the aircraft, age should be considered in a trade off with the acquisition costs considering also major maintenance checks and expected overhauling.

The last factor could be important as a consequence of the higher thrust required and the possible structural wear caused during towing. The higher thrust requirement, as a consequence of a heavier reinforced B747 requiring more thrust and leading to higher engine wear, was accounted for by adding a 2% increase in maintenance labor hours per year.

5.1.1.2.6 Indirect and Other Further Ownership Costs

This section describes the IOC and other ownership costs related to the IAC recovery operations, including vehicles and facilities.

In addition to the acquired aircraft, a new landing strip would be necessary in Kourou to reduce transportation costs and risk associated to transporting the stage from the Feliy Eboue International Airport, Cayenne, at 75 km from the launch facility. Furthermore, this would reduce potential risk associated to operating the returning stage near residential areas and in a commercial airport. The costs from this type of facility can vary considerably. For example, the Orbiter Landing Facility used for the Space Shuttle, with a 4.5 km length runway and 90 meters wide, with a price tag of 22 $M dollars in 1975, could now cost around 102 $M dollars (2018). On the other hand, the industrial commercial airport of Teruel, Spain, with a 2.8 km length runway and 45 meters wide, used for large aircraft maintenance operations and storage, cost around 59.2 M$ in 2011. Other small private airports of 2 km of runway length could cost around 15 M$, based on some USA airports for sale in 2019[8], such as the Griffin-Spalding County Airport in Georgia.

Irrespectively of the price, it is assumed that this cost would be provided by Arianespace, ESA, or other governmental agencies, since the airport would also be suitable for payload processing, which currently arrives to Cayenne via airplane and then travels 75 km by road or to the Paricabo docking area by ship taking longer time. Therefore, the airport landing fee estimation used in Section 5.1.1.2 is assumed enough, although it is probable that the launch site user fee (currently around 1 M$ per launch + 4 M$ of fixed costs per year) would increase as a consequence of the use of these installations. Nevertheless, a key issue for cost saving strategies here would be to regulate spaceport fees in a similar way as commercial airports.

Regarding vehicles for operations, once the stage has landed and arrived to a waiting position, a recovery convoy is deployed to service and examine the recovered vehicle and prepare it for towing operations to the Stage Processing Facility. For the Space Shuttle, more than 25 vehicles were required to conduct all the safety operations. Based on the Space Shuttle recovery convoy, the following additional vehicles are considered necessary.

The safety operations considered are based on the ones performed for the Space Shuttle post-landing operations. In this later case, the safety operations took approximately 2 hours after the stage landed with 2 hours of team preparation and purge system chill down before the actual landing. It has to be noted that for the Space Shuttle, these were hazards associated to hypergolic and toxic propellant used for the Attitude and Orbit Control System, which are not considered for this analysis, as well as astronauts on-board which required medical evaluation and had to deboard safely. This also explains the required team of approximately 150 trained personal. A reduced team is assumed, based also on observed SpaceX employees working on the stage securing operations after landing. For the 2-hour preparation before the mission, it was assumed that each worker would perform one task to be conservative, and the minimum between the assumed maximum of 46 employees and the total number of workers is used.

Firstly, an initial atmosphere check looking for possible fuel/oxidizers in the surroundings takes place, taking approximately 15 minutes. Once done, the recovery convoy and personal can approach the

[8] [Available at https://www.loopnet.com/,11.03.2019]

vehicle and conduct the propellant and pressurant purging and draining operations, taking approximately 50 minutes as for the Space Shuttle. The vehicle is then prepared for towing by positioning the taxi vehicle in the front wheel while control surfaces and the landing gear are locked. This operation can take approximately 30 minutes. These activities are listed in Table 5-7

Table 5-7: IAC Safety Activities

Activity	Time (hh:mm:ss)	Employees	WorkHours
Team Preparation and Purge Chill down	2:00:00	46	92.0
Safe Atmosphere Check	0:15:00	12	3.0
Access Preparations	0:15:00	12	3.0
Propellant/Pressurant Purge and Fuel Draining	0:50:00	12	10.0
Towing Vehicle Preparation	0:30:00		
Lock Control Surfaces	0:15:00	6	1.5
Landing Gear Lock	0:15:00	6	1.5
Total			**111**
Total + 20% Margin			**133**

The transportation to the SPF is assumed to be performed by a towing vehicle, as was done for the Space Shuttle. In this later case, the vehicle traveled 2 miles from the Space Shuttle Landing Facility to the Orbiter Processing Facility, with the whole operation taking approximately 2 hours. To do so, once the stage has completed all the safety operations including the landing gear lock pins, the towing vehicle is positioned in front of the stage and connected to the front wheel. After this preparation activities have finished, the towing occurs.

It is assumed that an off-the-shelf towing vehicle such as the commercial TaxiBot is used. It is estimated that this vehicle costs around 1.5 M$. A drawback of these vehicles is the heavy maintenance required, which is estimated to be annually 7.5% of the price of a new tug vehicle. Nevertheless, the vehicle wouldn't be used as often as for commercial airline operations, and therefore its maintenance costs can be considerably lower. In addition, its diesel consumption is considered negligible for the short distance traveled[9]. The taxibot can operate at 20 knots or more when towing. Therefore, it would only take around 5 minutes to tow the stage to the SPF for a 3-kilometer distance, and 1.5 minutes to detach from it. This labor time, although negligible was accounted for in the model.

For mission control operations it was assumed that a group of aerospace engineers are overlooking the operations and data acquisition at the mission control center, as was done for the Space Shuttle. This is taken from a FESTIP concept study, mentioning that 15 engineers would be required to overlook the operations plus a fraction of support engineers, totaling around 20 engineers if a high degree of autonomy is used [25].

5.1.1.3 Cost Breakdown of Recovery Costs

The cost breakdown for an exemplary recovery mission with IAC using the B-747-400F is shown in Figure 5-5 to Figure 5-7. Concerning direct costs, the major contributor are fuel costs with almost 2/3 of the total direct recovery costs. All remaining direct costs are small compared to the fuel costs with

[9] It is estimated to consume just 30 liters of diesel per operation. Bankers Capital Signed a Letter of Intent with Israel Aerospace Industries for Purchase of TaxiBot Aircraft Towing Units worth $97 Million, iac.co.il [Available at http://www.iai.co.il/2013/36756-44608-en/MediaRoom.aspx, 05.03.2019]

the 2nd and 3rd highest costs by landing fees and crew. The crew in this case is a team of aerospace engineers and UAV pilots that are able to remotely control and monitor the capturing aircraft.

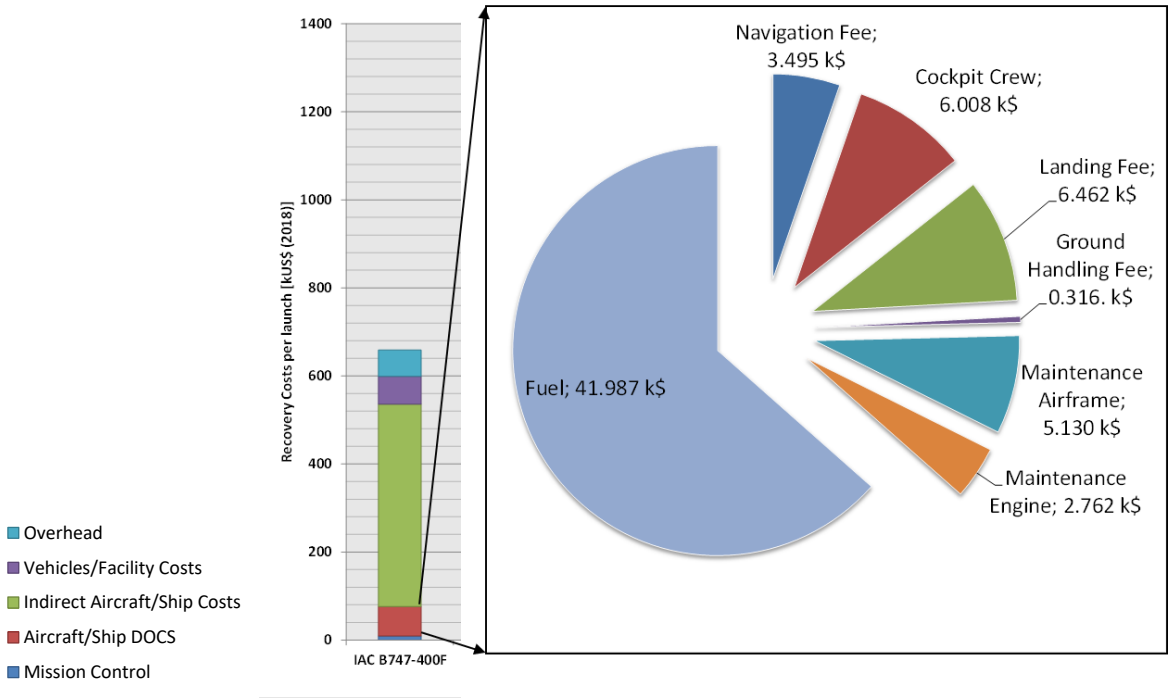

Figure 5-5: Direct Cost Breakdown for exemplary IAC recovery mission

Indirect costs are, compared to the direct costs, much higher due to the low number of missions per year. Whereas a commercial airline has to make sure that an aircraft flies as often as possible to be economically viable, this requirement is not valid for the In-Air-Capturing operations plan. Hence, the share of depreciation and interest get much higher per mission compared to commercial airliners (compare ~100 hours per year flight time with IAC vs. roughly 3000 hours flight time with commercial aircraft). Since indirect and ownership costs are the highest contributor to total recovery costs per mission it is of great importance to acquire an aircraft to a low acquisition price at good conditions. A very high acquisition price renders the recovery strategy too expensive.

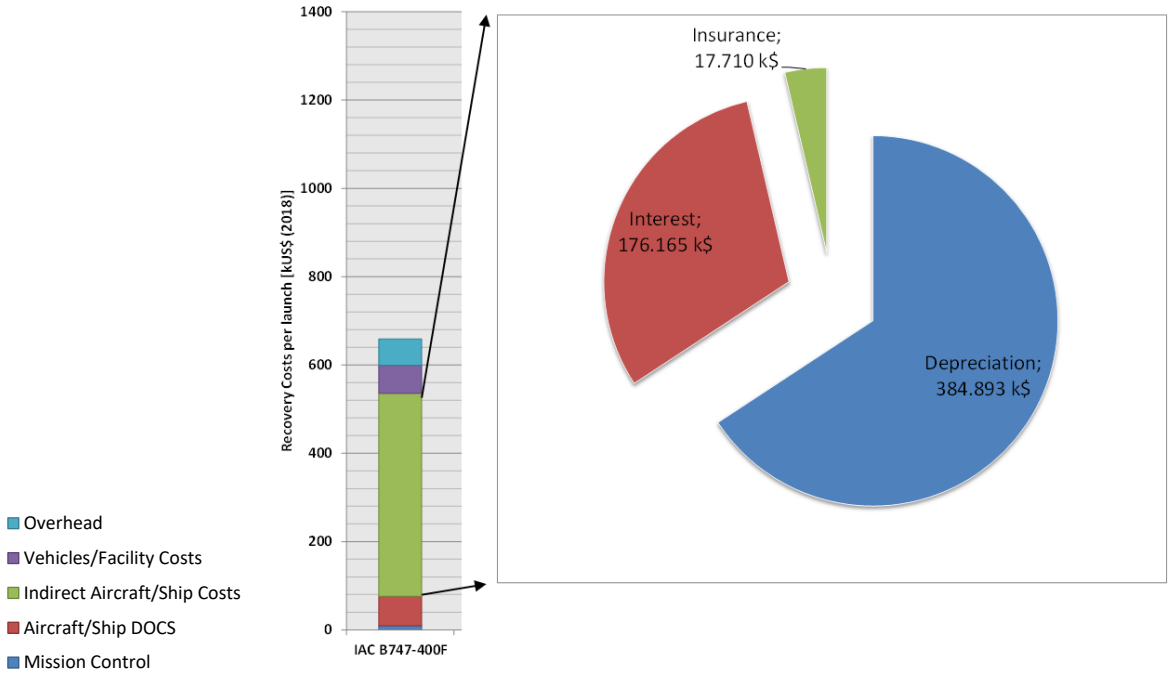

Figure 5-6: Indirect Cost Breakdown for exemplary IAC recovery mission

Last but not least the Figure 5-7 shows the cost breakdown for all additional vehicles and facilities costs. These are about the same magnitude as the direct operating costs of the aircraft. The vehicles/facilities cost are mainly driven by additional material costs which represent the cost of spare parts for the required vehicles and maintenance hours that have to be spend on said vehicles. The 2nd highest contributor to vehicles/facilities costs are the taxi vehicle which tows the stage on the airport (including acquisition) and additional post-flight operations, here referred to as airstrip operations.

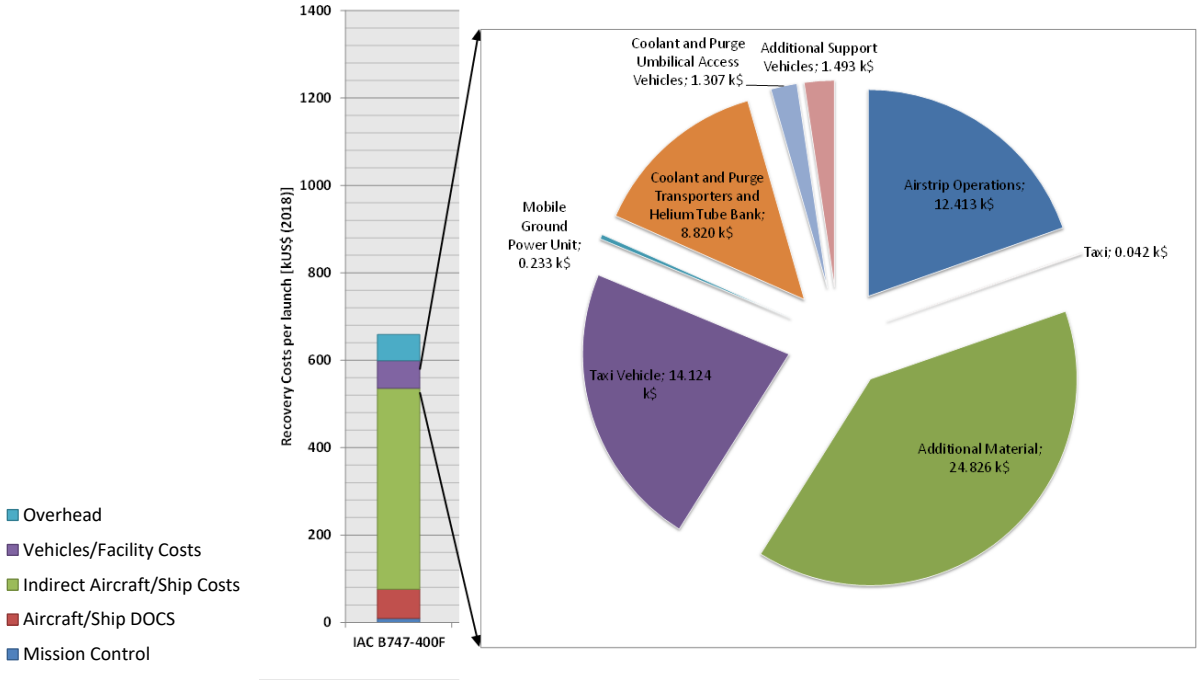

Figure 5-7: Vehicles and Facilities Cost Breakdown for exemplary IAC recovery mission

5.1.2 VL Downrange Landing, RTLS Cost

Down Range Landing (DRL) is a recovery mode suitable for GTO and other highly demanding missions which would require larger horizontal velocities at stage separation. Nevertheless, as opposed to the IAC method, it involves the use of a more systems (ships, harbor and activities) and longer time to transport the launch vehicle back to the landing site. This section will describe the different approaches used to estimate the costs associated to the DRL recovery mode. Nevertheless, since the focus lies on the In-Air-Capturing method, the modelling of this approach will only be explained briefly. For further detail consolidate [19].

Two main approaches are currently envisioned for the down range recovery of large reusable vertical landing vehicles. Blue Origin recently acquired a large used 11000 DWT Roll-On Roll-Off ship for recovery of its New Glenn first stage[10]. Nevertheless, only the Space X approach of landing on an ocean barge is currently being used commercially.

Roll-on Roll-off (RoRo) ships are designed for wheeled cargo, in contrast to Lift-on Lift-off (LoLo) ships which operate with a crane to load and unload cargo: These are currently also used by Arianespace and CNES to transport components the Ariane 5, Vega and Soyuz launchers from Europe to French Guiana[11], and are operated by the ship owner company Mairitime Nantaise, which owns RoRo and ConRo ships (Mixture between RoRo and LoLo), under a 15 year contract.

[10] Used Ro/Ro will become Blue Origin's Rocket Landing Pad, The Maritime Executive [Available at https://www.maritime-executive.com/article/used-ro-ro-will-become-blue-origin-s-rocket-landing-pad, 07.03.2019]

[11] Maritime Nantaise, our fleet [Available at https://www.compagnie-maritime-nantaise.com/en/our-fleet/,08.03.2019]

Space X is currently using a fleet of ships for their recovery operations[12]. For landing, they are using an Autonomous Spaceport Drone Ship (ASDS), based on upgraded ocean Marmac barges. To tow these barges, tugboats are employed to transport the ASDS, such as the Pacific Freedom operated by Pacific Tugboat Service, and also additional ones while arriving to harbor to assist in docking operations. Furthermore, the operations are aided by 49-meter length supply vessels operated by the vessel owner Guice Offshore LLC ('Go'), carrying crew and material. With this concept, Space X is achieving a 48-hour turnaround between booster delivery and port departure for next mission for their ASDS ships.

For the recovery operations estimation, the reference vehicles listed in Table 5-8 are used based on the ships mentioned in the discussion above. Nevertheless, ConRo ships might also be attractive for landing reusable rockets because of the large available deck for container cargo combined with its RoRo versatility.

The ships considered as representative of their type for this analysis are shown in Figure 5-8 and Table 5-8. A summary of ships used in the aerospace industry is shown in section 5.1.

[12] SpaceX Marine Fleet, Active and Retired ASDSs, Spacex subreddit [Available at https://www.reddit.com/r/spacex/wiki/asds 08.03.2019]

Table 5-8: Characteristics of ships considered for the analysis

Ship	Length (m)	Beam (m)	Draft (m)	Deadweight (t)	BHP (hp)	Maximum Service Speed (knots)
RoRo 2700 lane meter	193	26	7.4	14200	22026	21.6
Tug Boat	29.8	11	4	-	4300	12
Ocean Barge	91.4	30.5	4.8	10267	-	-
Support Vessel	49.9	11	3	659	1750	12

Figure 5-8: Ships considered for DRL. Top left is the RoRo vessel bought by Blue Origin to use as landing and recovery ship. Top right one is the ASDS platform used by SpaceX for rocket landings. Bottom left one are the Go Searcher and Go Navigator supply vessels

In contrast to the aircraft DOC model for ownership costs, other cash costs are considered as ownership, to differentiate between charter rates (which includes crew etc., but does not include fuel, rates, cargo handling and bunkering) and direct ownership of a vessel. The total ownership costs can be computed as follows (in an annual or per launch basis)

$$C_{OWN} = C_{DEP} + C_{INT} + C_{INS} + C_{RE/MAN} + C_{CREW} + C_{VIC} \quad (5\text{-}35)$$

Depreciation of physical assets is a major DOCs for ships. A distinction was made here considering a residual value of 10% similar to the aircraft model, with a linear depreciation rate and a depreciation period of 15 years. The depreciation residual value is assumed negligible for the ship upgrades.

Interests are computed in the same way as for the aircraft DOC model, with the same compound interest rate per year, payments per year and payment period. Although not considered it is assumed necessary for today's financial market situation.

The ship annual insurance premium has been assumed as 1% of the ship initial acquisition costs (including upgrade). This is then given as follows

$$C_{INS}^{yr} = 0.01 * C_{ACQ} \tag{5-36}$$

Repairs and maintenance costs are assumed to be around 10% of the ship annual capital costs (acquisition and upgrade).

$$C_{RE/MAN}^{yr} = 0.1 * \left(C_{ACQ}^{yr} + C_{UP}^{yr}\right) \tag{5-37}$$

Annual crewing costs are based on the average workyear costs for the maritime sector as specified in section 5.1. This is based on minimum safe-manning requirements of 18 for the RoRo vessel, and 8 for the tug boat. It is expected that this minimum varies per country. In this way, crew costs become one of the biggest contributors to ownership costs, especially for the cheaper tug boats and support vessels. For FY 2018, this value is the following.

$$C_{CREW}^{yr} = n\text{-}_{CREW} * 112.707 \frac{k\$}{crew} \tag{5-38}$$

Victual costs are a small amount of the ownership costs accounting for consumables required to maintain the crew during the trip. This are based on the factor of new 11% of the RoRo ship DOC crew costs observed in [19]. The costs per launch were normalized as if the crew was used the 365 days of the year.

$$C_{VIC}^{l} = 0.11 C_{CREW}^{l} * \frac{L}{365} \tag{5-39}$$

Cash costs for ship DOC estimation represent the costs which are not included in charter rates, such as fuel and rates. The total cash costs can be computed as follows

$$C_{CASH} = C_{FUEL} + C_{FEE,FUEL} + C_{FEE,NAV} + C_{FEE,BERTH} + C_{FEE,CARGO} + C_{DOCK} \tag{5-40}$$

Fuel prices for the ships are based on the average Rotterdam bunker prices[13] for Low Sulphur Marine gas oil (required for European Emission Control Areas) between March 2018 and March 2019 of 600 $/metric ton. Nevertheless, a spread of 245 $/metric ton was observed due to the high variability, and it is expected that the price could rise in the future as a consequence of future carbon pricing frameworks, as was mentioned for aviation jet fuel in section 5.1.1.2. The United Nations Conference on Trade and Development mentions a proposed tax of 300 $/metric ton of CO2 for the maritime industry, which would make bunker prices more than 2 times more expensive. In addition, ships use a combination of diesel/gasoil and marine fuel (lower price) for their operations. This distinction is left for future work on refining the ship performance, and the worst case (most expensive) was chosen.

Bunker rates applicable in the French Guyana region in the CNES/CSG refueling facility are used, of 7.51 €/metric ton. The fuel consumption for each vehicle are based on typical fuel consumptions observed in the literature for similar Space X and Blue Origin acquired ships and are listed in Table 5-9. It is also assumed that the fuel consumption at rest is 3% of the value.

Table 5-9: Fuel Consumption for the Analyzed Ships

Ship	Cruise Fuel Consumption (ton/day)

[13] Global Average Bunker Price, shipandbunker.com [Available at https://shipandbunker.com/prices/av/global/av-glb-global-average-bunker-price,07.03.2019]

RoRo	61.2
Tug	8
Platform	Assumed negligible
Supply Vessels	5

As explained in [19], another important factor for voyage costs are the port dues, mooring/berth and cargo handling rates. These vary considerably from harbor to harbor, and therefore there are no attempts in the literature to obtain empirical relations to model them. Certain models mentioned that mooring/berth and cargo handling dues are rarely available as they are managed by private companies and terminal operators. Nevertheless, and attempt was made to model these rates by consulting the rates applying at the Grand Port Maritime of Guyana and applying a conversion factor from Euros to Dollars.

As the document did not account for aerospace vehicles for the cargo handling charges, a value based on Port Canaveral tariff modification of 500 $ per ton of aerospace vehicle is used, or 15 k$ per unit in 2016 $ (whichever is smaller). This tariff accounted for port degradation caused by the use of the voluminous vehicle.

In addition, it was observed that SpaceX barge operations require the use of two additional tug boats for docking and undocking. The applicable rates were based on Port Canaveral tug boat rates. One of these is considered also to assist in the RoRo operations docking, with a corresponding price of 1825$ per docking operation with the stage + 1500$ for possible 3 hours delays. For the barge, a price of 950$ per docking and undocking operation is applied with a 50% increase due to its unpowered operation. Additional 3 possible delay hours are considered.

5.1.3 Comparison of Recovery Costs

The costs of recovery per launch for different return methods for VL and HL stages are shown in Figure 5-9. The costs are given in US$ with respect to the economic conditions of 2018. For In-Air-Capturing, the costs of the B-747, the A380 and the A330 NEO are presented. For VL recovery the SpaceX and Blue Origin barge/ship recovery methods and RTLS costs are added. The RTLS costs are also more or less valid for the HL flyback when assuming similar efforts in landing strip construction. The reference HL stage for the mission calculation is a ~50 ton landing mass stage and for VL a ~45 ton landing mass stage. However, the impact of landing mass on the mission is negligible due to the comparatively low direct launch costs in all cases, as will be explained in the following.

The recovery costs end up between 250 k$ (RTLS) to 670 k$ (SpaceX barge landing) to almost a million US$ for the Blue Origin method for VL related methods. Recovering the stage via IAC costs 650 k$ to 1.25 million US$ depending on the selected aircraft. The greatest share, regardless of VL or HL, is made up of indirect costs and overhead costs. This great share is due to the depreciation of the acquisition and modification costs over all launches assuming a remaining lifetime of 15 years. Hence, the recovery costs are highly dependent on the aircraft price which explains the high recovery costs for the A380.

Direct costs, including fuel and crew costs, landing fees, navigational fees or harbor fees and costs for extra services account for only roughly 100k$ per mission or 1.5 million – 2.5 million US$ per year depending on the recovery method. Of these direct costs 2/3 of costs are related to fuel for IAC. For VL methods, the greatest share of direct costs is due to crew costs. The facility and vehicles costs are higher for the VL recovery methods which can be explained by the fact that crane acquisition costs are increasing total costs. Contrary, the IAC costs don’t include depreciation costs of the airstrip or hangar building. Including those costs would add additional 250 k$-400 k$ per launch.

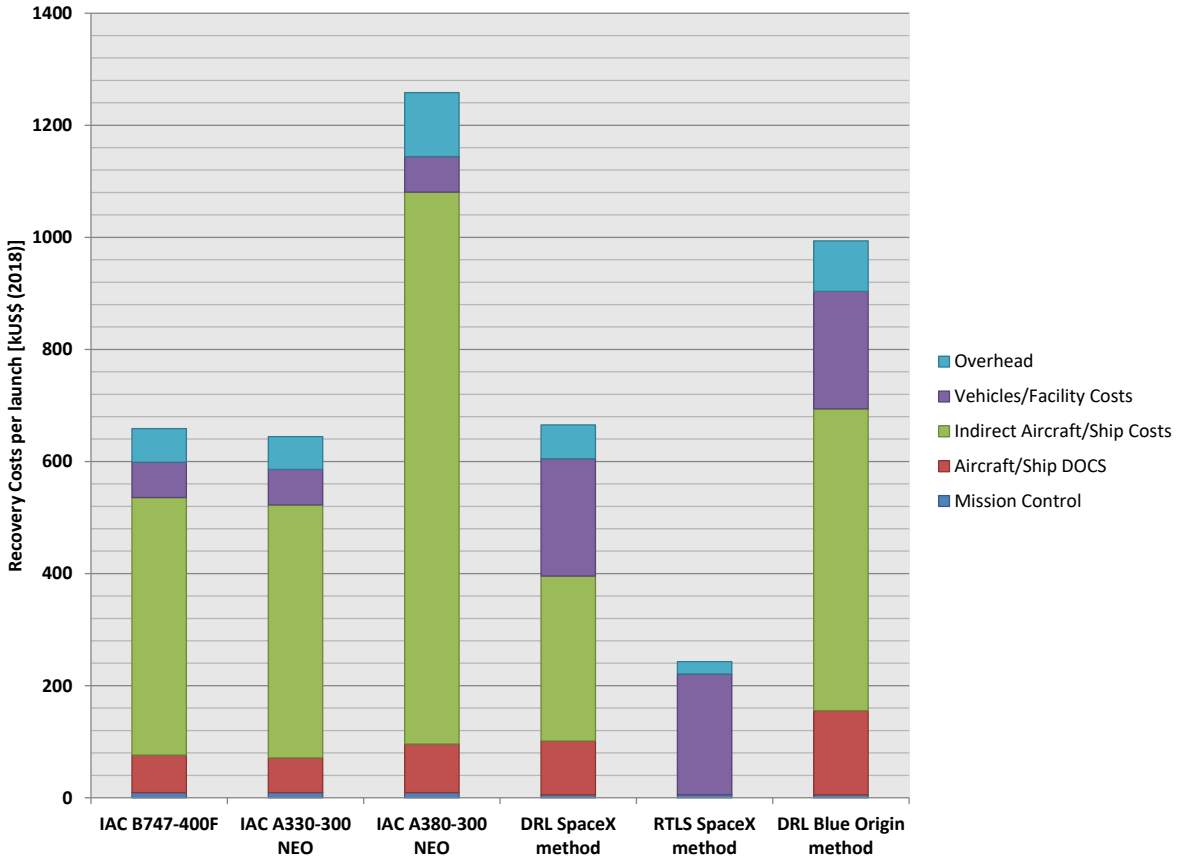

Figure 5-9: Recovery Cost breakdown for different return strategies

As expected, the recovery costs are certainly dependent on the launch rate. Figure 5-10 shows that dependency over launch rates from 5 to 45 launches per year. The same assumptions as described previously were used for this calculation. The recovery costs calculated with the top-down model TRANSCOST were added for comparison. In this model, the recovery costs are calculated according to equation (5-1) where L is the launch rate m_{rec} is the mass of the recovered stage/hardware and fi are country- and business dependent factors.

$$WYr_{REC}^{TRANSCOST} = \frac{1.5}{L}(7 * L^{0.7} + m_{rec}^{0.83}) * f_i \quad (5\text{-}1)$$

The recovery costs depend exponentially on the launch costs with a negative exponent. Hence, the decrease of costs per launch in the comparable low launch rate regime is greater whereas the costs approach a boundary value when reaching very high launch rates. Nevertheless, doubling the launch rate from 15 to 30 launches per year would result in a decrease of -30% for the SpaceX method, -40% for the Blue Origin method and -35% for IAC. Using IAC as recovery method seems to be favorable for a launch rate greater than 15 launches per year. The recovery costs of using RTLS are negligible since they fall below 200 k$ per launch with a launch rate greater than 20 launches per year. The recovery costs calculated with TRANSCOST are considerably higher. This can be explained by the fact that the recovery CER is based on the recovery operations of the Space Shuttle solid boosters, which required a relative high effort due to the fact that it was the first time that rocket hardware was ever recovered.

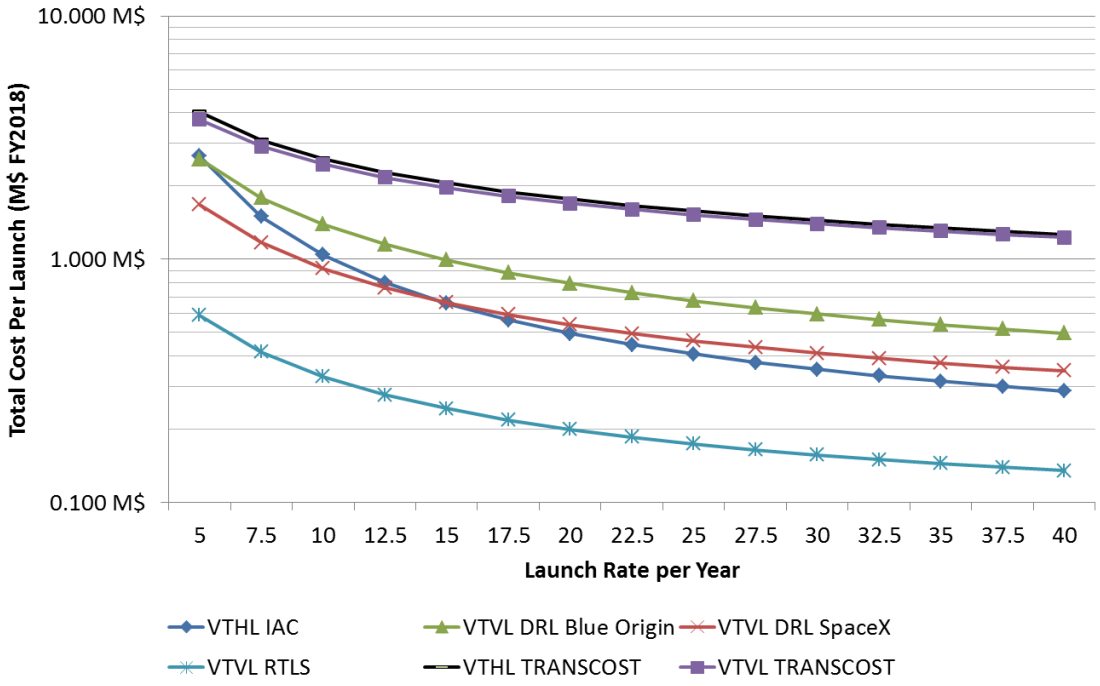

Figure 5-10: Recovery Costs per launch in M$ (economic conditions: 2018) for VTVL and VTHL recovery methods

5.2 Total Launch Costs

The total launch costs were calculated using the TransCost model. This model is using a top-down approach to calculate costs. Hence, a sufficiently large database has to be available to derive trends from cost data on historical or operational launch vehicles. As already explained in the introduction in section 5 this leads to a problem considering cost analysis of RLV with TransCost: the lack of sufficient and reliable cost data on RLVs.

The general idea behind TransCost is the calculation of costs based on so-called CERs (cost estimation relationships). Generally, these CERs are calculating the cost based on Workyear cost which can be translated into a monetary value for different economic conditions and business models. The CERs for launcher stages, engines and components are generally formulated as shown in equation (5-2). Here, M is the stage or component mass, x and a are stage/component specific factors that depend on propellant choice, engine cycle and further parameters. f_n are multiple factors that reflect different market conditions, business models, overhead shares, team and project experience and so on and are thus highly dependent on the company or space agency developing and building the respective launch vehicle. An example of a TransCost CER is shown in Figure 5-11.

$$Cost = \sum_{n} f_n \, a \cdot M^x \tag{5-2}$$

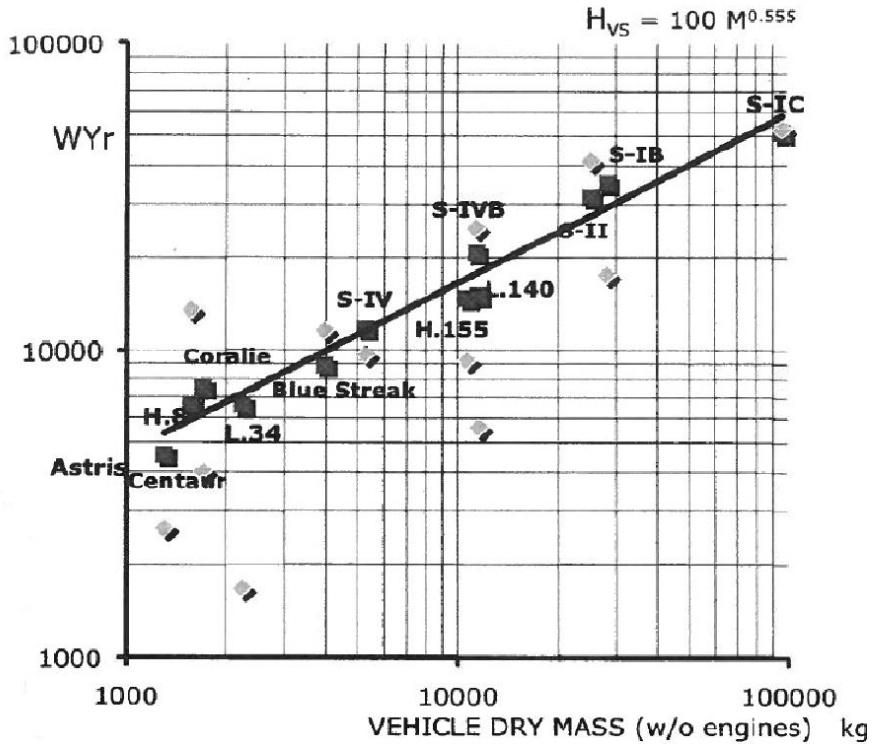

Figure 5-11: TransCost CER for expendable, liquid-propulsion launch vehicle stages

The TransCost model, whereas giving acceptable to good results for expendable launch vehicles, is at this point not entirely applicable to reusable launch vehicles. A modification of the model is necessary since it is assumed that the costs of winged stages are not expected to be much higher than those of vertical landing stages. This should be considered and improved in the economic analysis which should be updated in the course of the FALCon project.

However, as a first parametric study, the total launch costs herein were calculated by combining the TRANSCOST model with the in-house established recovery model and are expressed with respect to the costs of an expendable launch vehicle. Since absolute values can only be determined with better knowledge of the production procedures, work processes, required personnel, overhead costs and acquisition costs and so on a relative comparison between RLV and ELV costs makes more sense in this context. Hence, all costs presented herein are related to the respective costs of a comparable ELV system to identify breakeven points and determine ranges in which the RLVs might offer economic advantages over ELVs. However, at this stage the total launch costs are subject to very high uncertainties and should thus be taken as a preliminary glimpse at cost modelling of RLVs and not as a final and undeniable result.

Figure 5-12 shows the normalized average launch costs of the RLV hydrogen launchers over a period of 10 years. The costs are normalized with respect to the costs of the VL vehicle being operated as expendable vehicle, meaning that all recovery hardware is stripped off the vehicle and all propellant is used to accelerate the stage. The average is determined by calculating the cost of the launcher over 10 years and dividing the total costs by the number of launches. Furthermore, the costs are given for a launch rate of 10 launches/year and different refurbishment factors (see section 2.4 for the definition of the refurbishment factor). Any points below the 1.0 line are regions where the ELV would be cheaper than an ELV. It is visible that too high refurbishment costs lead to increasing launch costs which lead to economically inviable solutions. If the refurbishment factor drops beneath 0.4, the RLV is cheaper than the respective ELV with greater advantage the lower the refurbishment costs are. Interestingly, while expecting a great cost decrease with an increase in reuses for less than 10 reuses, the averaged costs stagnate for more than 20 reuses for a refurbishment factor between 0 and 0.1. For higher refurbishment, a slight increase in costs for a high number of reuses can even be observed. This indicates that extensive number of reuses might not in all cases be of preference for a RLV.

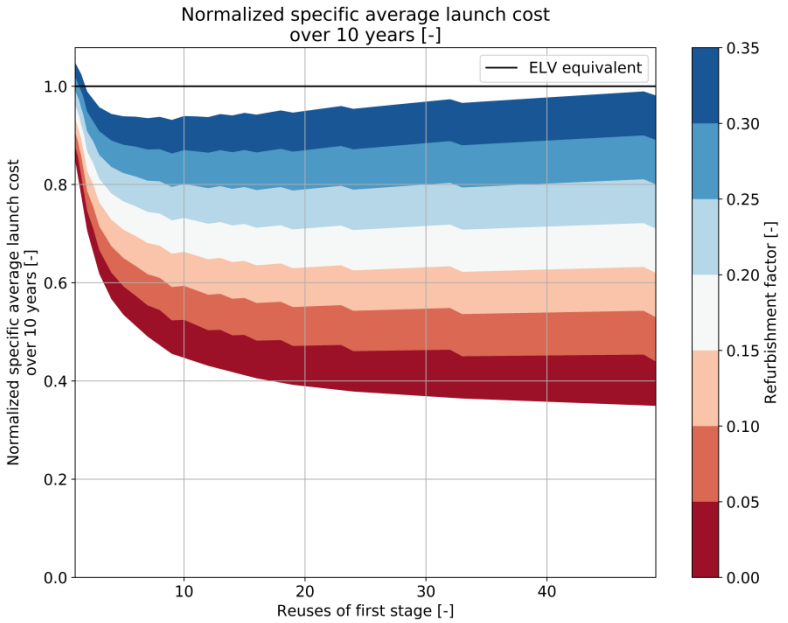

Figure 5-12: Normalized average launch costs for the RLV hydrogen stages for different reusability factors at a launch rate of 10 launches/year

The total launch costs of RLVs are also dependent on the launch rate. Figure 5-13 shows that dependence for refurbishment factors of 0.25, 0.5, 0.75 and 1 which represents the ELV. An increase in launch rate leads to a reduction of launch costs in all cases. However, the reduction is comparable for ELV and RLV. The greatest driver for reducing the launch costs is decreasing the refurbishment factor, since only the RLV with a refurbishment factor of 0.25 is cheaper than the respective ELV launcher and that only for sufficiently high numbers of reuse.

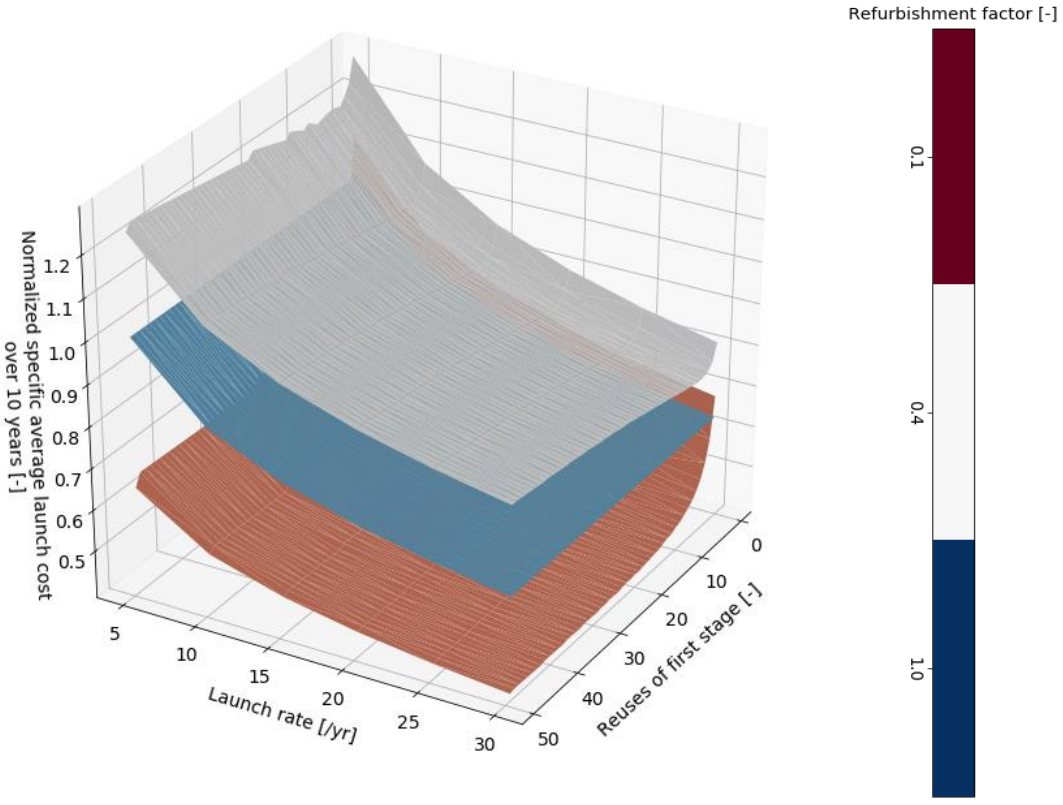

Figure 5-13: Normalized average launch costs for the RLV hydrogen stages for different launch rates, number of reuses and reusability factors

In general, it should be noted that this model is a preliminary model. Hence, any cost values and relations presented depend highly on the assumptions that are input into the model. These assumptions depend on the business model, the country, team experience and further factors and the stage mass. An increase in stage mass leads to higher costs, which is why hydrogen seems also a good choice from an economic point of view. However, in the future course of economic studies of RLVs, the cost model shall be enhanced to include uncertainties and worst-cases to allow a more accurate determination of the overall costs.

5.3 Subscale Scenario Economic Analysis

Currently, there are several small-sat launch vehicles under development or already on market. Among the most popular, the Rocketlab Electron, the Virgin Orbit Launcher One and the Firefly aerospace launch vehicle are the most mentionable. However, only the Rocketlab Electron has flown successfully and has delivered payload to orbit. The Electron launch vehicle is interesting for the FALCon project since Rocketlab recently mentioned that they would be trying to capture and recover the first stage by so-called mid-air retrieval. Contrary to the FALCon IAC technology, Rocketlab plans to use a helicopter to capture the Electron first stage as shown in Figure 5-14. [27]

Figure 5-14: Electron dummy stage being captured by a helicopter

The use of a helicopter has several advantages: a helicopter can hover or fly at very low velocity to capture. This is of advantage in case of capturing a stage that is attached to a parafoil as seen in Figure 5-14. However, the range of a helicopter is limited. In case of the FALCon In-Air-Capturing a winged stage is assumed, so a small airplane could be used to capture the returning stage. Possible aircraft for this task could be turboprop cargo machines, such as the Cessna Skycourier, the ATR 72 or the Dash 8 (see Figure 5-15).

Figure 5-15: Cessna Skycourier (left) and ATR 72 (right)

In the following, two different sections will be presented. The first one will focus on defining a premise and requirements for a subscale launch vehicle scenario to use In-Air-Capturing in an economically viable sense. This means that the results of the previous heavy-lift analysis will be used to derive a set of assumptions or requirements that are necessary for a small-scale scenario to work. Then, in the following section, a preliminary analysis of the costs of recovery using a turboprop-propelled aircraft as shown in the picture above is performed. Both sections will be used to evaluate the economic viability of IAC on a smallsat launch vehicle.

5.3.1 Premise

The results from sections 5.1 and 5.2 can be used to derive some requirements or assumptions that are necessary for a small-sat vehicle to be economically viable. Those requirements will be elaborated in the following.

- ***Low relative Cost Share of IAC by plane with regards to total launch costs:*** As seen in the previous sections, the recovery costs can range from 600 to 1200 kUS$ when using commercial turbofan aircraft. This is a relatively low share compared to the total launch costs of a medium to heavy-lift vehicle. SpaceX charges around 60 million US$ for a Falcon 9 flight and Ariane 5 launches cost around 130 million US$. Hence, the share of the recovery costs would range from 1.7% to less than 1% with respect to total launch costs. In case of a small-sat launch vehicle, the total launch costs are lower. Electron charges around 5 million US$ per launch with the Electron. Hence, recovering a returning stage of that mass with an A340 adds a relative share that is much higher compared to the total launch costs, thus rendering it economically unviable for such vehicles. As result, the premise here is that the share of recovery costs added by the IAC method is as low as possible.
- ***Costs added by introducing reusability have to be lower compared to using an ELV.*** This premise is valid for all launch vehicles. In summary, reusability of a launch vehicle adds costs that are not present for an ELV. These costs that are added by making the stage reusable (additional hardware, software, recovery costs, infrastructure, post-processing, refurbishment…) have to be less than what it would cost to produce a new stage. In case of small-sat launch vehicles, this can get difficult due to the fact that costs in general are much lower compared to a heavy-lift vehicle.
- ***Low reduced payload capability by adding reusability.*** Any reusable launch vehicle will experience a payload penalty due to adding either hardware mass (wings, parachute, landing gear…) or propellant for return maneuvering compared to an ELV. Since the mass of a small-sat launch vehicle is low in general, any payload penalty will either require sizing up the vehicle or risking to not capture the whole small-sat market. Due to the lower masses compared to heavy-lift launchers, the margins here are much tighter.
- ***Small-sat launch vehicle usually have a higher share of overhead and fixed costs to total launch costs.*** Compared to heavy-lift vehicle, where the major share of costs is due to the necessity to produce heavy hardware, smaller launch vehicles have a higher share of fixed

costs [18]. Hence, introducing reusability will not have as high of an impact on costs as it will have on a heavy-lift launch vehicle.

Some of these points are summed up in Figure 5-16, where the total launch costs are plotted over vehicle payload capability. The higher the payload capability and hence mass of the vehicle, the lower the costs per mass to orbit. This plot, which was taken from TRANSCOST, also shows that there is a point where adding reusability to the launch vehicle doesn't make any sense, since the costs added by recovers get higher than comparable ELV costs beyond a certain point.

In summary, a small-sat launch vehicle has much tighter margins for being reusable compared to a heavy-lift vehicle due to the generally lower mass, lower share of production costs and the high impact on payload capability. Hence, reusability here makes sense if the added mass is relatively low, the recovery costs are much lower than that for IAC by A340-type aircraft or barge landing on SpaceX-like barges, the impact on payload capability is in a range that allows to serve the whole small-sat market and the added costs by reusability are lower. As seen in the previous sections, this calls for a method that rather uses parachutes or parafoils and no additional stage propellant to recover the stage.

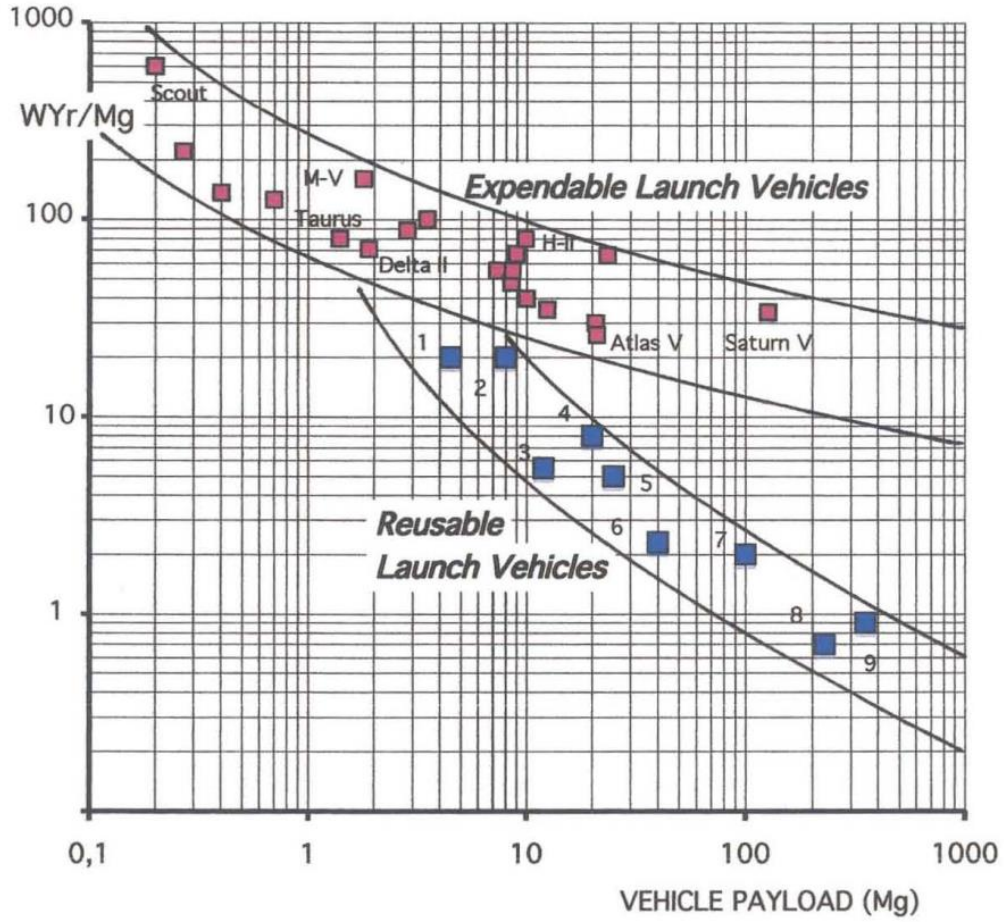

Figure 5-16: Theoretical Specific Transportation Cost of Expendable and Reusable Launch Vehicles vs. Payload Capability to LEO (RLV-Projects: 1= Kistler K-1, 2 =Slinger TSTO, 3 =MBB BETA 11, 4 = Lockheed Martin Venture Star", 5 =MBB BETA III, 6 = Chrysler SERV, 7 = BETA IV, 8 = Boeing SST0'76, 9 = TUB NEPTUNE) - No development cost amortization included. [18]

5.3.2 Recovery Costs for Turboprop cargo aircraft

As mentioned earlier, the recovery costs using a smaller turboprop cargo aircraft are calculated to get a range of expected costs with such vehicles. Turboprop cargo aircraft are not as powerful as turbofan-driven commercial aircraft, but they generally have lower specific fuel consumption and are

sufficiently powerful to carry empty small-sat stages. In this analysis, two different aircraft were assumed: the ATR 72 and the Dash 8 turboprop aircraft. The specifics of these aircraft are shown in Table 5-10. The same cost model as for the full-scale vehicle was used to determine the recovery costs but assuming a third of the personnel to do post-flight-processing (20 workers).

It is important to note that the analysis presented was performed on a preliminary basis. It would be a further important step to check the performance specifications of the envisioned aircraft for the In-Air-Capturing for small vehicles with the aircraft manufacturer. Questions such as range capability, towing capability and all other points that have to be addresses for the heavy lift scenario would also have to be addressed for the subscale scenario.

Figure 5-17: De Havilland DHC-8 (Dash 8)

Table 5-10: Turboprop aircraft specifications

Aircrafts		ATR 72-600	Dash 8 – Q400
$Maximum\ Takeoff\ Weight$	[t]	23	30.5
$Operational\ Empty\ Weight$	[t]	13.3	17.8
m_{MFW}	[t]	5	6.5
S_{ac}	[m²]	61	64
$Cruise\ Velocity$	[km/h]	510	556-667
Range	[km]	1528	2040
Fuel Consumption	[kg/km]	1.49	1.83
Acquisition Price Used	[MUS$]	5.5	3.5

The recovery costs were calculated assuming second-hand acquisition prices as shown in the table above. Furthermore, it was assumed that both vehicles are loaded with fuel to their maximum. The results compared to the turbofan B747 aircraft are shown in Figure 5-18. The recovery costs using the light turboprop aircraft are much less than the B747 costs, mainly due to the lower acquisition costs. The added costs range are around 150000 – 170000 US$ per launch, assuming 15 launches per year. The DOCs are less compared to the B747, mainly due to the lower mass of the turboprop aircraft and the better specific fuel consumption of those engines. Overhead and facility costs are reduced due to less workers required (however, this assumption would have to be verified by assessment of aircraft industry) and the aircraft mass and space. Thus, smaller hangars and vehicles could be used.

Taking the premises of section 5.3.1 into account, using IAC for small-sat launchers is a quite challenging task. The recovery costs, based on the preliminary analysis done within this section, could be reasonably low to allow using IAC for small-sat launchers. The share of recovery costs using a

smaller turboprop aircraft (150000 $) to total launch costs (5 million US$ for Electron) is 3% and thus comparable to the heavy-lift scenario. However, to fully determine the economic viability of IAC for small-sat launchers, a more detailed analysis using more profound data would have to be performed. This analysis should investigate the impact on launcher performance when adding wings and recovery hardware to a small-sat launcher and the extra mass added. Furthermore, the additional production and refurbishment costs have to be evaluated. Certainly, it will be more challenging to use IAC for small-sat launch vehicles, but not impossible though. The margins of finding a technical and economical viable vehicle are tighter compared to heavy-lift vehicle however.

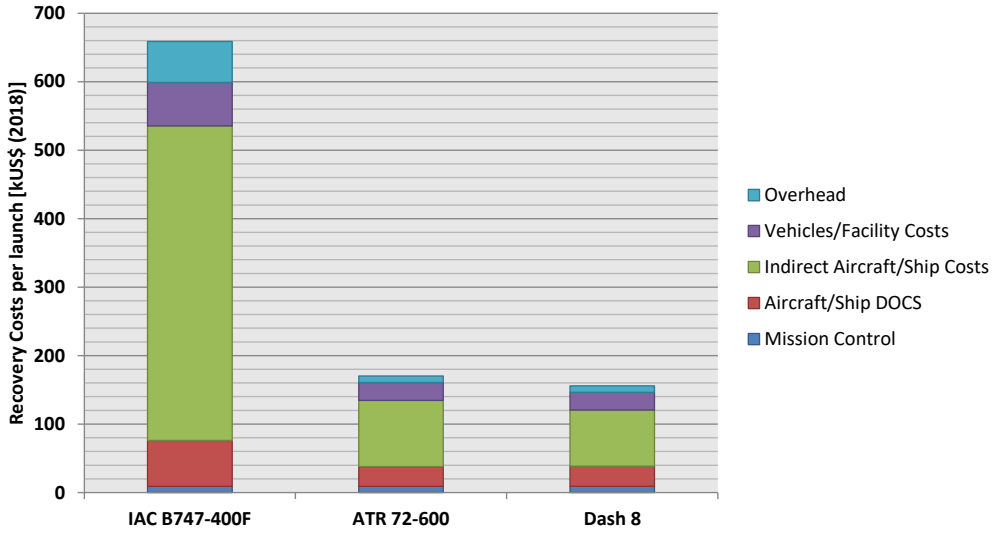

Figure 5-18: Recovery Cost breakdown for turbofan passenger aircraft (B747) and turboprop aircraft (ATR 72 and Dash 8)

5.4 Outlook

In the course of the FALCon study it is important to position the IAC procedure with respect to other RLV strategies to highlights its advantages and economic benefits and future potential to develop competitive launch vehicles in Europe. From a technical point-of-view the IAC method offers the potential to build powerful and comparably light and compact launch vehicles. From an economic perspective however, certain open points still remain that have to be answered.

The cost model that was derived in-house is based on a bottom-up estimation approach where the work, tasks and hardware are broken down into smaller packages or parts to estimate the costs of those smaller packages. Since aircraft and ship operations are a well-explored field of cost estimation with a lot of models and data available the determination of said recovery costs is much more straight-forward then the estimation of RLV stage and engine development and production cost. Hence, the estimation of these costs shall be the focus of the analyses that follow in the work package 2.3 of the FALCon project.

The further tasks and ideas considered for this workpackage 2.3 include the following:

- **Improvement of TransCost model** and especially the formulas for RLVs to determine more accurate launch costs. A strategy would be to try a more “bottom-up” focused approach as it was pursued for the recovery costs
- Literature survey and **implementation of a statistical cost model** using an approach based on uncertainty and probability estimation. This could allow the estimation of RLV costs based on known uncertainties and would return a cost estimation with a confidence interval [21].
- **Validation of cost model** by cost data from Ariane 5, Ariane 6 and future Ariane assumptions and ideas

6 RLV Reference Stage

An important task within WP 2 of the FALCon project is the definition of the RLV reference launcher and especially the reusable first stage that serves as reference stage for the full-scale In-Air-Capturing simulation in WP 7. This section focuses on the reference stage of the three-stage-to-orbit concept with a first stage with foldable wings as it was presented at the IAC 2019 [22].

6.1 Assumptions and Stage Design Requirements

The launcher is to be designed for the most suitable combination of high commonality in major components and providing good mission flexibility. The upper payload range should be in the 10 to 15 tons GTO-class and should include multiple payload capability. Using an adapted, reduced size upper segment, smaller satellites have to be carried to different LEO. The expendable section is designed as two-stage system, hence the launcher results 3-stage to orbit configuration.

The RLV-configuration was designed using the following mission requirements:

- GTO: 250 km x 35786 km
- Launch site: CSG, Kourou, French Guiana
- **Target Payload: ≥ 13 tons**
- **First Stage is captured by towing aircraft after re-entry**
- **L/D in subsonics for In-Air-Capturing ≥ 6**

Staged combustion cycle rocket engines with a moderate 16 MPa chamber pressure are baseline of the propulsion system. A Full-Flow Staged Combustion Cycle with a fuel-rich preburner gas turbine driving the LH2-pump and an oxidizer-rich preburner gas turbine driving the LOX-pump has been defined by DLR under the name SpaceLiner Main Engine (SLME) [23]. The expansion ratios of the booster and passenger stage/ orbiter engines are adapted to their respective optimums; while the mass flow, turbo-machinery, and combustion chamber are assumed to remain identical in the baseline configuration.

The SpaceLiner 7 has the requirement of vacuum thrust up to 2350 kN and sea-level thrust of 2100 kN for the booster engine and 2400 kN, 2000 kN respectively for the passenger stage. All these values are given at a mixture ratio of 6.5 with a nominal operational MR-range requirement from 6.5 to 5.5. Table 6-1 gives an overview about major SLME engine operation data for the nominal MR-range as obtained by cycle analyses.

The size of the SLME in the smaller booster configuration is a maximum diameter of 1800 mm and overall length of 2981 mm. The larger passenger stage SLME has a maximum diameter of 2370 mm and overall length of 3893 mm. A size comparison of the two variants and overall arrangement of the engine components is published in [23].

The engine masses are estimated at 3375 kg with the large nozzle for the passenger stage and at 3096 kg for the booster stage. These values are equivalent to vacuum T/W at MR=6.0 of 68.5 and 72.6.

Table 6-1: SpaceLiner Main Engine (SLME) technical data as used by reusable and expendable stage [22]

	RLV Booster	2nd ELV stage
Mixture ratio [-]	6.5	5.5
Chamber pressure [MPa]	16.9	15.1
Mass flow per engine [kg/s]	555	481
Expansion ratio [-]	33	59
Specific impulse in vacuum [s]	435	451
Specific impulse at sea level [s]	390	*357*
Thrust in vacuum [kN]	2356	2116
Thrust at sea level [kN]	2111	1678

The basic stage design and layout are shown in Figure 6-1. As already mentioned, the launcher is design as three stage system with the first stage as winged RLV stage in parallel with the expendable 2nd and 3rd stage. As propellants, LOX (white tanks) and LH2 (red tanks) are used. The first reusable stage is equipped with 4 SLME engines, the 2nd stage is equipped with one vacuum-optimized SLME and the 3rd stage uses the Vinci engine.

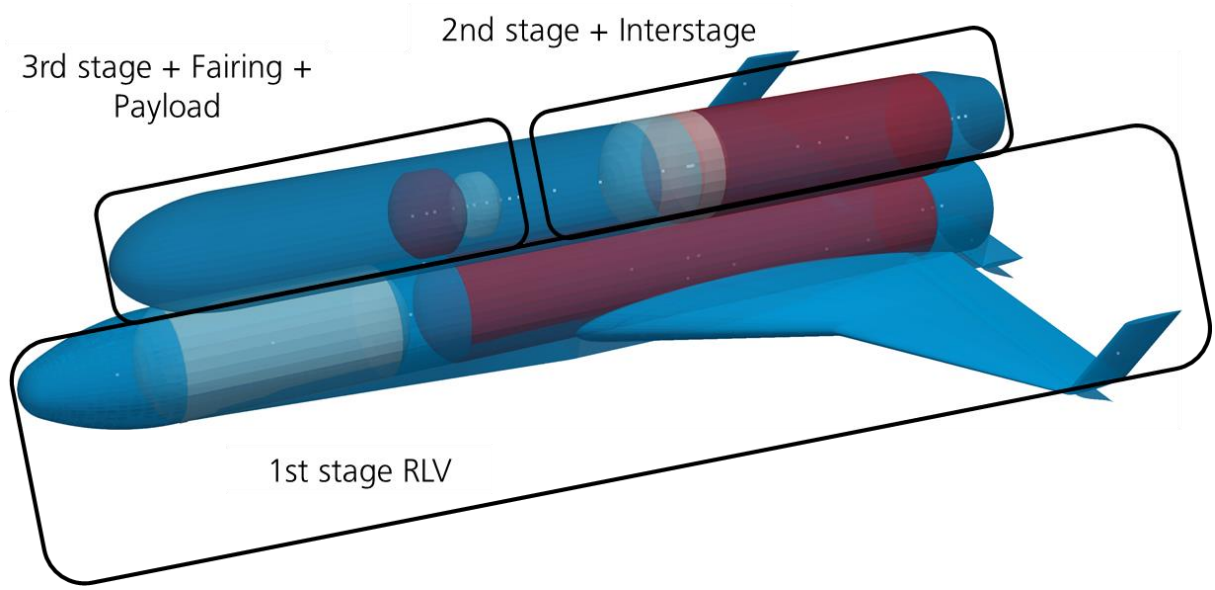

Figure 6-1: Layout and tank positions of 3STO configuration, fixed-wings

The ascent phase is split into two steps. First, the second stage is injected into an intermediate orbit with an apogee height of 600 km, a perigee height of 25 km and an inclination of 5.4°. Following a ballistic flight phase, the third stage is ignited so that it reaches the apogee at half burn time, thus performing a Hohmann transfer into the designated GTO with 600 km perigee and 35786 km apogee and 5.4° inclination. The flight trajectory for the fixed wing configuration is shown in Figure 6-2.

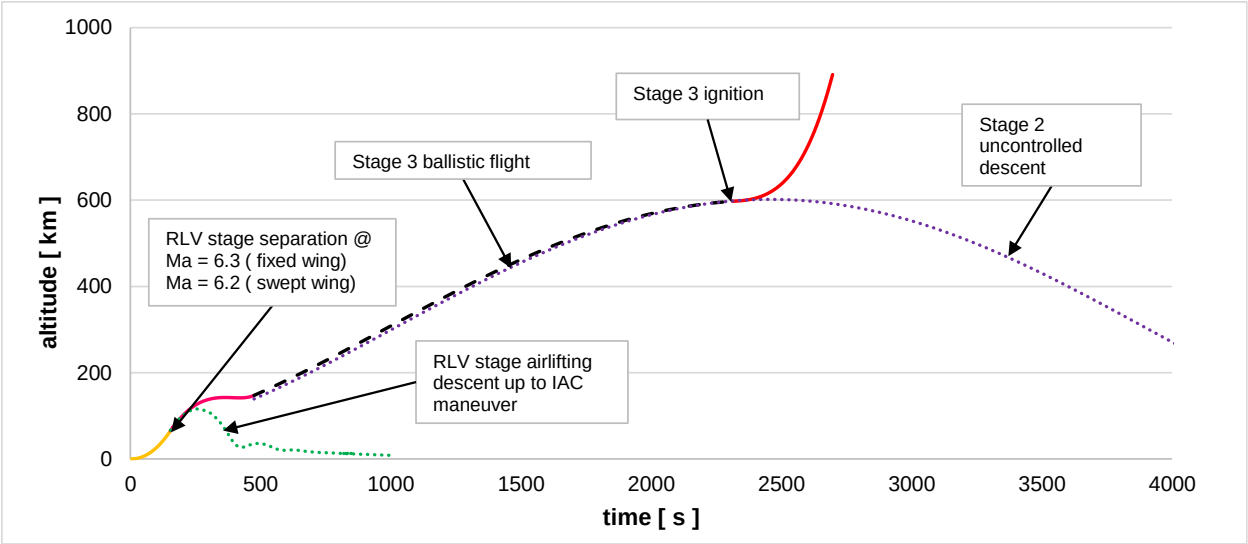

Figure 6-2: Ascent flight trajectory of the RLV with mission events [22]

6.2 RLV stage geometry with moving / folding wings

In the wake of investigations on RLVs at DLR a certain problematic concerning winged first stages was discovered. In certain flight conditions during re-entry of winged RLV stages, a shock-shock interaction between the fuselage bow shock and the wing's leading edge shock can lead to increased heat loads at the interaction front (see Figure 6-3). This problem might be solved by increasing the TPS thickness or changing materials at the interaction front or potentially better by moving the wings out of the bow shock.

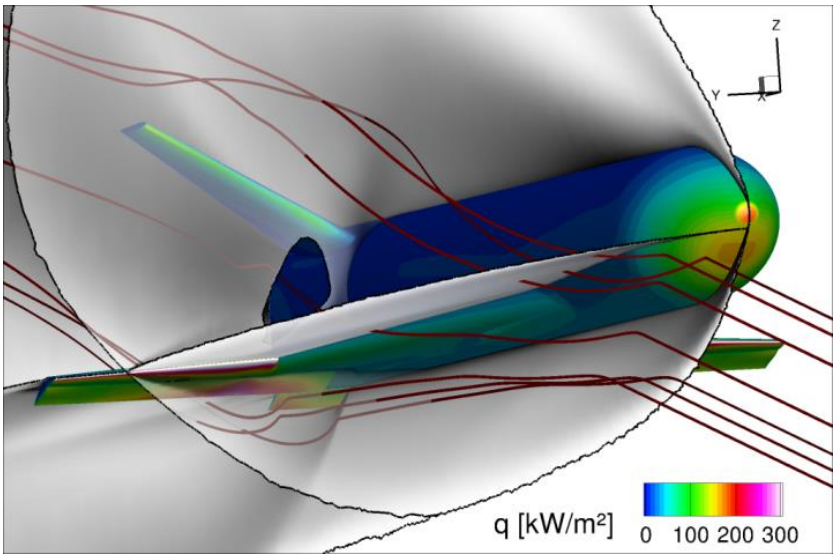

Figure 6-3: Shock-shock interaction of a winged RLV stage during re-entry

With retractable wings the effective span during re-entry could be limited to make sure that the wings are not lying within the shock-shock interaction. When transitioning to subsonic speed, the wing could be extended to allow for a higher L/D, in some cases even higher than with a fixed-wing configuration.

Variable geometry wings in aeronautics have been under investigation at least since the mid of the 20th century and numerous concepts and operational aircraft have been studied and realized. RLV first stages with variable wings have been considered in the USSR in the context of Energia Buran evolution and later also in DLR [24].

The wing geometry parameters and the wing position with respect to the fuselage are offering several degrees of freedom to the design. Moreover, the impact of parameter variation on the different

disciplines is strongly coupled. E.g. wing geometry is affecting mass and vehicle CoG-position while both impact flight dynamic behavior and trimming.

A favorable swept-wing configuration was found by comparing a vast range of different possible wing configurations to allow for a design that fulfils all requirements:

- High L/D of at least 6 allowing for adequate gliding path angles during In-Air-Capturing
- Small span in hypersonics to avoid shock-shock interaction
- Landing Speed of ≤ 105 m/s
- Trimmable to high AoAs in hypersonics to minimize heat flux

The first stage diameter and length is similar to the core stage of an Ariane 5 or 6 with 5.4 m. The wing span of the inner wing is around 20.2 m the span of the outer wing is 16.7 m which adds up to a total span with wings extended of 35.5 m (see Table 6-2).

Table 6-2: Major stage dimensions of the RLV stage and of the launcher RLVC4-III-B

H340 (RLV stage)	
total length (incl. bodyflap)	59.5 m
fuselage diameter	5.4 m
total span (deployed wing)	35.5 m
H150 ELV	
total length (incl. fairing)	46.5 m
fuselage diameter	5.4 m
H16 ELV	
total length	4.0
fuselage diameter	4.0

The convergent preliminary design of the variable-wing first stage is presented in Figure 6-4 which also shows the difference between the re-entry configuration with the wings folded and the transonic and subsonic configuration with wings extended. The outer wing is stored inside the inner wing during re-entry and is connected via the folding mechanism to the outer wing. It is visible that the outer wing extends over the chord length of the inner wing so that the outmost parts extend outside. This makes it necessary for the inner wing to be open at the trailing edge to accommodate the protruding part of the outer wing.

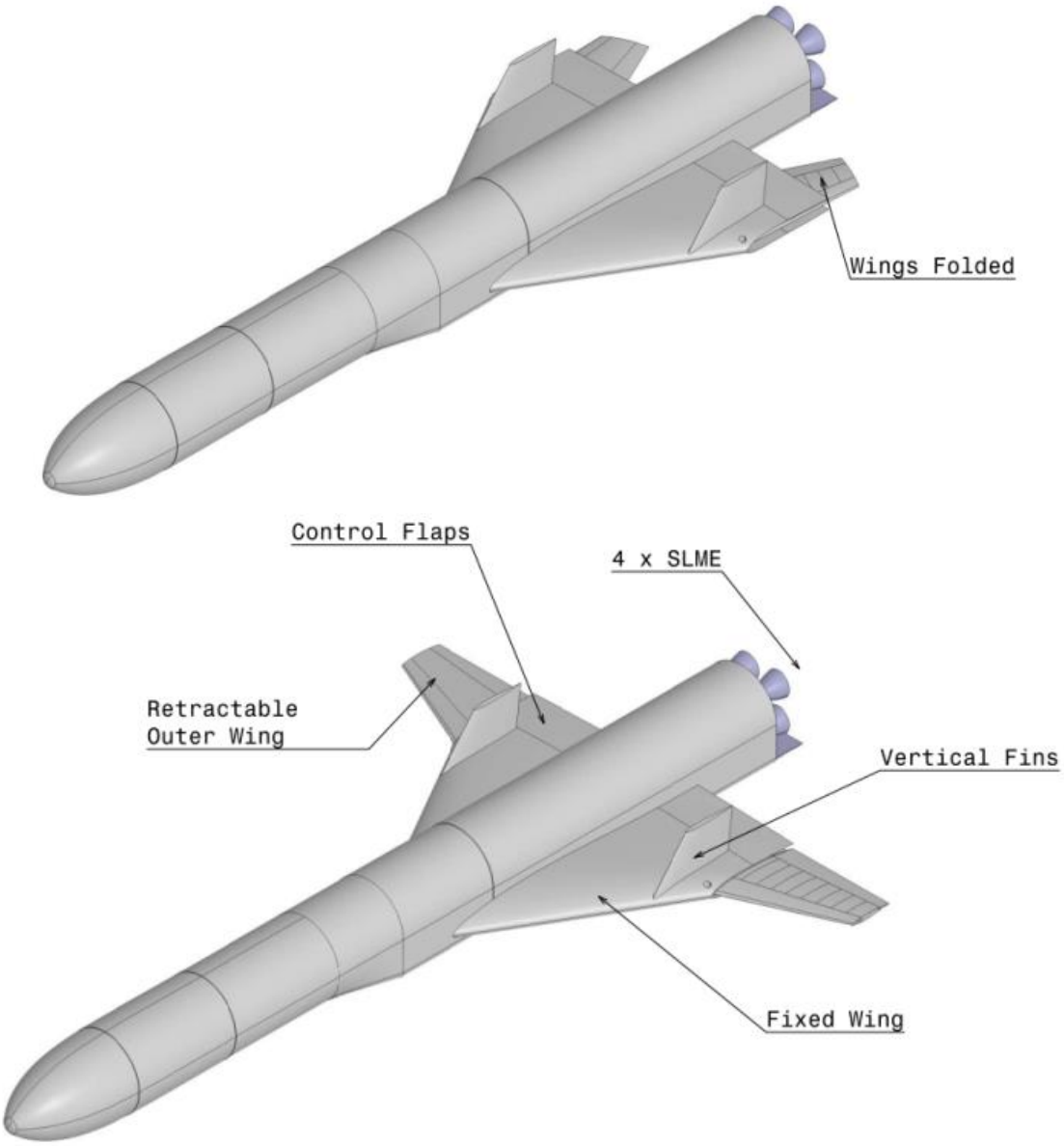

Figure 6-4: Conceptual Design of Folding-Wing First stage RLVC4-III-B with wings folded (top) and wings extended (bottom)

An internal view of the preliminary wing design including structures layout of both wing parts and the flaps is shown in Figure 6-5. The upper and lower rear parts of the fixed wing can be deployed as spoilers and thus adopt the role of non-existing trailing edge flaps. The inner rib and spar structure has to leave out space to accommodate for the outer wing. The landing gear box is positioned to consider sufficient distance to the CoG while allowing AoAs of 12° during landing. Any detailed landing gear design is not yet performed which might require modifications to the structural layout presented in Figure 6-5.

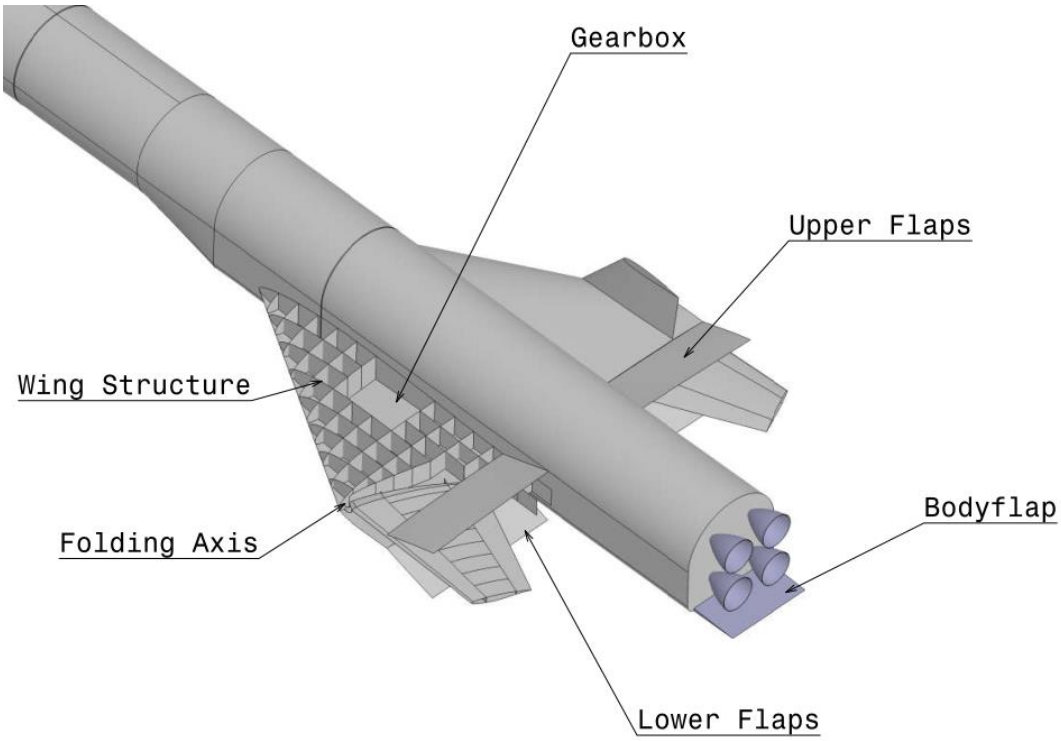

Figure 6-5: Preliminary structural layout of the folding wing stage RLVC4-III-B

6.3 Aerodynamic performance

The lift-to-drag ratio of the folding wing configuration is shown in Figure 6-6. In untrimmed subsonic flight, the L/D reaches values of 8 for untrimmed and slightly above 6.5 for trimmed conditions. This is a good value since it leads to a flight path angle of -8.75° during the In-Air-Capturing maneuver. The maximum trimmed L/D in hypersonic is 2 to 2.5. However, during re-entry the AoA is ought to be as high as possible to produce sufficient drag to decelerate the vehicle and sufficient lift to keep the maximum heat flux within boundaries. Hence, the L/D at re-entry conditions with AoAs of around 40°-50° is around 1.

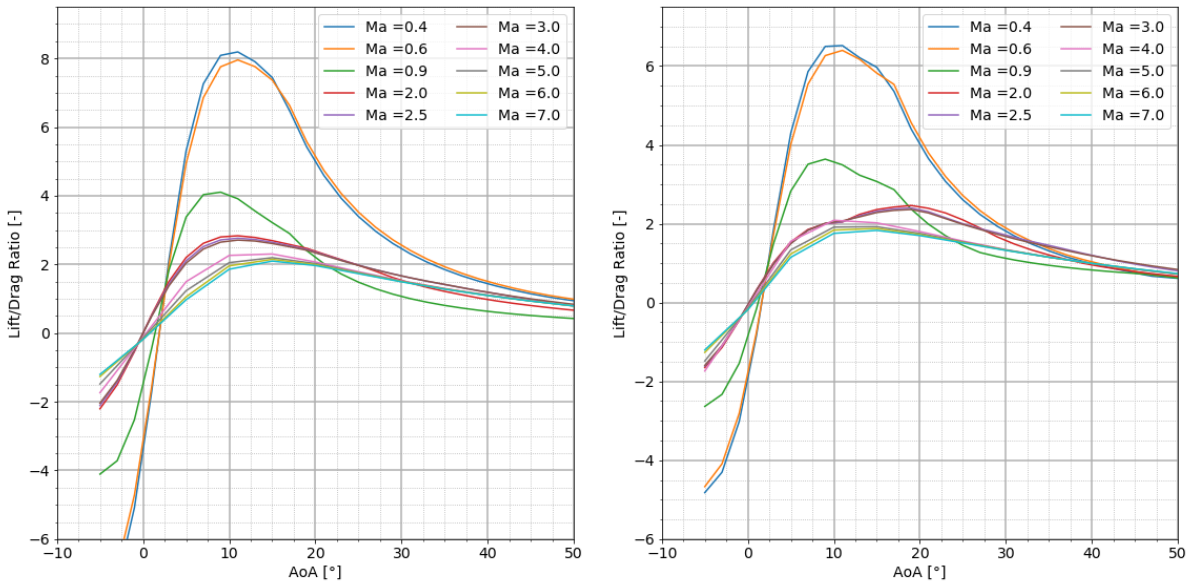

Figure 6-6: L/D of the folding wing configuration for untrimmed (left) and trimmed (right) flight

A further question that has to be answered is the trimmability of the vehicle in all flight conditions. As already mentioned, hypersonics requires high AoAs to control the re-entry. Figure 6-7 shows the moment coefficients for the folding wing stage from Mach 4 upwards. A stable trim point is found at cm=0 and $\partial cm/\partial \alpha \leq 0$. Hence, stable trim points can be found at high AoAs from Mach 4 upwards with a broader range of trimmable AoAs for higher Mach numbers.

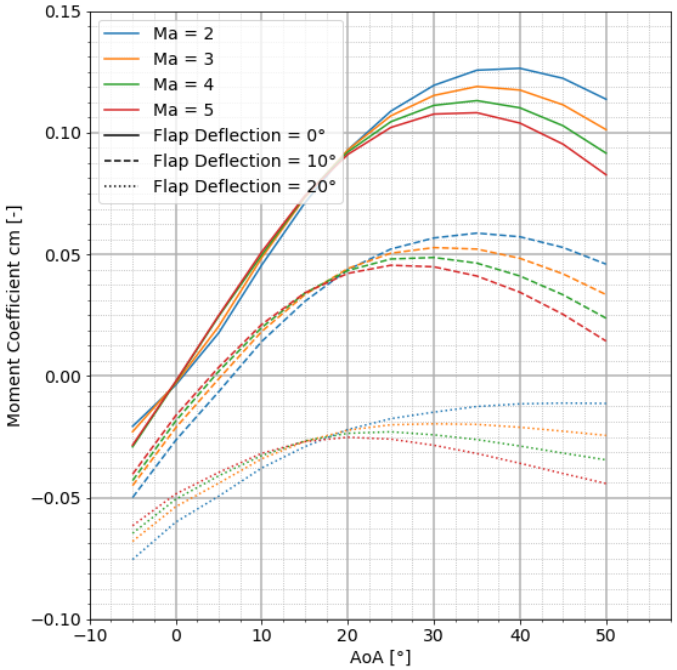

Figure 6-7: Moment Coefficients in hypersonics for folding wing first stage

6.4 Performance and Mass

The mass breakdown of the complete launcher with the folding-wing first stage is shown in Table 6-3. However, it is important to note that any folding wing design requires a folding mechanism with a certain mass. In this preliminary design phase the additional mass due to this folding mechanism was not considered yet. Only the additional mass by the overall greater wing area was considered.

Table 6-3: Launcher mass breakdown

H340 (RLV stage)	
Ascent Propellant	340000 kg
Dry Mass	69670 kg
GLOW	417800 kg
Structural Index incl. Engines	20.0%
H150 ELV	
Ascent Propellant	150000 kg
Deorbit Propellant	-
Dry Mass	17310 kg
GLOW including fairing	174210 kg
Structural Index incl. Engine w/o fairing	11.3%
H16 ELV	

Ascent Propellant	15300 kg
Deorbit Propellant	500 kg
Dry Mass	4225 kg
GLOW (incl. P/L)	32800 kg
Structural Index incl. Engine and multiple payload adapter	25.5%
separated payload GTO	12000 kg
Total GLOW	**624825 kg**

Figure 6-8 shows the ascent trajectory of the complete vehicle into the low transfer orbit. The ascent burns of 1st and 2nd stage propel the 3rd stage and payload to an altitude of roughly 140 km. The 3rd stage coasts along the ballistic trajectory (see section 6.1!) until reaching the equator where it ignites its engine to provide the final Δv required to reach GTO (not shown in Figure 6-8). RLV stage separation occurs at slightly less than 2 km/s (Mach 6.3) and an altitude of 64.3 km resulting in a dynamic pressure well below 1 kPa allowing a safe separation maneuver of the RLV and ELV stages in parallel arrangement. Further, the 2nd stage ignition is delayed by several seconds that the RLV has sufficient time for distancing. Full thrust of the single SLME on the H150 is assumed to be reached 8 s after separation when the upper segment is already in more than 70 km altitude (Figure 6-8). After approximately another 5 minutes of acceleration the MECO-conditions of the transfer LEO are achieved.

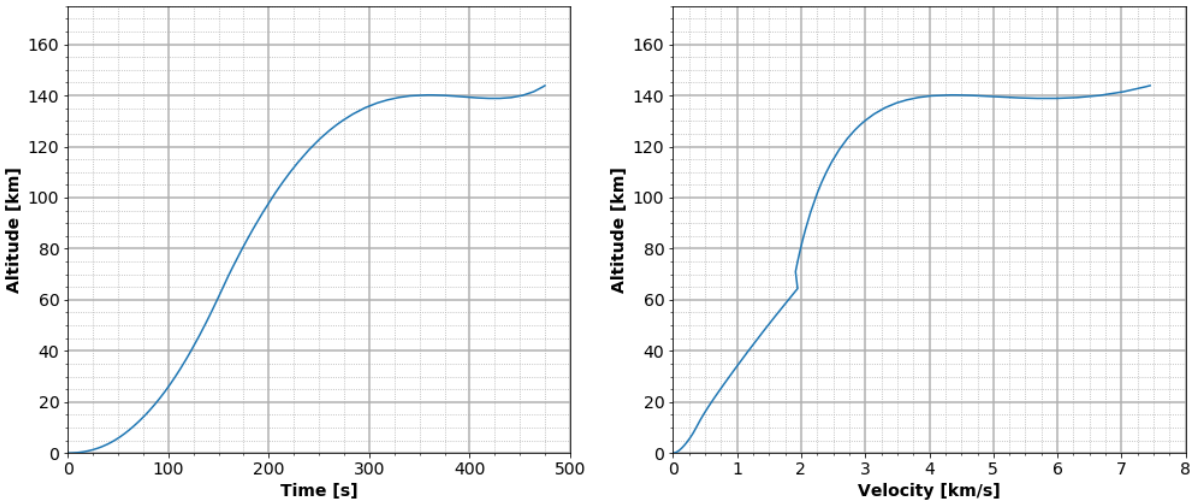

Figure 6-8: Ascent trajectory of 3STO RLVC4-III-B in transfer orbit 30 km x 600 km

6.5 Re-entry and corresponding loads

After its MECO and stage separation the winged RLV stage ascents in ballistic flight to an apogee slightly above 100 km (Figure 6-9). Around 200 seconds after stage separation during the stage's descent a rapid increase in aerodynamic forces and loads can be observed. The re-entry AoA is kept at 45° in the beginning of the atmospheric flight phase before α is rapidly reduced to less than 20° to limit the n_z load factor to a maximum of 3.5 g. The vehicle is controlled in a smooth reentry corridor without extensive skipping by adapting AoA and by banking which also initiates its heading change towards the launch site. The movable outer wing is preliminary assumed to be deployed at supersonic Mach number of 3 at an altitude of around 25 km. These conditions might be slightly adapted in future work to perform the transition maneuver at minimum dynamic pressure. After transitioning to subsonic velocity, the stage enters a steady gliding flight with an AoA that provides it the maximum trimmable L/D and flight path angle of around -8° favorable to starting the "in-air-capturing" maneuver approximately 12 minutes after stage separation.

The TPS of the system was preliminarily defined according to the calculated thermal loads experienced during re-entry of the GTO-mission. Figure 6-10 presents a distribution of windward side surface areas distinguished by the maximum external temperature reached during the mission. These areas help in selecting the most suitable TPS-type and usually each of them is designed with a constant insulation thickness in its sector. Depending on the expected temperature, the respective areas are covered with FRSI (Felt Reusable Surface Insulation) in lower temperature zones from 400 K - 600 K maximum surface temperature, AFRSI (advanced flexible reusable surface insulation) for 600 K – 900 K surface temperature, and TABI (tailored advanced blanket insulation) for temperatures from 900 K – 1200 K. The one-dimensional TPS sizing analyses performed for the complete vehicle along the full reentry trajectory intend to provide mission-dependent TPS mass, but not a preliminary functional architecture of this subsystem.

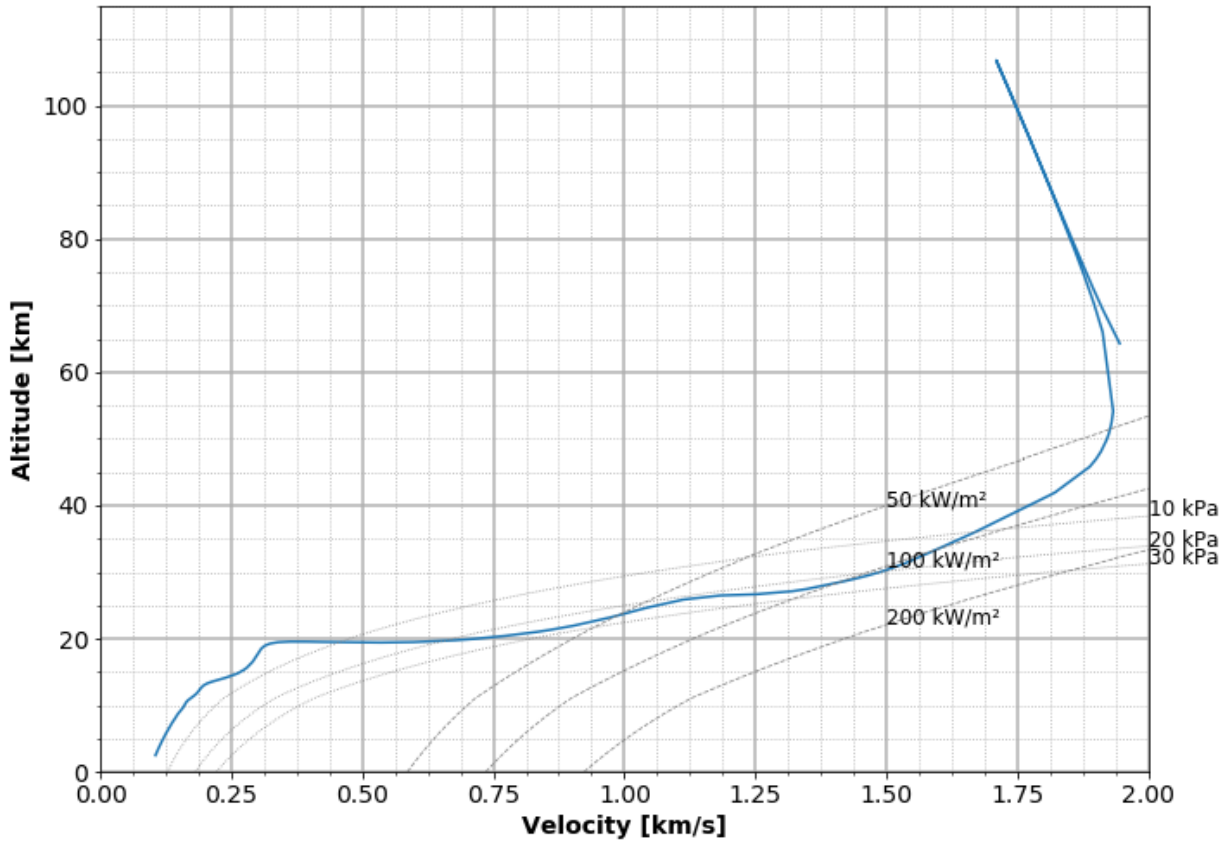

Figure 6-9: Descent trajectory (altitude vs. flight speed) of winged RLVC4-III-B first stage

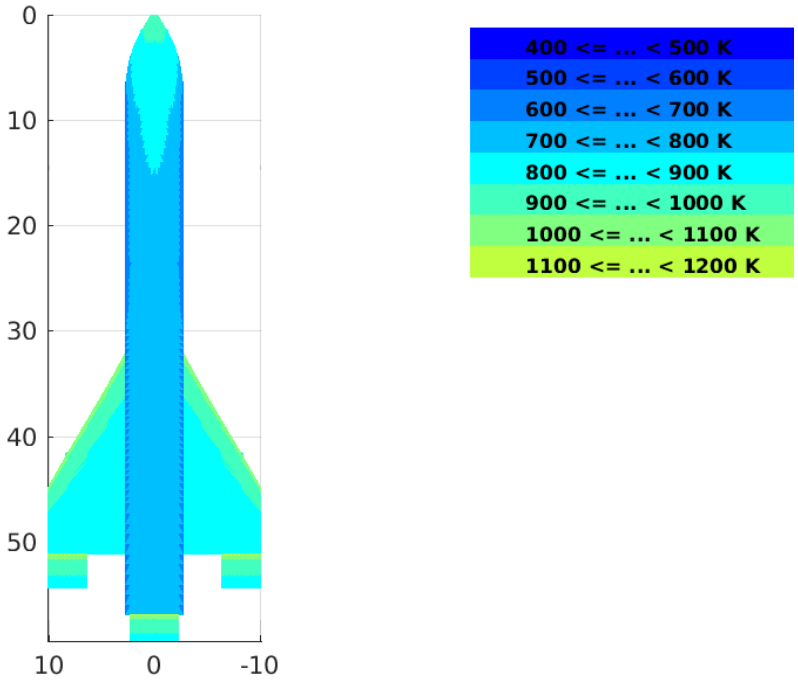

Figure 6-10: Areas of maximum temperature reached on the windward side of RLVC4-III-B first stage during re-entry

6.6 ASTOS Configuration and Trajectory Optimization

In this section, two scenarios will be analyzed using ASTOS software. The VTVL scenario contains the results of the optimization in case of a Vertical Landing scenario. The VTHL scenario contains the results of the optimization in case of an In-Air Capturing scenario, which ends with predefined capturing conditions imposed on altitude and Mach number/velocity.

By **Optimal Trajectory** we understand the following:

- Optimal evolution of states that put the vehicle into the desired target orbit and/or ground location
- Optimal attitude profile (control)
- Optimal masses (vehicle design)
- Optimal cost function (best mathematical cost possible)
- Satisfaction of all imposed constraints, being Initial/Final boundary constraints or path constraints

It is to be noted that the following ASTOS Configuration Optimization is adapting the propellant loading of all stages but keeps each stage structural index constant. This approach is somehow academic for launcher sizing and will be critically assessed when comparing obtained results with the reference stage launcher design of the previous sections 6.2 through 6.4.

6.6.1 FALCon VTVL Scenario

In this scenario the trajectory optimization of the ascent and fly back path of the RLV is performed using the ASTOS software. The first stage will perform a VTVL downrange landing (barge), but will have no constraint on landing location, in order to find the optimal landing location. The optimization is performed in 3-DoF.

6.6.1.1 Scenario setup and assumptions

6.6.1.1.1 Target mission

The launch site is located on Kourou. The location has the following coordinates and approximate altitude:

Table 6-4: Kourou Launch Site

Launch Site	Latitude [°]	Longitude [°]	Altitude [m]
Kourou	5.240322	-52.768602	0

The target orbit and payload are the following:

Table 6-5: Target Orbit and Payload

Target Orbit	Apogee [km]	Perigee [km]	Inclination [°]	Payload [kg]
GTO	35786.0	400.0	6	13000

6.6.1.1.2 Stage Data

The initial assumptions regarding the stage masses are stated in the table below. The data was provided by DLR in Bremen and was derived by a preliminary design of the respective launcher.

Table 6-6: Launcher Stage Data

Stage 1	
SI (including engines)	17.2 %
Baseline Propellant Mass	347 t
Stage 2	
SI (including engines)	11.9 %
Baseline Propellant Mass	153.5 t
Stage 3	
SI (including engines)	27.2 %
Baseline Propellant Mass	17 t
Fairing	
Total Mass	3000 kg

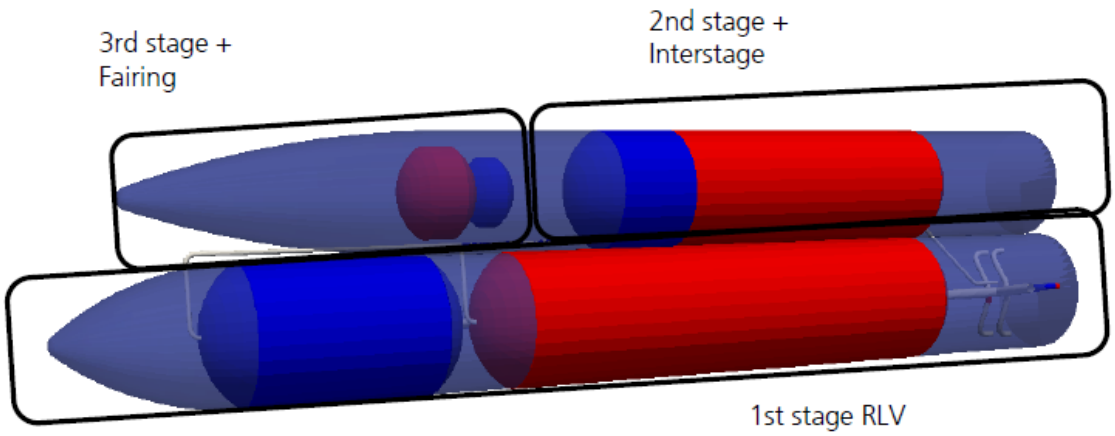

Figure 6-11: FALCon VTVL three stage to orbit system design

The Structural Index (SI) is defined as:

$$SI = \frac{m_{dry}}{m_{propellant}} \tag{6-1}$$

6.6.1.1.3 Engine Data

The assumptions regarding the engines used in the optimization process are stated in the table below. Further details about engine data can also be found in Table 6-1. It is important to mention that the VL version requires the SLME engines to be throttled during the return maneuver burns. These engines can be throttled down to 85%. However, throttling down the engines leads to a change in Isp (compare Table 6-7). Nevertheless, modeling the change in Isp is not possible with neither the ASTOS tool nor the DLR tool tosca. The change in Isp due to throttling is however so minor that the effect of that simplification on the outcome of the trajectory simulations is negligible.

Table 6-7: SLME Engine Data

1st Stage Engine: SpaceLiner Main Engine Derivative	
ISP Sea Level	390 s
ISP Vacuum	435 s
ISP Sea Level throttled	386 s
ISP vacuum throttled	438 s
O/F	6.5 (100%)
Massflow	553 kg/s (100%)
Number of engines in 1st Stage	4
Engine Throttle Capability	85 – 100 %
2nd Stage Engine: SLME Derivative with higher expansion ratio	
ISP Vacuum	451 s
O/F	5.5
Massflow	479 kg/s
Number of engines in 2nd Stage	1
Engine Throttle Capability	No
3rd Stage Engine: Vinci	
ISP Vacuum	457 s

1st Stage Engine: SpaceLiner Main Engine Derivative	
O/F	5.8
Massflow	39 kg/s
Number of engines in 3rd Stage	1
Engine Throttle Capability	No

The maximum number of engines of stage 1 were used only in the ascent phases. In the descent phases (Brake Before Atmosphere and Landing Brake) only one engine is used with a throttle capability of 85%-100%.

6.6.1.1.4 Aerodynamic Data

For this scenario we have used simplified aerodynamics, namely C_{Drag} and C_{Lift}.

The VTVL aerodynamics were provided both for the ascent and descent phases. The reference area considered in the ascent aerodynamics is 29 m^2. The reference area considered in the descent aerodynamics is 49.3 m^2. The aerodynamics for the angle of attack of 150 to 210 degrees are provided for the engine-first flight phases. The drag and lift coefficient curves for the whole flight of the full vehicle configuration are shown in Figure 6-12. The respective coefficients for the return flight of the first stage are shown in Figure 6-13.

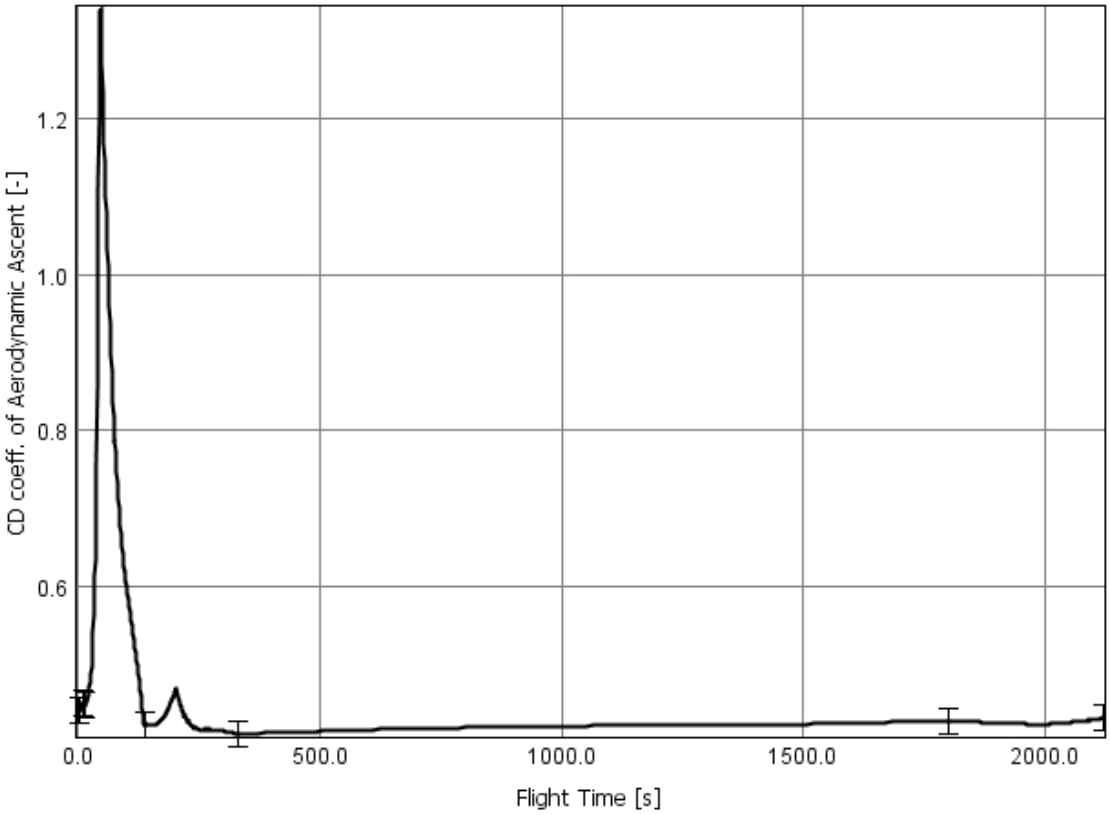

Figure 6-12: Drag Coefficient used in the Full Vehicle Ascent trajectory

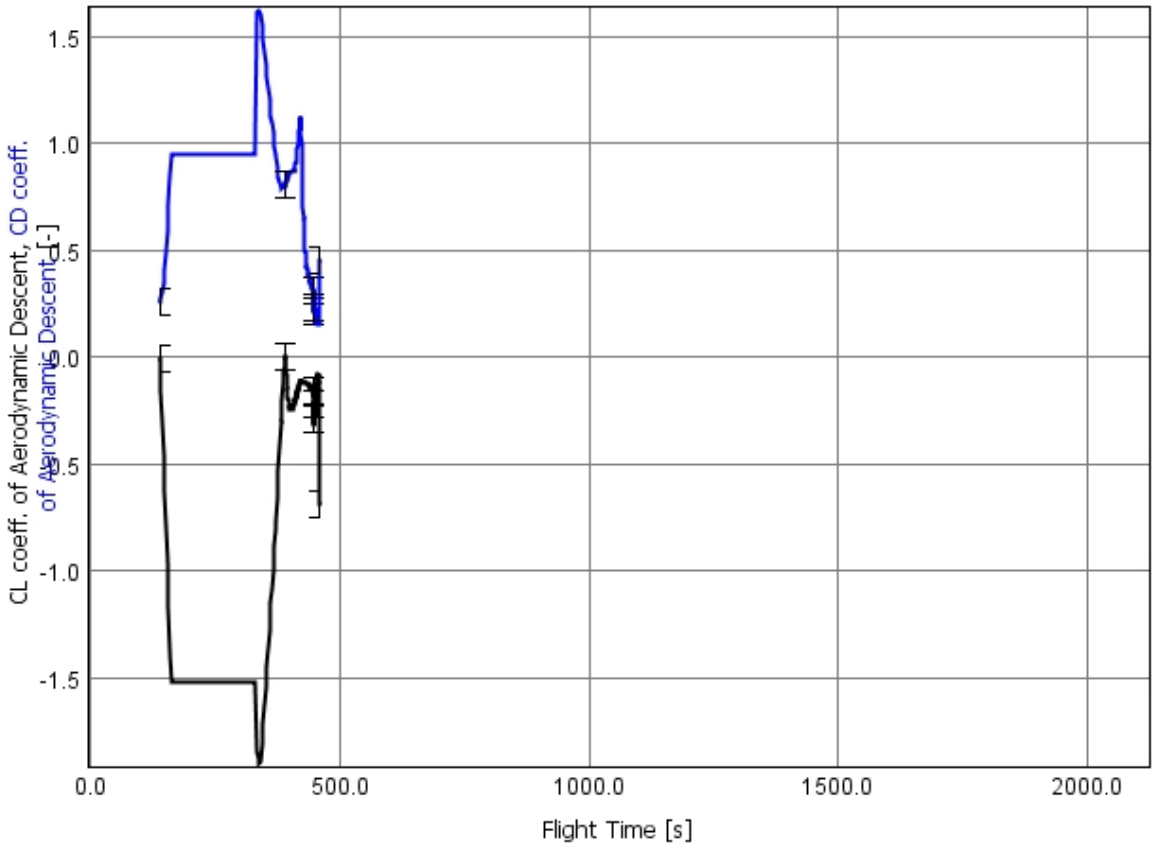

Figure 6-13: Lift and Drag Coefficients used in the Stage 1 Descent trajectory

6.6.1.1.5 Mission Phases

The mission phases in the VTVL scenario are detailed in the following tables.

Table 6-8: 1st Stage Mission Phases

Phase	Optimal Duration [s]
Lift Off	5.42055496468959
Pitch Over	6.8271823986924
Pitch Constant	1.9803444040130003
Gravity Turn	124.785967952048
Flip Maneuver	252.344341650794
Coast	55.368536827303
Burn Before Atmosphere	2.4236814539745
Coast Before Landing	0.1
Landing Burn	9.63452538991504

Table 6-9: Full Vehicle Mission Phases

Phase	Optimal Duration [s]
Lift Off	5.42055496468959

Phase	Optimal Duration [s]
Pitch Over	6.8271823986924
Pitch Constant	1.9803444040130003
Gravity Turn	124.785967952048
Fire Coast	0.5
Stage 2 Burn	190.284428510682
Coast to Injection	1471.89339509488
Stage 3 Burn	318.679467260699

6.6.1.1.6 Mission Constraints

The mission constraints, apart from the initial state and the target orbit are detailed in the following table.

Table 6-10: Mission Constraints

Constraint	Value
Maximum convective heat flux for nose radius of 0.5 m	200 kW/m^2
Maximum longitudinal load Factor	7
Maximum lateral load factor	3
Maximum Fairing Separation Heat Flux	1135 W/m^2
Maximum dynamic pressure	130 kPa
Maximum pitch rate during RCS phases	5 deg/s
Maximum pitch rate during RCS phases	5 deg/s
Maximum pitch rate in aerodynamically controlled phases	3 deg/s
Maximum yaw rate in aerodynamically controlled phases	3 deg/s
Final Altitude of 1st Stage	0 m
Maximum landing velocity of 1st stage	3 m/s
Final Minimum Perigee Altitude	400 km
Final Minimum Apogee Altitude	35786 km
Final Inclination	6 °

6.6.1.1.7 Cost Function

The cost function used in the optimization process is Minimum Initial Propellant. This cost term minimizes the total propellant mass of the vehicle at the beginning of a phase. Using this cost function, propellant mass of each stage is optimized in order to satisfy all the optimality criteria.

6.6.1.2 Optimization Results

6.6.1.2.1 Masses

The optimal masses are compared with the baseline masses in the table below. The baseline masses are from the preliminary design established at DLR. The GLOM of the RLV launcher calculated with the optimization procedure from ASTOS is about 17% less compared to the DLR SART baseline model. The 2nd stage experiences the greatest relative loss in propellant mass and the RLV stage's

propellant mass decreases by roughly 39%. This decrease in mass can partly be explained by the fact that the ASTOS tool uses an optimization algorithm to minimize the mass. However, further reasons can lead to the observed differences in mass.

First, it is important to note that the masses at DLR were obtained using a quasi-optimization. This quasi optimization is treating the ascent and descent phases separately, a combined optimization of both phases is not possible. Furthermore, the ascent is divided into two subsections that are separately optimized. Hence, the obtained trajectories might not be the global optimum. A major contribution to the big mass reduction is the absence of a significant re-entry burn. While in the DLR simulated trajectory the re-entry burn is around 12 s, the ASTOS optimized trajectory features a 2 s re-entry burn. A short burn reduces the amount of propellant needed and thus the “inert mass” which has to be accelerated during ascent. The consequence is great reduction in mass. Nevertheless, it is debatable if such a short re-entry burn might not be too short since it is an unknown to which extent the RLV stage can withstand the re-entry loads.

Other reasons for the observed differences are the simplified approach with a constant structural index. Hence, with a decrease in propellant mass the SI is assumed to stay constant. However, for launch vehicles the SI increases with lower propellant masses, thus leading to relatively higher dry masses. Since this effect is not linear it is difficult to determine its exact effect on the calculated masses. Furthermore, the ascent orbit has a great influence on the mission performance. Since the ascent orbits can differ from the ASTOS to the DLR version, this can have a major impact on performance as well.

Table 6-11: Final Optimized Masses

	Baseline Mass [kg]	Optimized Mass [kg]
1st Stage Propellant Mass	347000	320042.2047
1st Stage Dry Mass	59684	54036.77159
2nd Stage Propellant Mass	153500	92941.82221
2nd Stage Dry Mass	18266	10846.40271
3rd Stage Propellant Mass	17000	12673.34066
3rd Stage Dry Mass	4624	3380.551789
Fairing	3000	3000
Payload	13000	13000
GLOW	**616074**	**509921.0937**

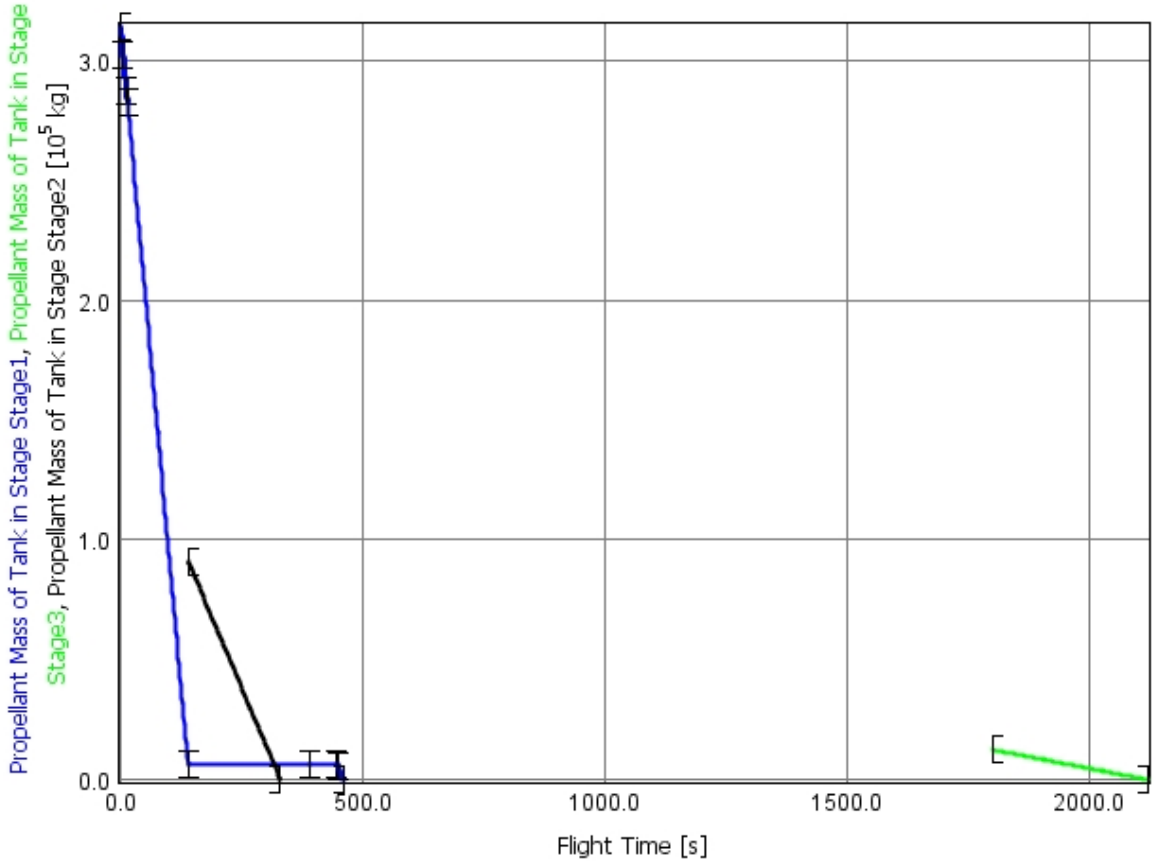

Figure 6-14: Optimal Propellant Masses of all the Stages over time

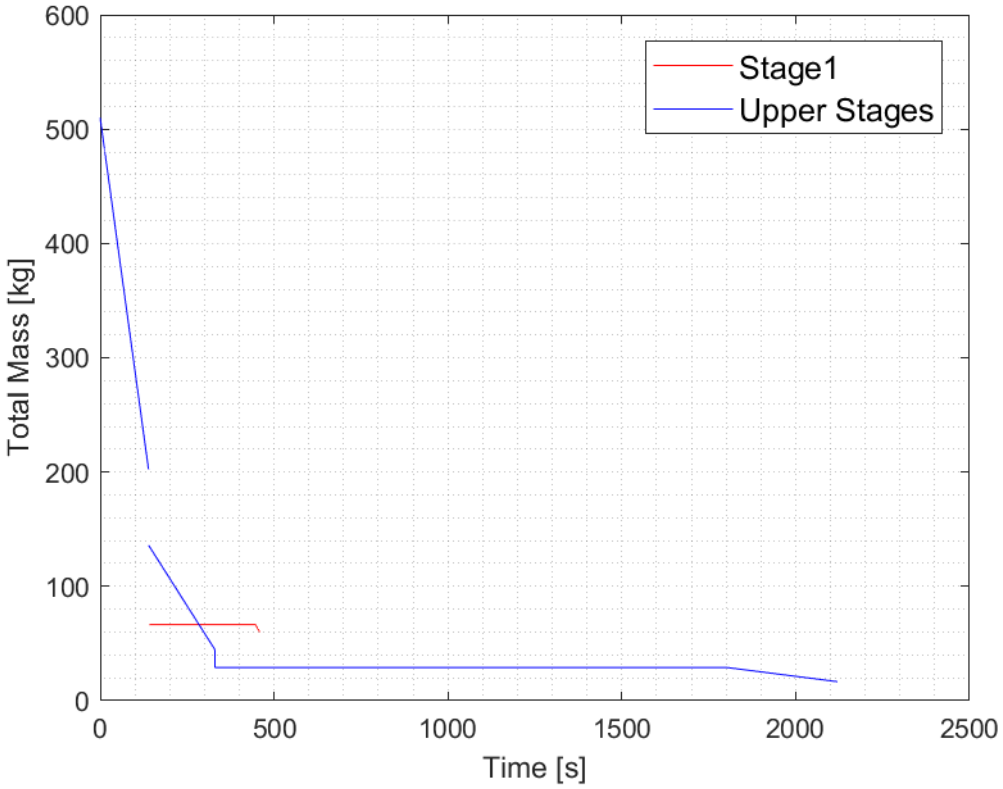

Figure 6-15: Optimal profile of the total mass of the vehicle

6.6.1.2.2 Constraints fulfillment

The constraints fulfillment can be checked in the table below.

Table 6-12: Mission Constraints Fulfillment

Constraint	Limit	Optimization
Maximum convective heat flux for nose radius of 0.5 m	200 kW/m^2	161 kW/m^2
Maximum longitudinal load factor	7	6.73
Maximum lateral load factor	3	2.46
Maximum Fairing Separation Heat Flux	1135 W/m^2	1135 W/m^2
Maximum dynamic pressure	130 kPa	106 kPa
Maximum pitch rate during RCS phases	5 deg/s	1.5 deg/s
Maximum yaw rate during RCS phases	5 deg/s	1.5 deg/s
Maximum pitch rate in aerodynamically controlled phases	3 deg/s	1 deg/s
Maximum yaw rate in aerodynamically controlled phases	3 deg/s	1.5 deg/s
Final Altitude of 1st Stage	0 m	0 m
Maximum landing velocity of 1st stage	3 m/s	3 m/s
Final Minimum Perigee Altitude	400 km	400 km
Final Minimum Apogee Altitude	35786 km	35786 km
Final Inclination	6 °	6 °

Details related to the constraints fulfillment can be seen in the figures below.

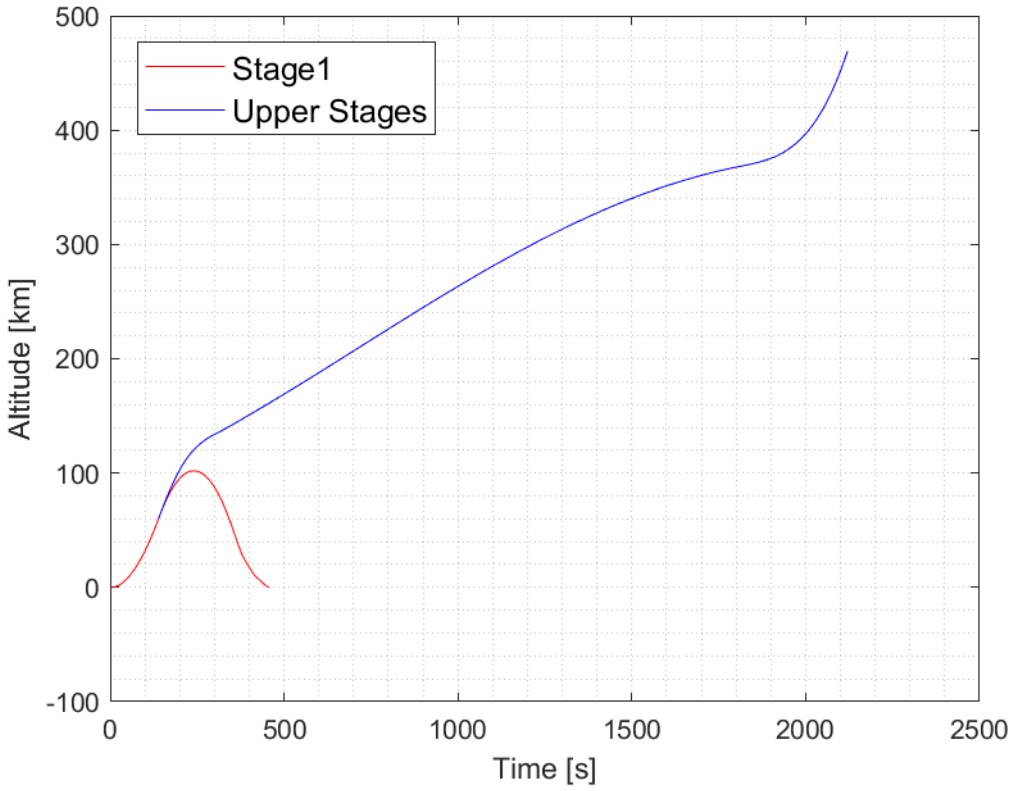

Figure 6-16: Altitude Profile

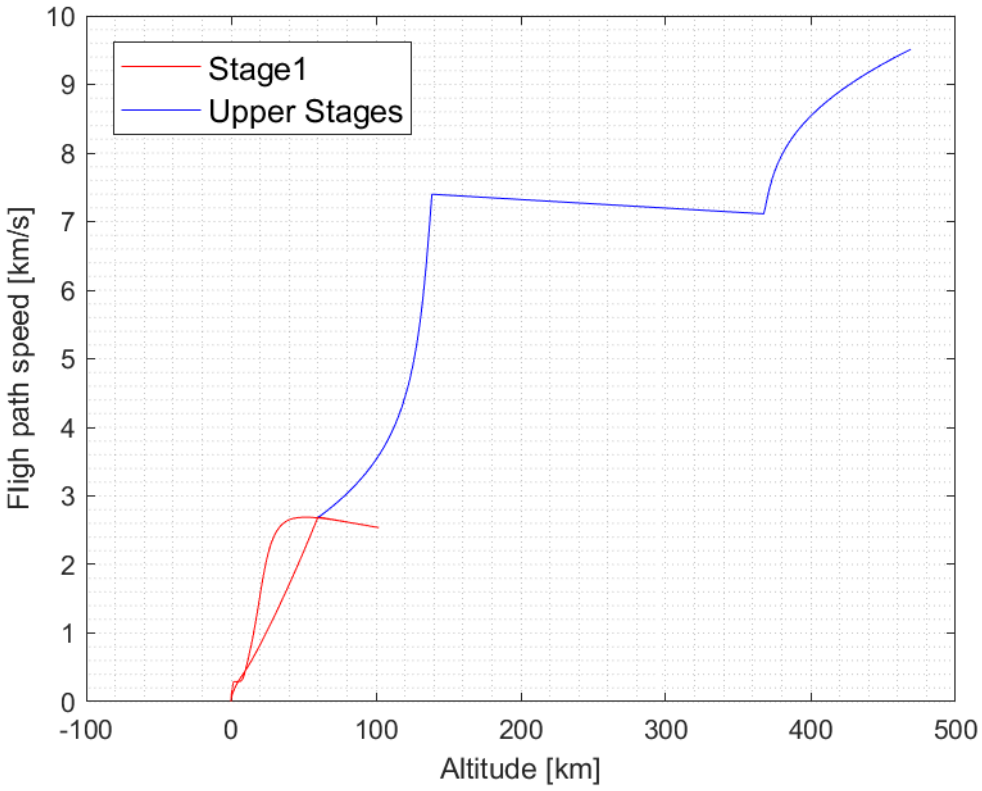

Figure 6-17: Altitude vs Flight Path Speed Profile

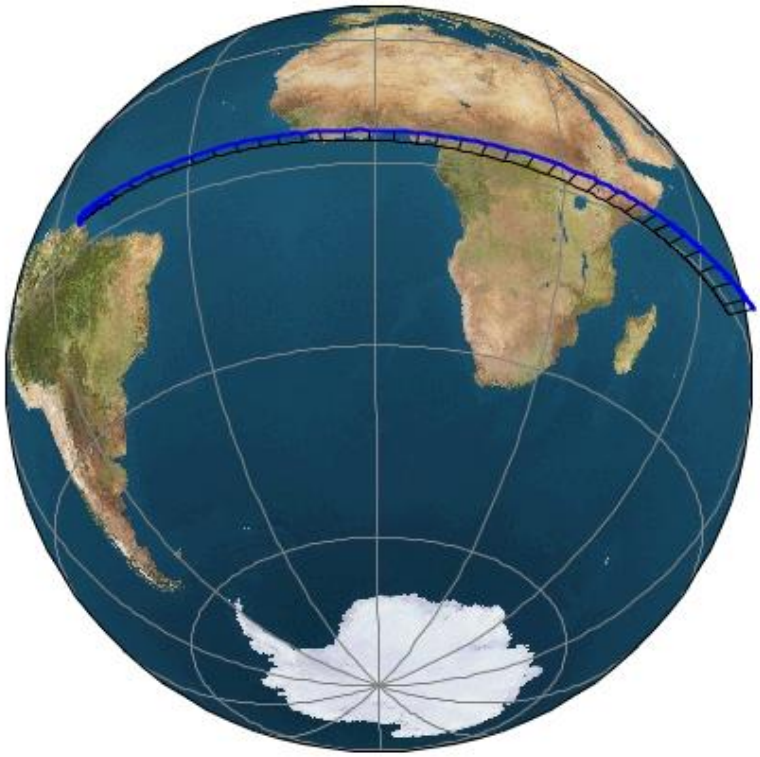

Figure 6-18: Satellite View of the Mission

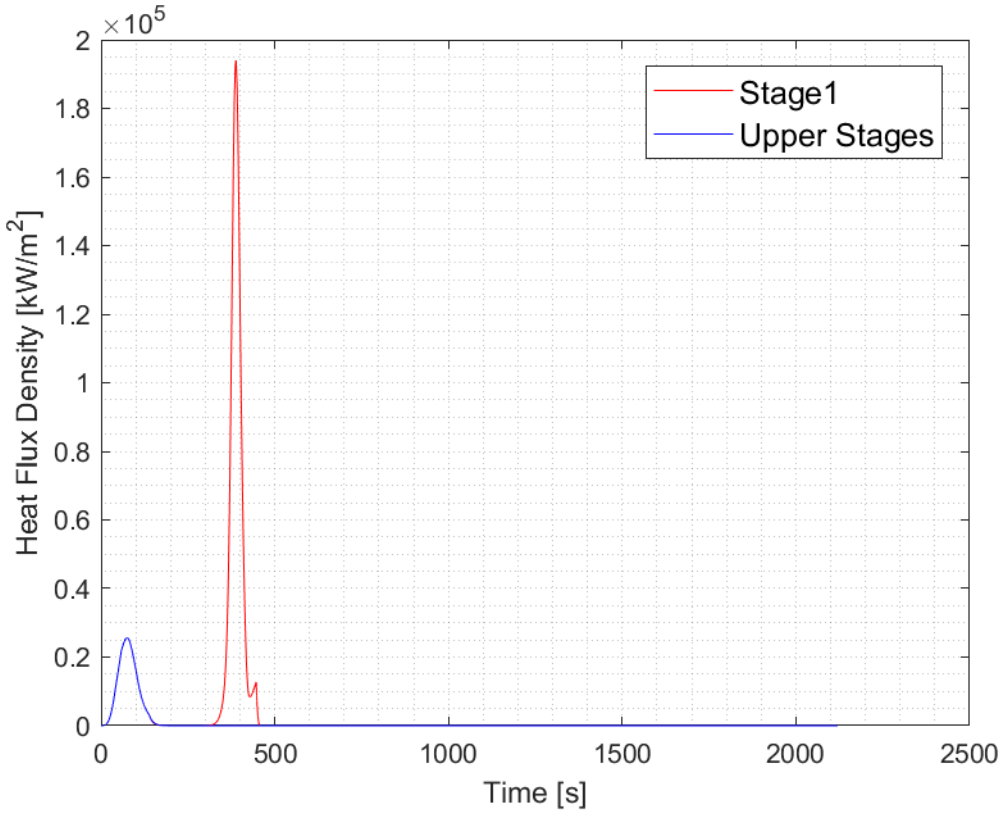

Figure 6-19: Heat Flux Density Profile (Free Stream)

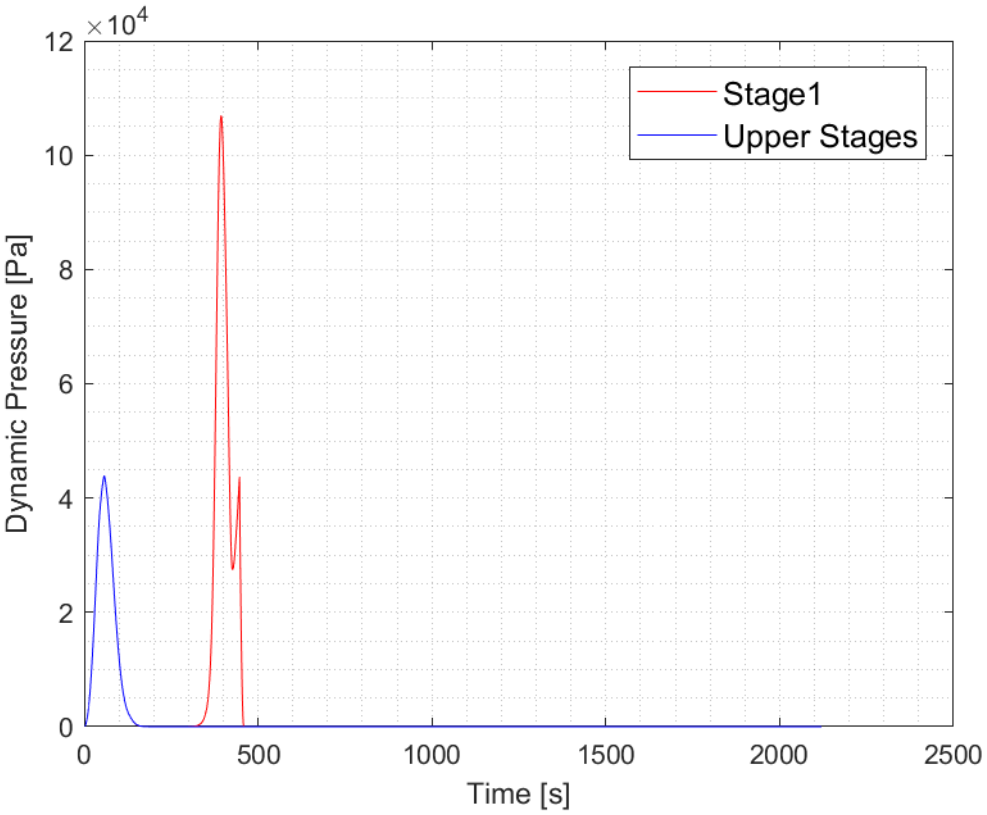

Figure 6-20: Dynamic Pressure Profile

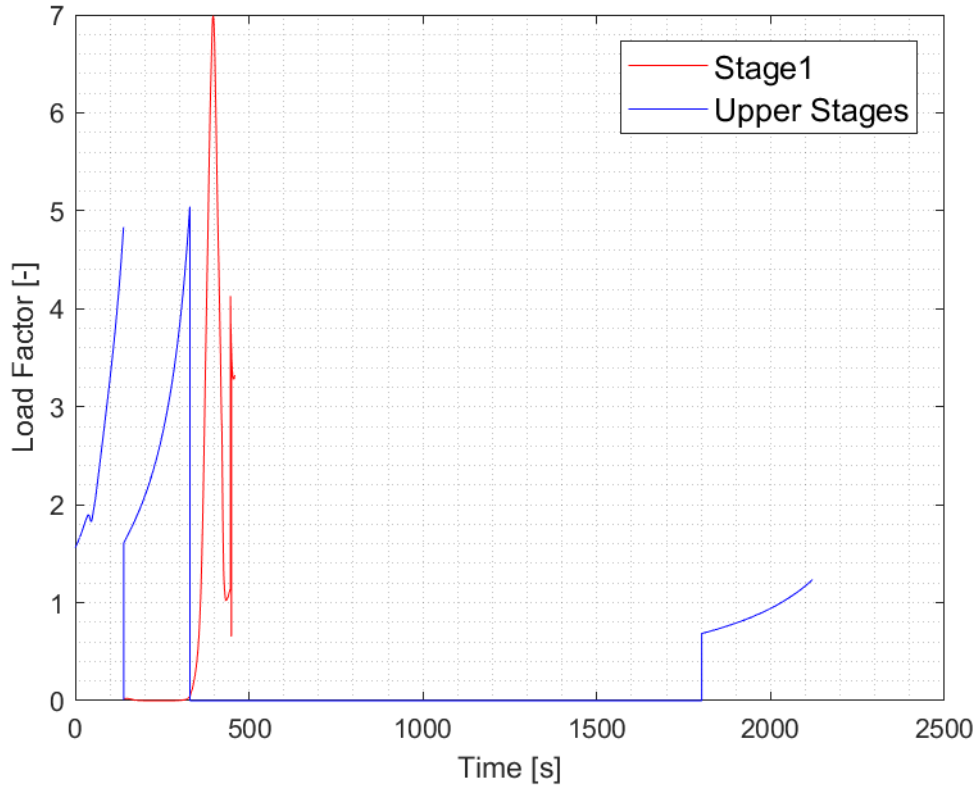

Figure 6-21: Total Load Factor Profile

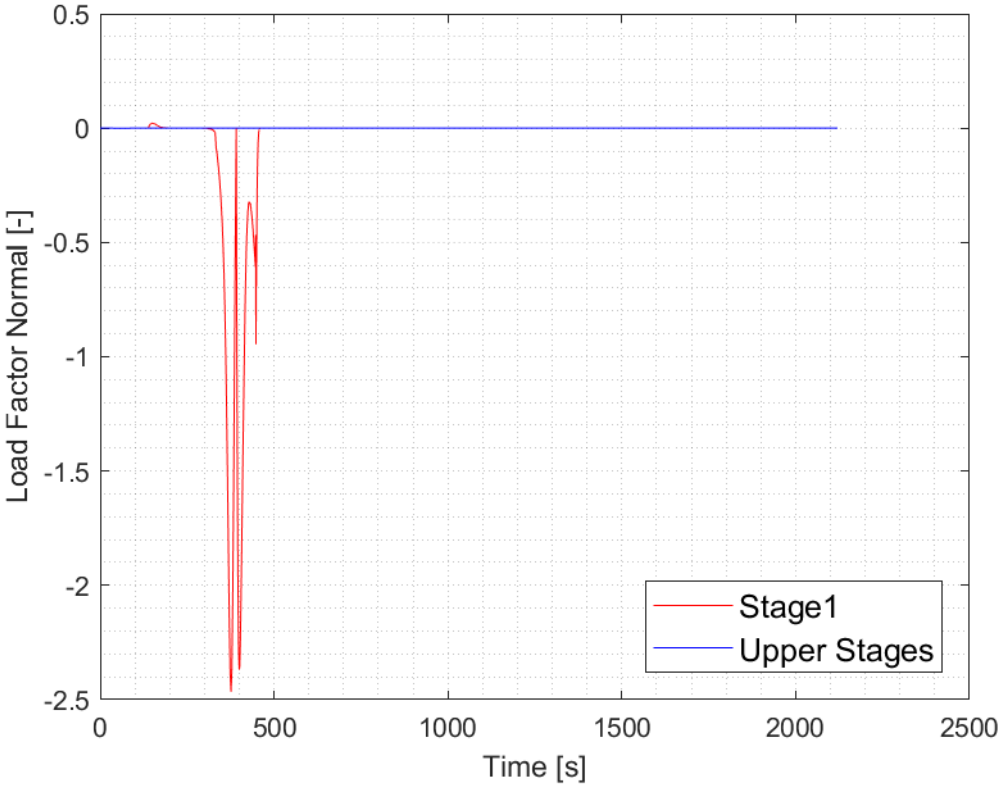

Figure 6-22: Load Factor Normal (nz)

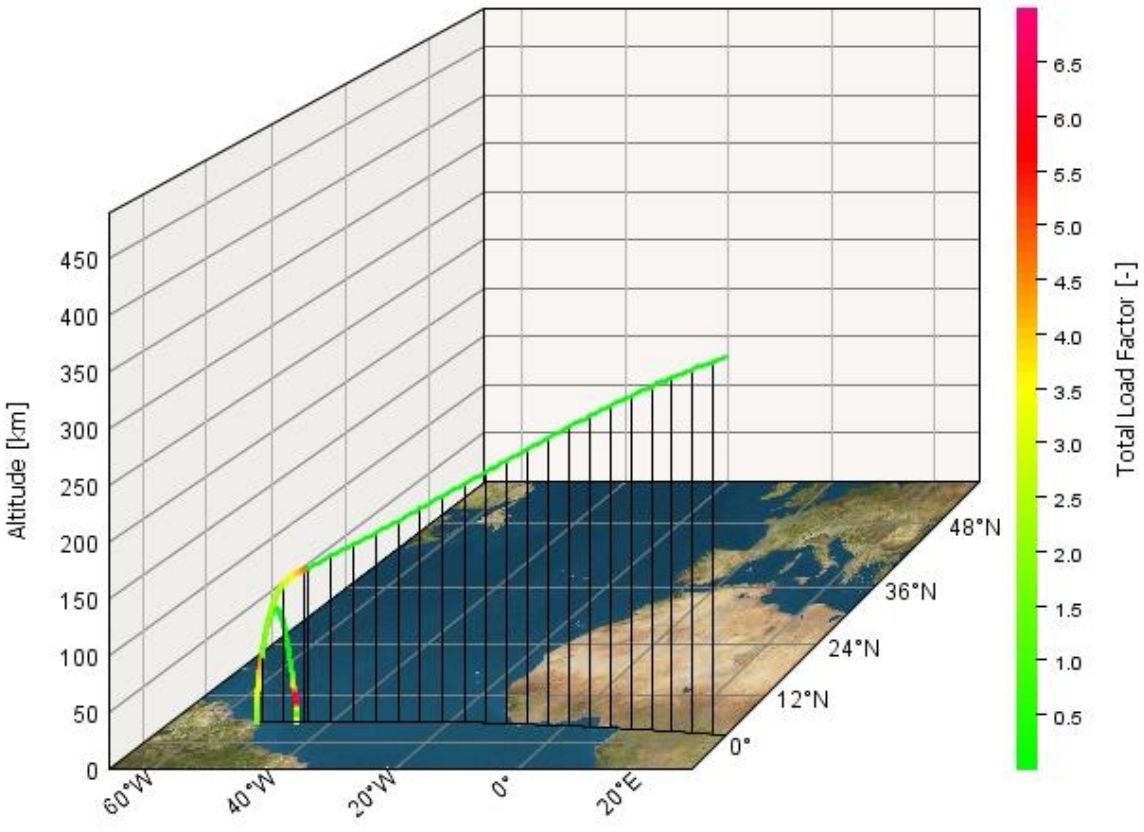

Figure 6-23: 3D Trajectory and Total Load Factor

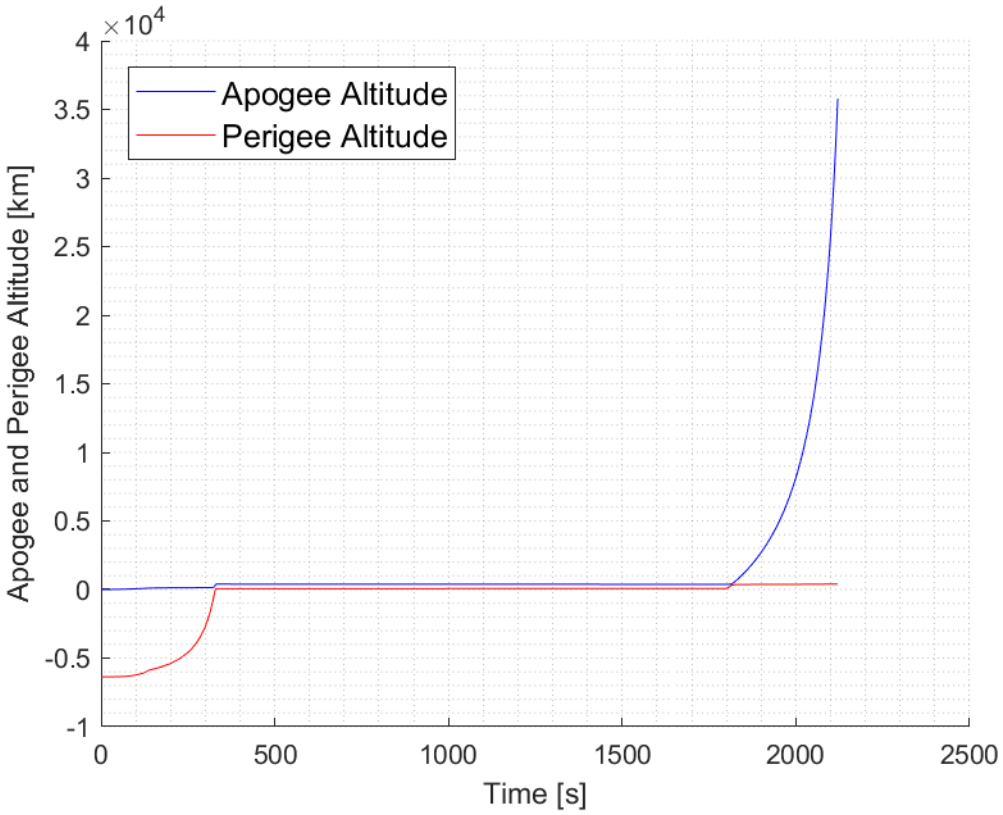

Figure 6-24: Final Orbit Profile

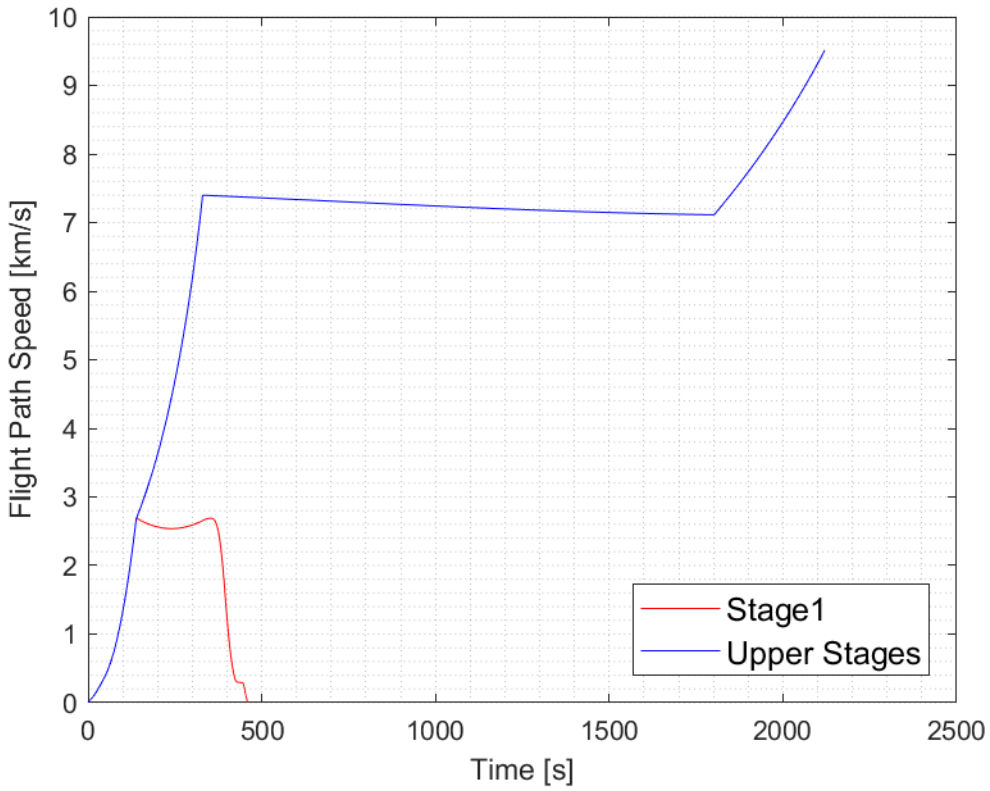

Figure 6-25: Flight-Path Speed Profile

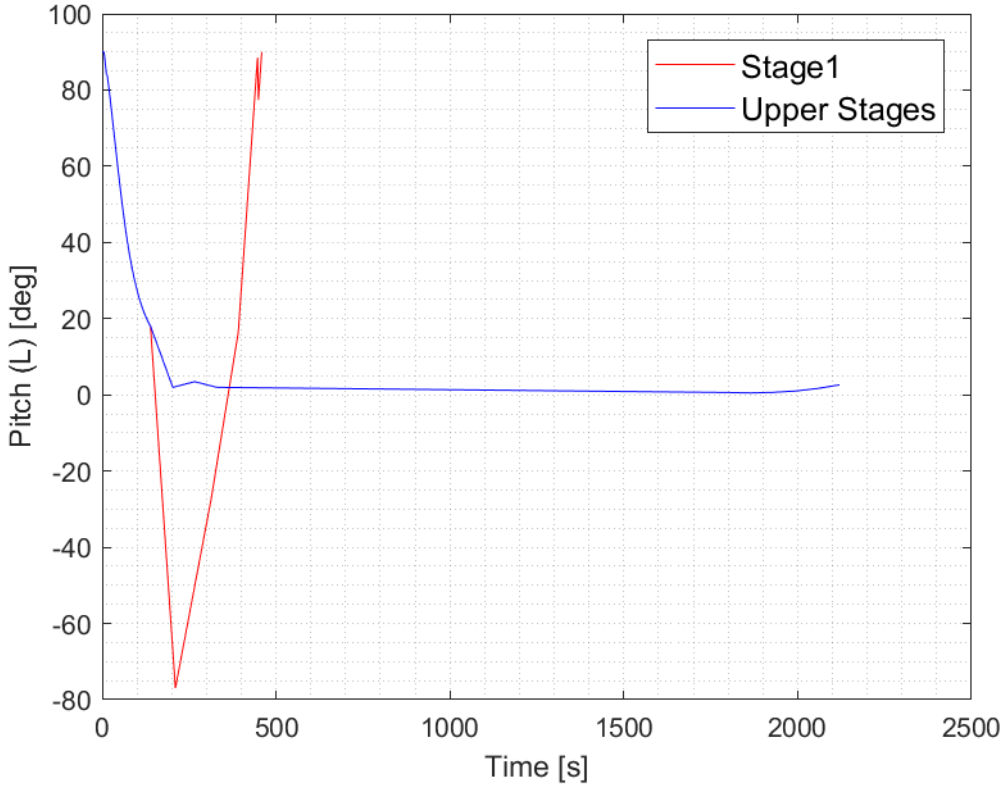

Figure 6-26: Pitch Profile

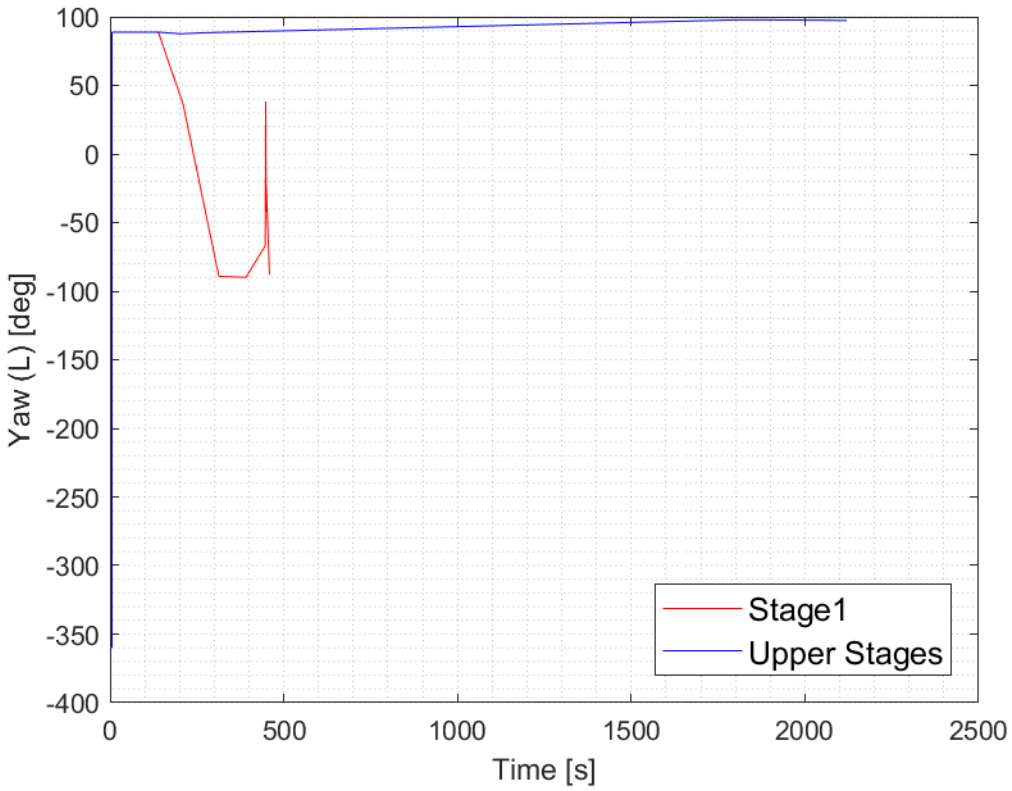

Figure 6-27: Yaw Profile

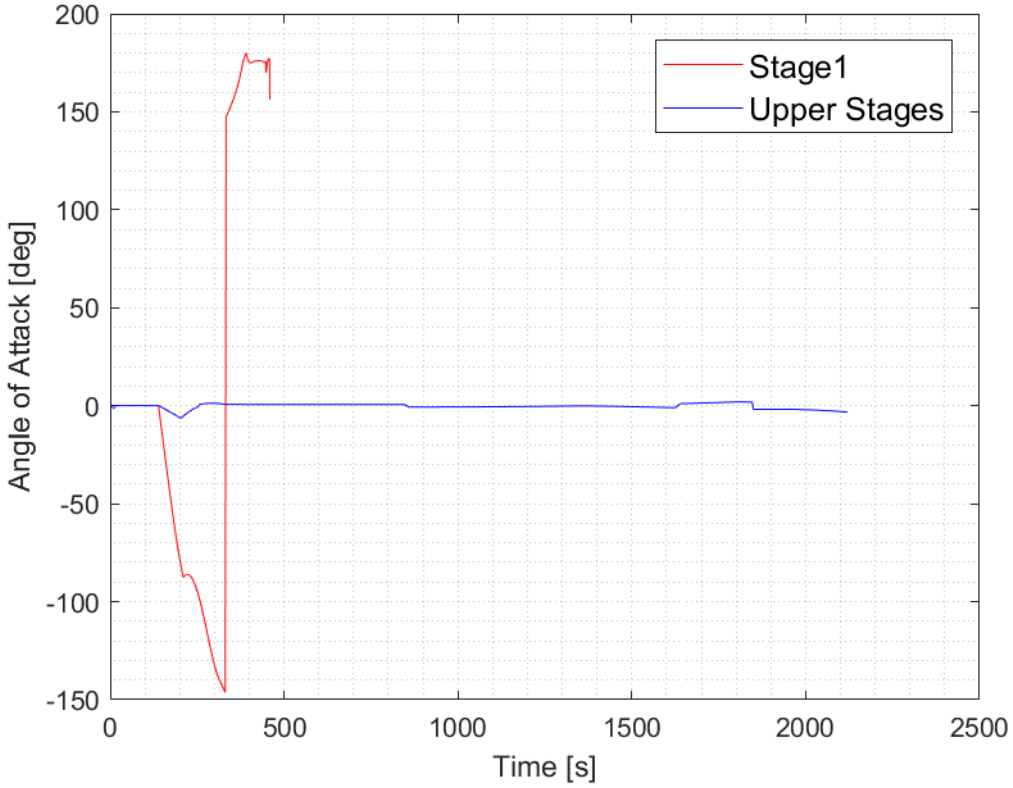

Figure 6-28: Angle of Attack Profile

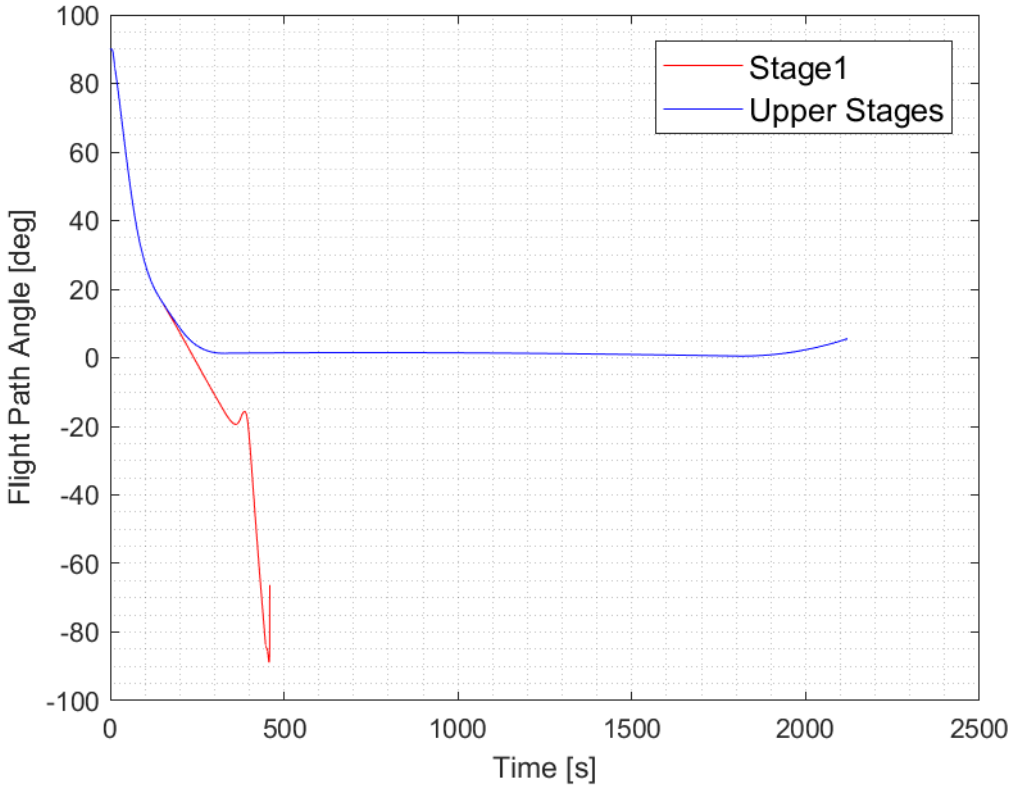

Figure 6-29: Flight path angle Profile

6.6.2 FALCon VTHL Scenario

In this scenario the trajectory optimization of the ascent and glide back path to an In-Air Capturing state of the RLV is performed using ASTOS software.

6.6.2.1 Scenario setup and assumptions

6.6.2.1.1 Target mission

The launch site is located in Kourou. The location has the following coordinates and approximate altitude:

Table 6-13: Kourou Launch Site

Launch Site	Latitude [°]	Longitude [°]	Altitude [m]
Kourou	5.240322	-52.768602	0

The target orbit and payload are the following:

Table 6-14: Target Orbit and Payload

Target Orbit	Apogee [km]	Perigee [km]	Inclination [°]	Payload [kg]
GTO	35786.0	400.0	6	13000

6.6.2.1.2 Stage Data

The initial assumptions regarding the stage masses are stated in the table below. As for the VTVL system the masses and design was established first at DLR and then provided to ASTOS for further optimization. The preliminary (baseline) data is described in Table 6-15. The structural indices are directly based on the full scale RLV reference launcher as presented in the previous sections 6.1 to 6.5.

Table 6-15: Stage Data

Stage 1	
SI (including engines)	20 %
Baseline Propellant Mass	340 t
Stage 2	
SI (including engines)	11.3 %
Baseline Propellant Mass	150 t
Stage 3	
SI (including engines)	25.5 %
Baseline Propellant Mass	15.8 t
Fairing	
Total Mass	3000 kg

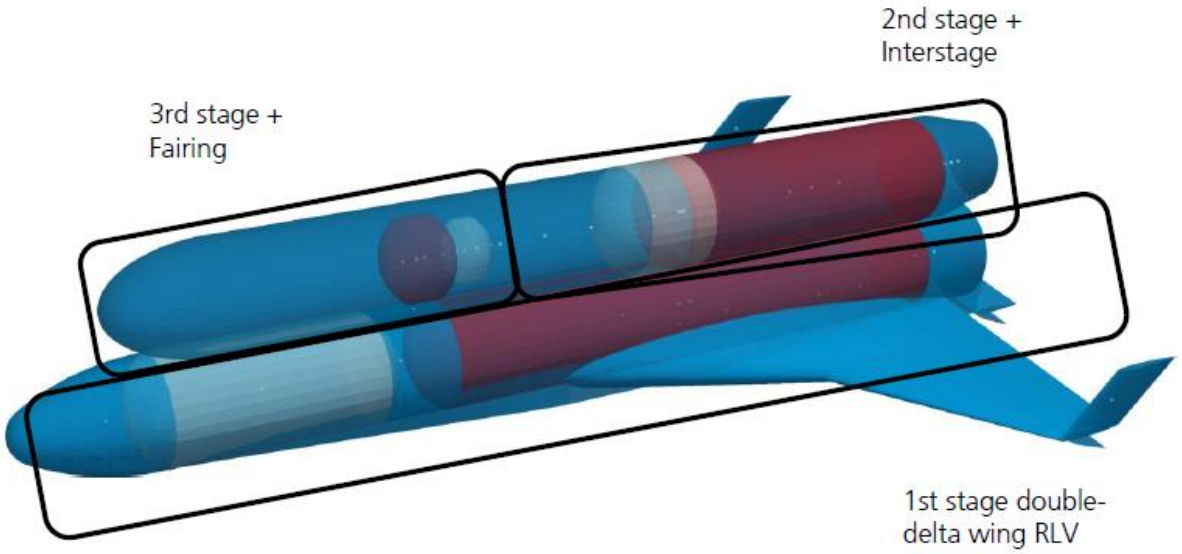

Figure 6-30: FALCon VTHL three stage to orbit system design

The Structural Index (SI) is defined as:

$$SI = \frac{m_{dry}}{m_{propellant}} \tag{6-2}$$

6.6.2.1.3 Engine Data

The assumptions regarding the engines used in the optimization process are stated in the table below (compare Table 6-7). In the descent phases no engine is used.

Table 6-16: SLME-Engine Data

1st Stage Engine: SpaceLiner Main Engine Derivative	
ISP Sea Level	390 s
ISP Vacuum	435 s
O/F	6.5 (100%)
Massflow	553 kg/s (100%)
Number of engines in 1st Stage	4
Engine Throttle Capability	85 – 100 %
2nd Stage Engine: SLME Derivative with higher expansion ratio	
ISP Vacuum	451 s
O/F	5.5
Massflow	479 kg/s
Number of engines in 2nd Stage	1
Engine Throttle Capability	No
3rd Stage Engine: Vinci	
ISP Vacuum	457 s
O/F	5.8

1st Stage Engine: SpaceLiner Main Engine Derivative	
Massflow	39 kg/s
Number of engines in 3rd Stage	1
Engine Throttle Capability	No

6.6.2.1.4 Aerodynamic Data

For this scenario we have used simplified aerodynamics, respectively C_{Drag} and C_{Lift}. The VTHL aerodynamics were provided both for the ascent and descent. The reference area considered in the ascent aerodynamics is 29 m^2. The reference area considered in the descent aerodynamics is 22.9 m^2. The respective aerodynamic coefficients for the full vehicle ascent are shown in Figure 6-31. The aerodynamic coefficients for the winged first stage are shown in Figure 6-32.

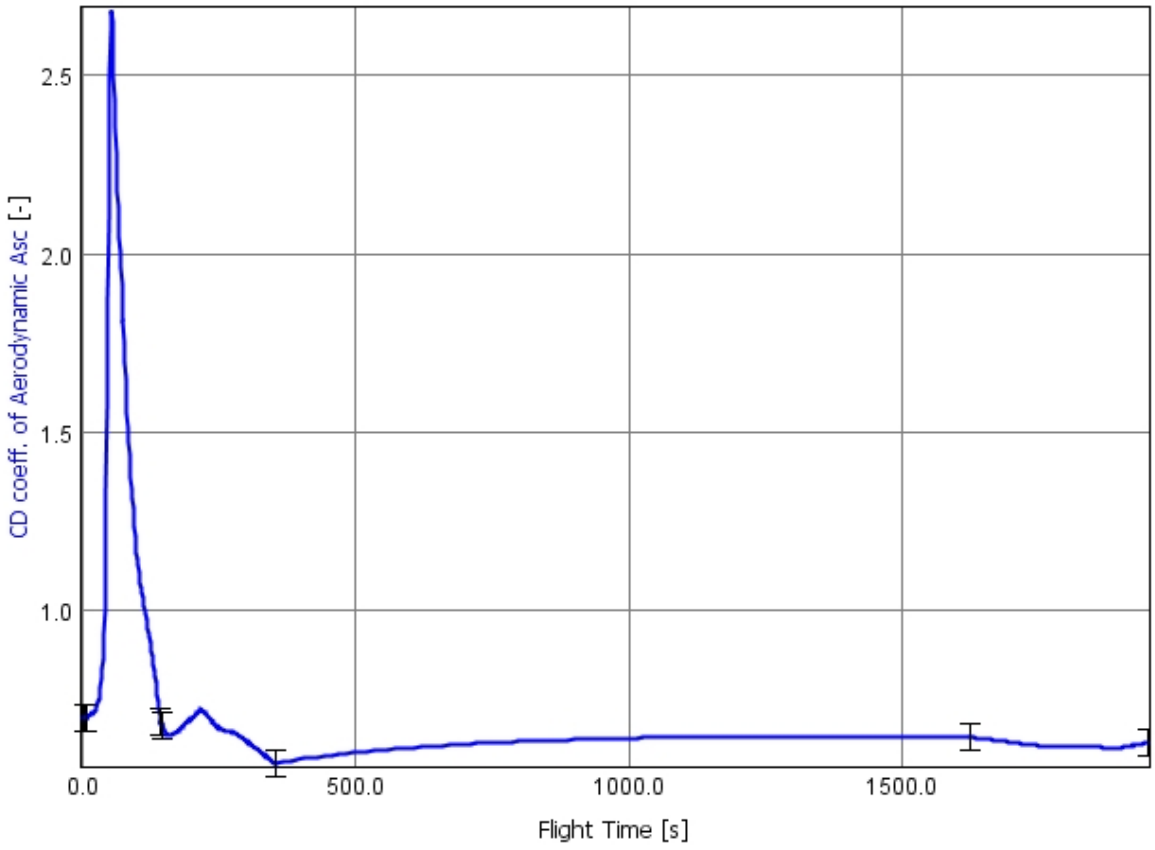

Figure 6-31: Drag Coefficient used in the Full Vehicle Ascent trajectory

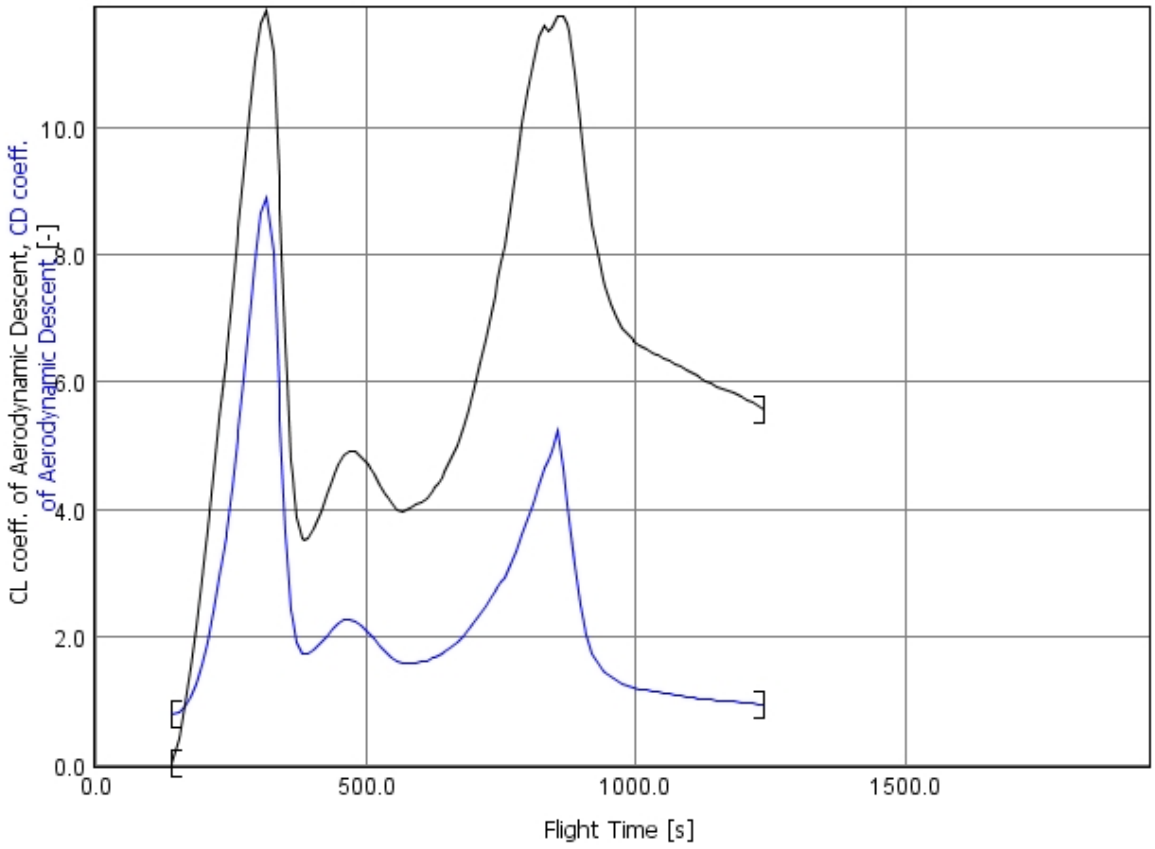

Figure 6-32: Lift and Drag Coefficients used in the Stage 1 Descent trajectory

6.6.2.1.5 Mission Phases

The mission phases in the VTHL scenario are detailed in the following tables.

Table 6-17: 1st Stage Mission Phases

Phase	Optimal Duration [s]
Lift Off	2.4715477825494
Pitch Over	3.5955643388664504
Pitch Constant	0.545389080338138
Gravity Turn	135.198638337174
Coast with Aerodynamic Brake	1095.42590303992

Table 6-18: Full Vehicle Mission Phases

Phase	Optimal Duration [s]
Lift Off	2.4715477825494
Pitch Over	3.5955643388664504
Pitch Constant	0.545389080338138
Gravity Turn	135.198638337174

Phase	Optimal Duration [s]
Fire Coast	5
Stage 2 Burn	206.90722350277298
Coast to Injection	1268.09166074986
Stage 3 Burn	326.557786084724

6.6.2.1.6 Mission Constraints

The mission constraints, apart from the initial state and the target orbit are detailed in the following table.

Table 6-19: Mission Constraints

Constraint	Value
Maximum convective heat flux for nose radius of 0.5 m	As low as possible
Maximum longitudinal load factor	7
Maximum lateral load factor	3.5
Maximum Fairing Separation Heat Flux	1135 W/m^2
Maximum dynamic pressure	45 kPa
Final Altitude of 1st Stage	9 km
In-Air Capturing Velocity of 1st stage	150 m/s
Final Minimum Perigee Altitude	400 km
Final Minimum Apogee Altitude	35786 km
Final Inclination	6 °

6.6.2.1.7 Cost Function

The cost function used in the optimization process is Minimum Initial Propellant. This cost term minimizes the total propellant mass of the vehicle at the beginning of a phase. Using this cost function, propellant mass of each stage is optimized in order to satisfy all the optimality criteria.

6.6.2.2 Optimization Results

6.6.2.2.1 Masses

The optimal masses are compared with the baseline masses in the table below. As for the VTVL, the masses obtained from the ASTOS optimization are much lower compared to the DLR masses. The same reasons that were explained for the VTVL are leading to the observed decrease. The relative decrease in GLOM is ~16%. Especially the 2nd stage experiences a great decrease, but not as pronounced as for the VL system. The reason for that is that the absence of a significant re-entry burn for the VL system greatly decreased the mass whereas the HL system decelerates via aerodynamic forces only.

Table 6-20: Final Optimized Masses

	Baseline Mass [kg]	Optimized Mass [kg]
1st Stage Propellant Mass	340000	319552.1734
1st Stage Dry Mass	69670	62737.24813
2nd Stage Propellant Mass	150000	101060.9987

	Baseline Mass [kg]	Optimized Mass [kg]
2nd Stage Dry Mass	17310	11199.26729
3rd Stage Propellant Mass	15800	12986.648
3rd Stage Dry Mass	4225	3247.617183
Fairing	3000	3000
Payload	13000	13000
GLOW	**624825**	**526783.9527**

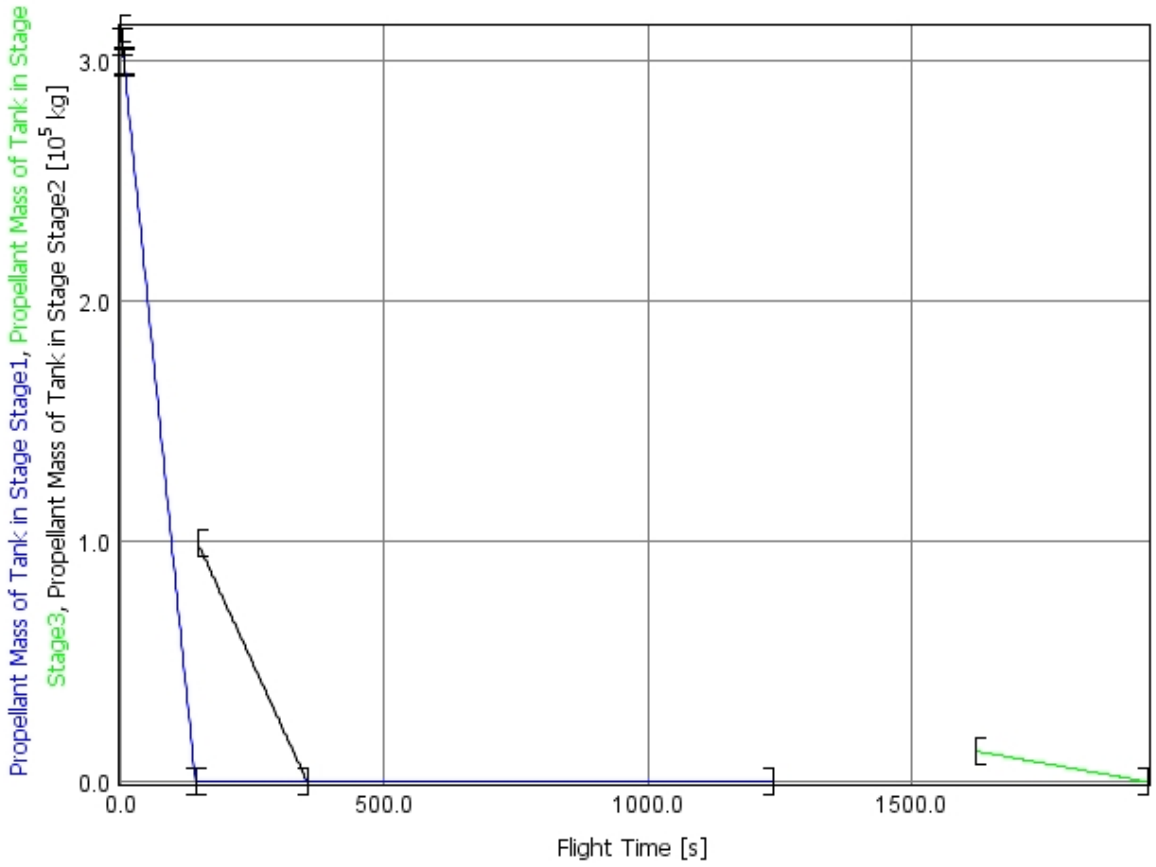

Figure 6-33: Optimal Propellant Masses of All the Stages over time

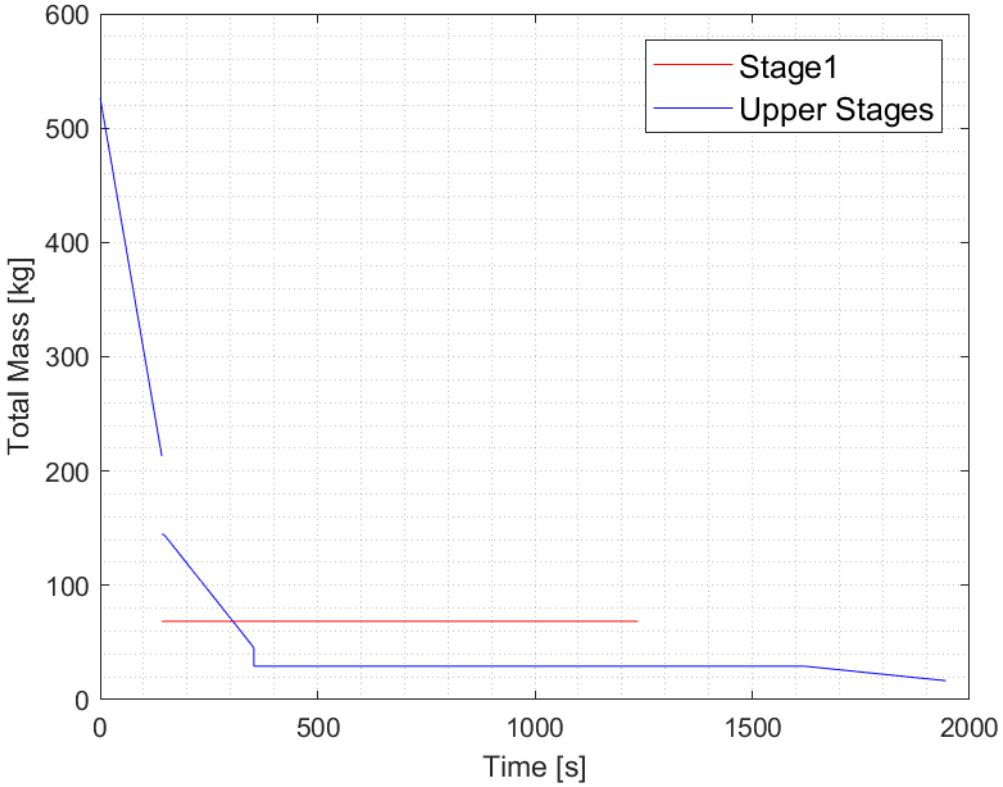

Figure 6-34: Optimal profile of the total mass of the vehicle

6.6.2.2.2 Constraints fulfillment

The constraints fulfillment can be checked in Table 6-21.

Table 6-21: Mission Constraints Fulfillment

Constraint	Limit	Optimization
Maximum convective heat flux for nose radius of 0.5 m	As low as possible	110.24 kW/m^2
Maximum longitudinal load factor	7	4.96
Maximum lateral load factor	3.5	3.25
Maximum Fairing Separation Heat Flux	1135 W/m^2	1135 W/m^2
Maximum dynamic pressure	45 kPa	33.95 kPa
Final Altitude of 1st Stage	9 km	8.99 km
In-Air Capturing Velocity of 1st stage	150 m/s	149 m/s
Final Minimum Perigee Altitude	400 km	400 km
Final Minimum Apogee Altitude	35786 km	35786 km
Final Inclination	6 °	6 °

Details related to the constraints fulfillment can be seen in the figures below.

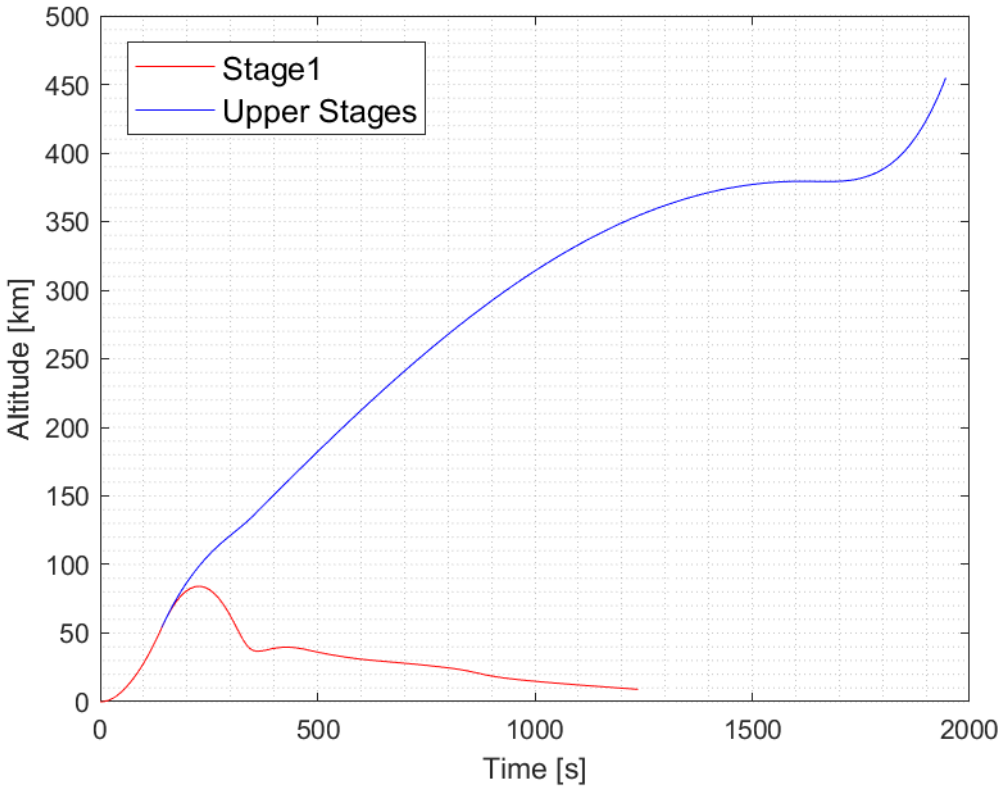

Figure 6-35: Altitude vs Time Profile

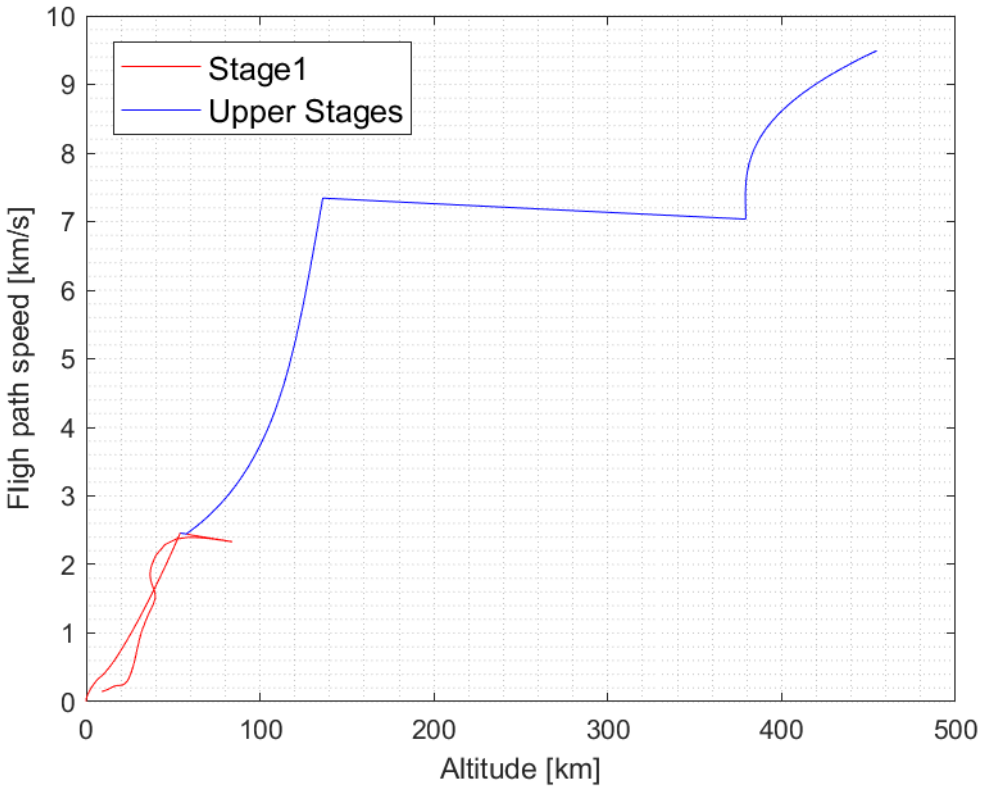

Figure 6-36: Altitude vs Flight Path Speed Profile

Figure 6-37: Satellite View of the Mission

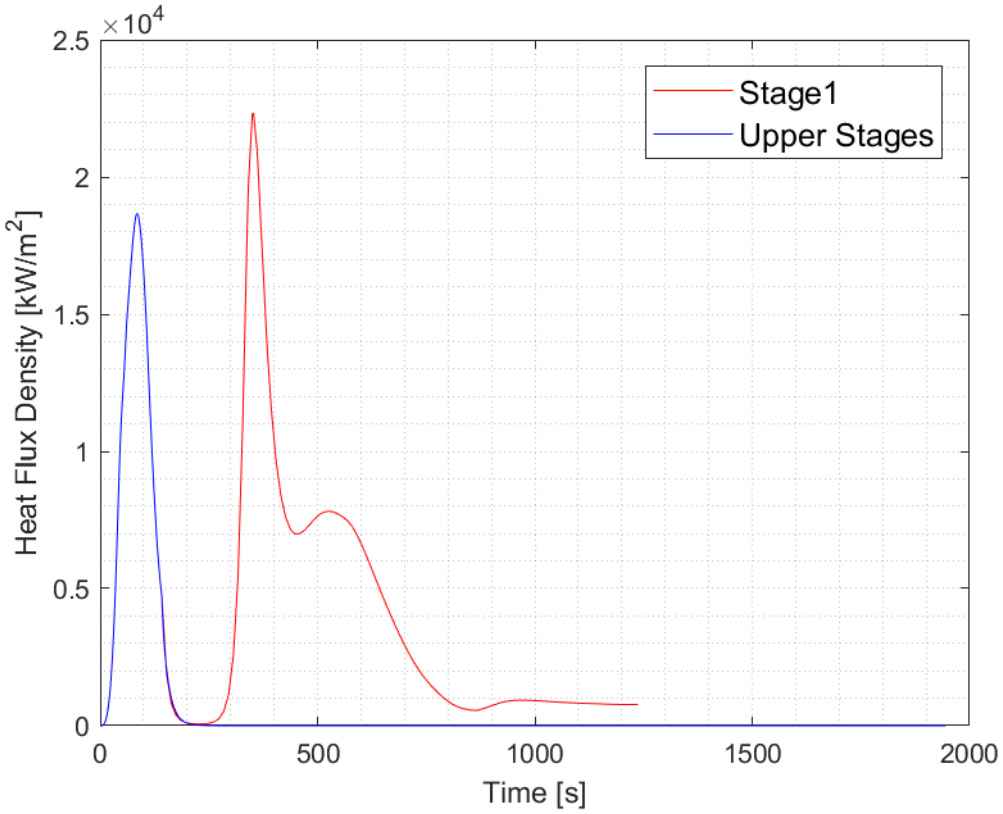

Figure 6-38: Heat Flux Density Profile (Free Stream)

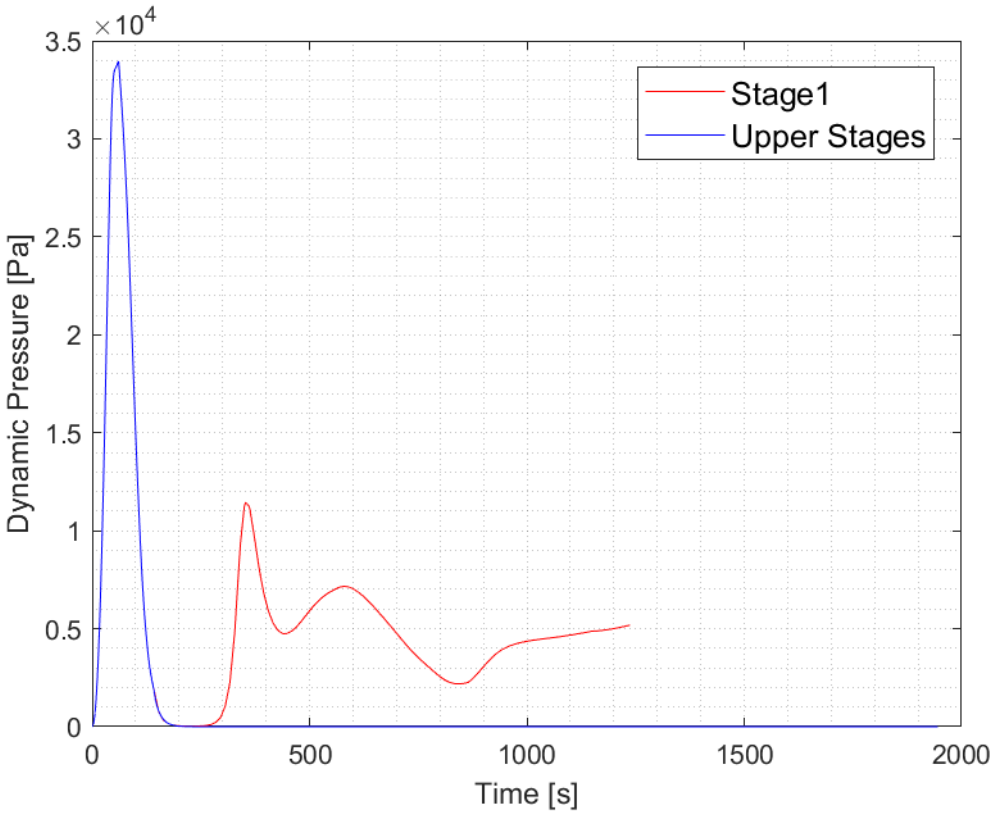

Figure 6-39: Dynamic Pressure Profile

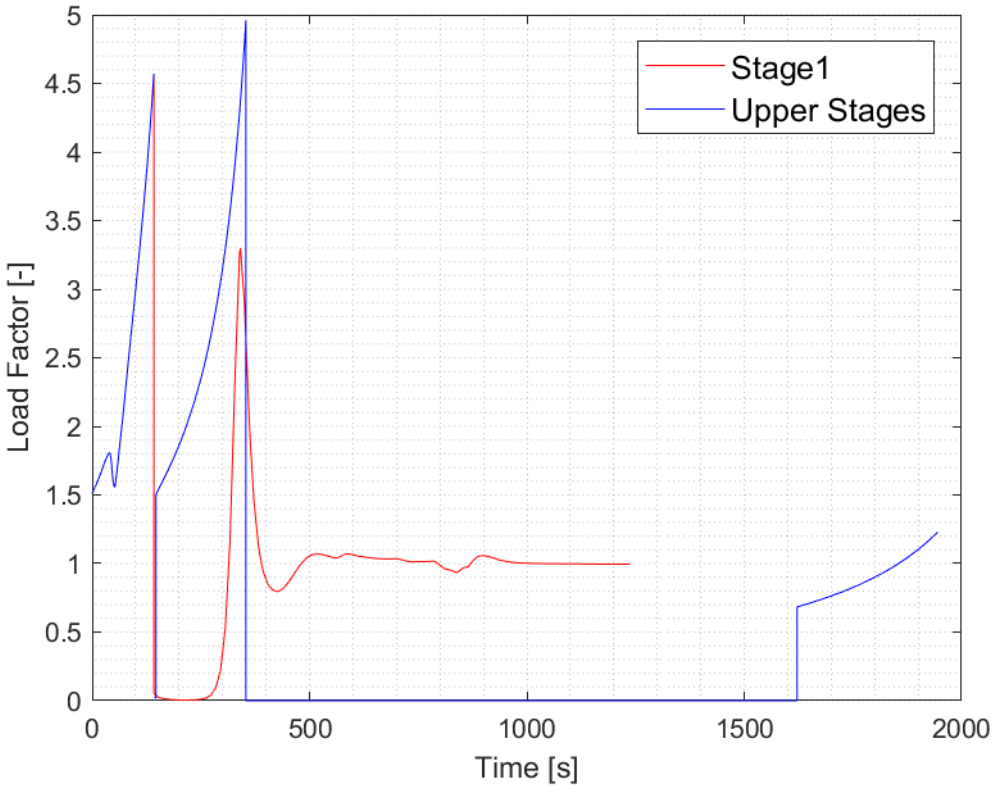

Figure 6-40: Total Load Factor Profile

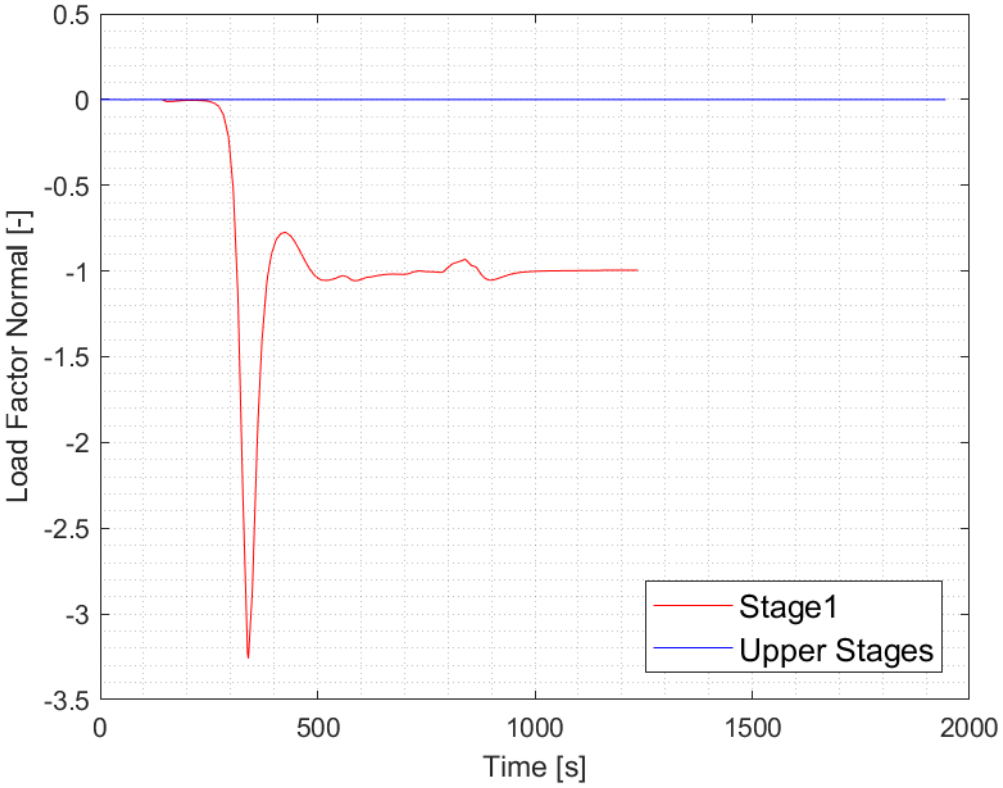

Figure 6-41 Load Factor Normal (nz)

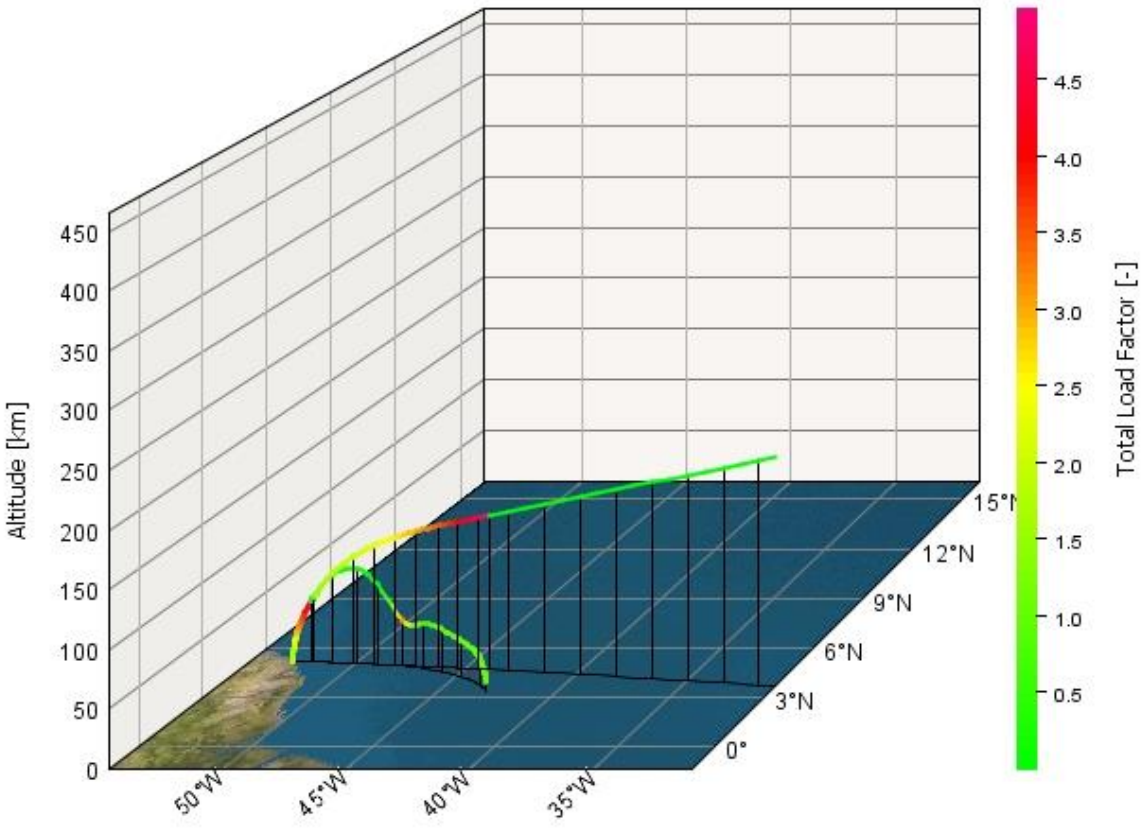

Figure 6-42: 3D Trajectory and Total Load Factor

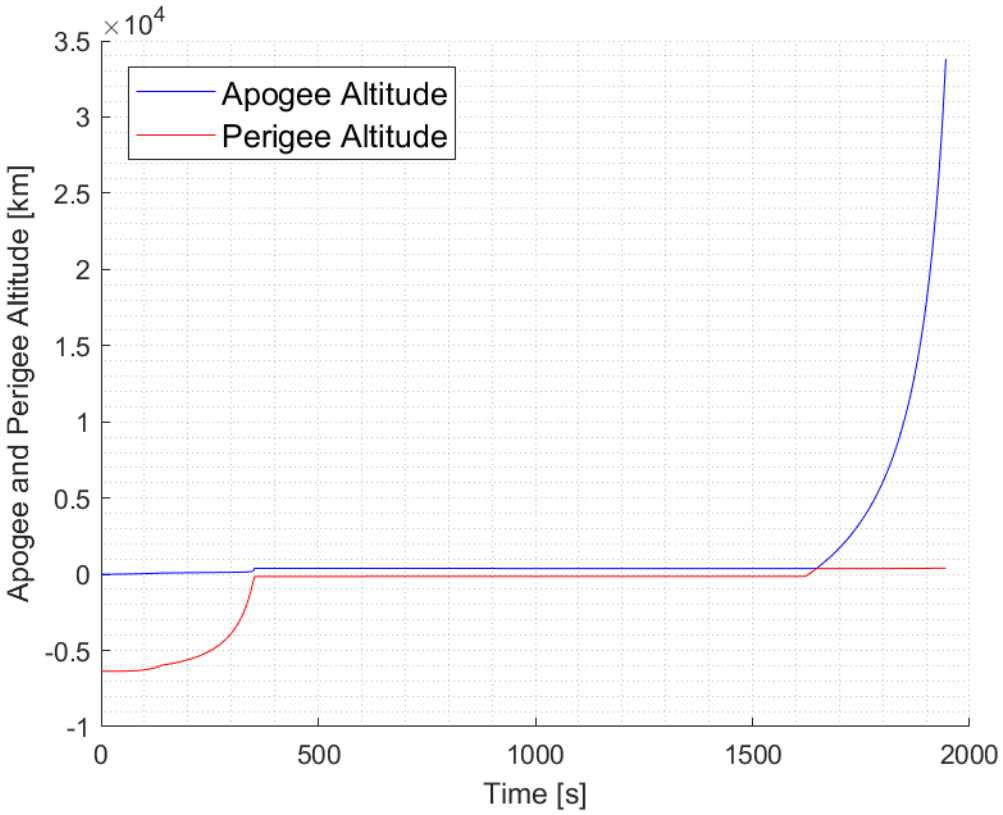

Figure 6-43: Final Orbit Profile

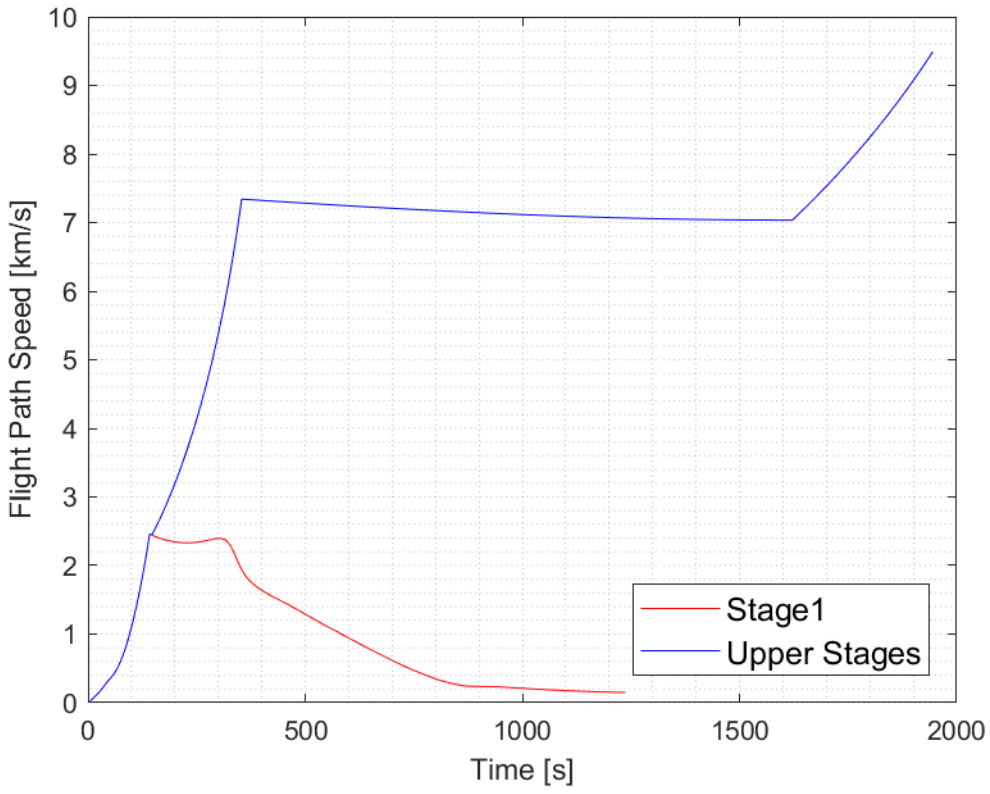

Figure 6-44: Flight-Path Speed Profile

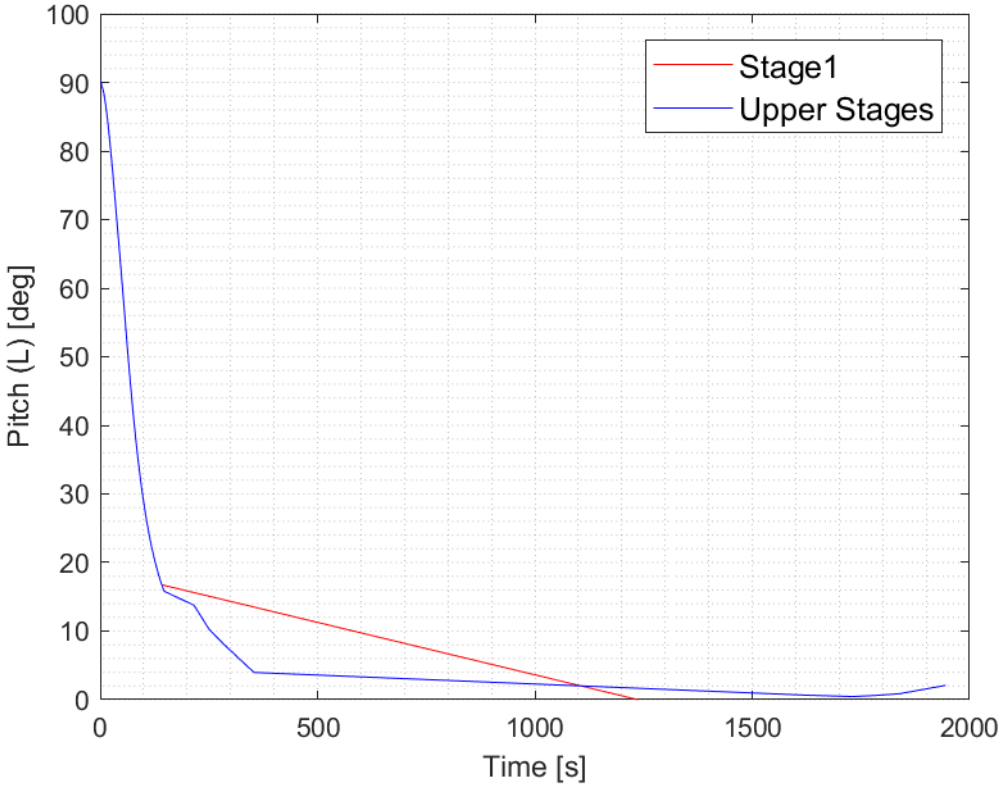

Figure 6-45: Pitch Profile

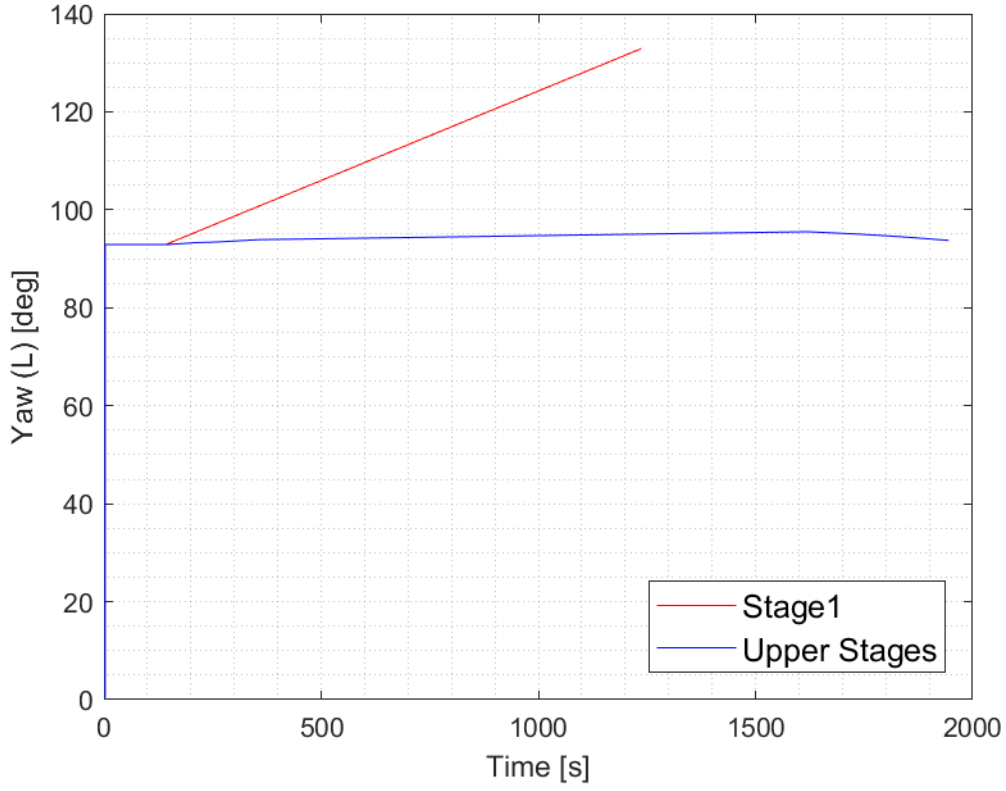

Figure 6-46: Yaw Profile

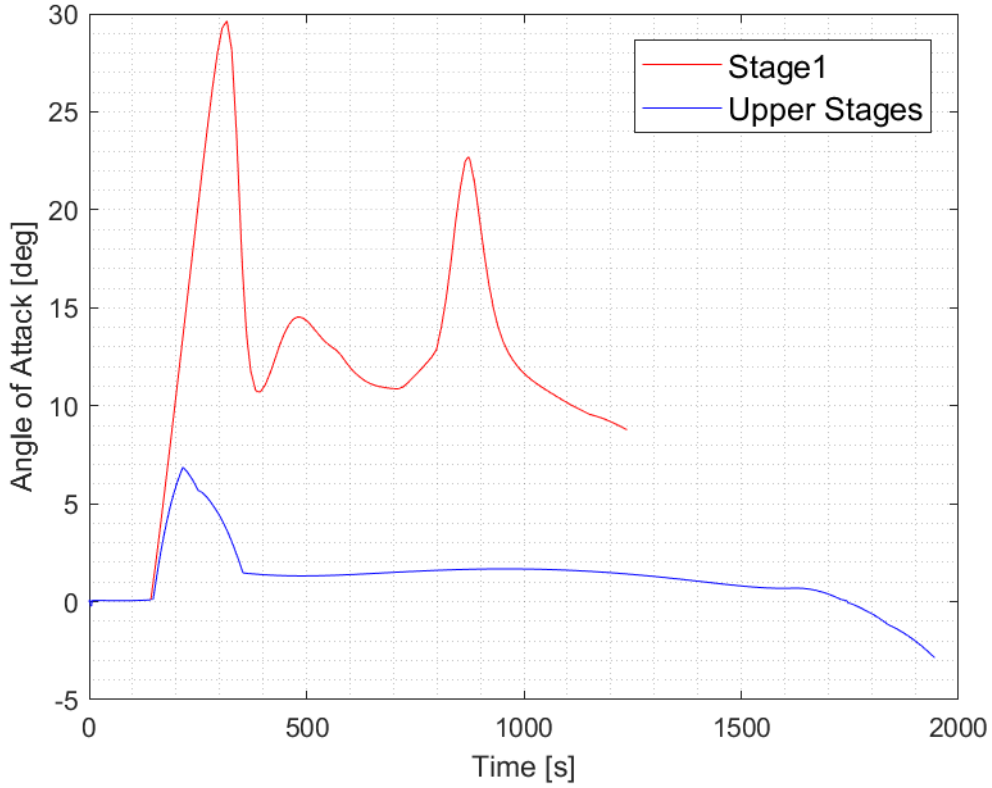

Figure 6-47: Angle of Attack Profile

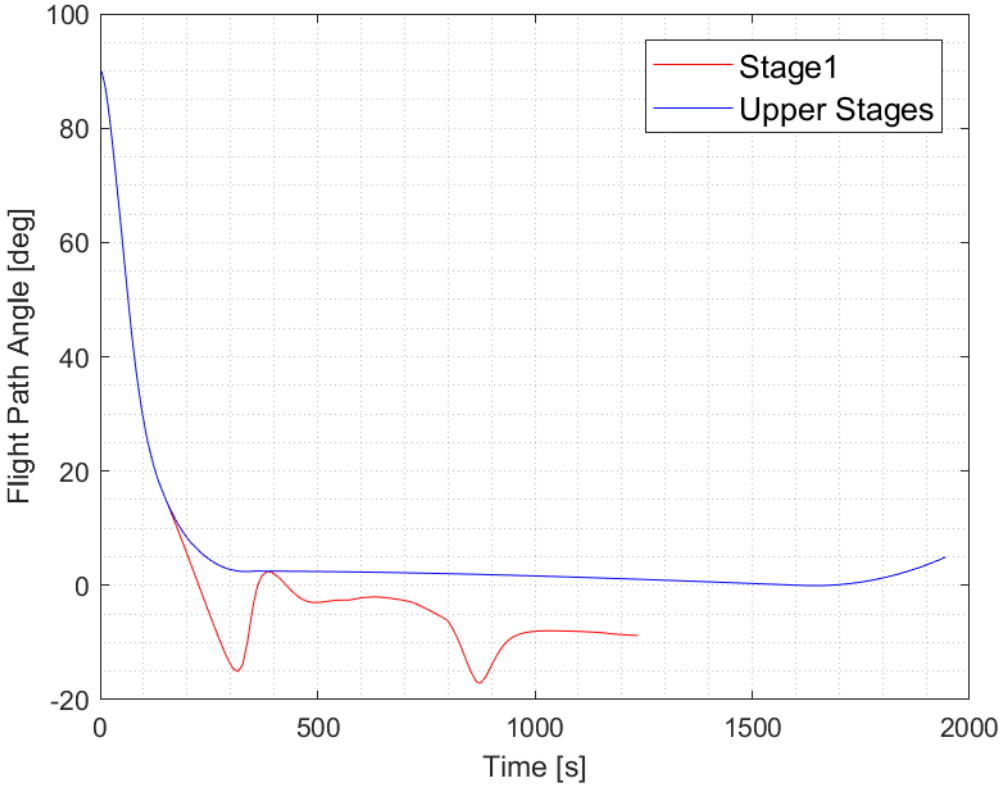

Figure 6-48: Flight path angle Profile

7 Conclusion

In this report the results of the task 2.1 of the Work Package 2 within the FALCon project are presented. This task focuses on the detailed analysis of different return options to position the “In-Air-Capturing” procedure into the framework of current efforts to reintroduce reusability to launch vehicles. Furthermore, the report shall help to put the different return methods into a perspective that allows a comparison of those methods to derive challenges, advantages and drawbacks of each method.

Therefore, four major return strategies were investigated in detail in this report. These were the vertical downrange landing with rocket propulsion and the RTLS landing with rocket propulsion, comparable to what SpaceX is doing with their Falcon 9 vehicle. Additionally, the horizontal landing method with own airbreathing propulsion system (Flyback Booster) and last the horizontal landing method with In-Air-Capturing were investigated.

Those methods were compared with respect to different objective criteria such as launch mass, payload performance, payload performance losses due to reusability, propellant and additional mass required, re-entry loads and size and geometry. From a strict system perspective, the VTHL launchers that perform In-Air-Capturing are the lightest and most performant systems, followed by the downrange vertical landing method. By using In-Air-Capturing, the launch mass can be reduced to values lower than those of the current Ariane 5 launch vehicle when using LOX/LH2 as propellants for a TSTO launcher with gas generator engines. This shows that, although adding mass by wings, fins and thermal protection, a reusable stage can be designed that is able to serve the nowadays launch market with a lower takeoff mass than the Ariane 5.

Considering re-entry and re-entry loads, the In-Air-Capturing method has the advantage of neglecting the need of additional propellant which leads to the low takeoff mass observed. While decelerating the stage with the rocket engines and landing it vertically requires a considerable amount of propellant, the winged stages decelerate by generating lift and drag by the big surface of the wings and the fuselage. However, re-entry loads are highly dependent on the re-entry conditions such as re-entry velocity and re-entry flight path angle. An advantage for light LOX/LH2 could be observed for winged stages in that case.

The economic analysis of reusable launch vehicles, based on early and preliminary assumptions, has shown that RLVs are able to lower the launch costs compared to expendable launch vehicle when meeting certain criteria. First, the number of reuses has to be sufficiently high and the refurbishment costs have to be low (minimum lower than 30% of the costs of a new stage). Furthermore, a high launch rate is of advantage for RLVs in general. If these criteria can be met, cost savings of 50% compared to ELVs are possible, based on the used preliminary model.

In this report the baseline RLV-stage for the full-scale In-Air-Capturing simulation intended to be used in WP7 is presented. This stage is based on a three-stage to orbit launcher which consists of a reusable winged first (reference) stage and an expendable second and third stage. The reference baseline is a double-delta wing stage with either foldable or fixed wings with a return mass of around 70 tons. The launcher is capable of delivering a large payload of 13 tons into GTO. The first stage re-enters the atmosphere after its MECO and should be captured by the towing airplane.

This report marks the end of the task 2.1 in WP 2. The economic analysis of reusable launchers however will continue in task 2.3. Results will be presented in a later report and the cost model will be continuously updated and validated with available data.

8 References

[1] NN: Grant agreement for: NUMBER — 821953 — FALCon, ANNEX 1 (part A) Research and Innovation action, Version date: 17/01/2019

[2] M. Sippel, C. Manfletti, H. Burkhardt, Long-term/Strategic Scenario for Reusable Booster Stages, Acta Astronautica, vol. 58, no. 4, pp. 209-221, 2003

[3] S. Stappert, J. Wilken, L. Bussler, M. Sippel, A Systematic Assessment and Comparison of Reusable First Stage Return Options, 70th International Astronautical Congress 2019, 21st – 25th October 2019, Washington DC, USA

[4] M. Sippel et al., Highly Efficient RLV-Return Mode "In-Air-Capturing" Progressing by Preparation of Subscale Flight Tests, 8th European Conference for Aeronautics and Space, Madrid, 1st – 4th July 2019

[5] S. Stappert et al., European Next Reusable Ariane (ENTRAIN): A Multidisciplinary Study on a VTVL and a VTHL Booster Stage, 70th International Astronautics Congress (IAC), Washington DC, USA, 21st – 26th October 2019

[6] Patentschrift (patent specification) DE 101 47 144 C1, Verfahren zum Bergen einer Stufe eines mehrstufigen Raumtransportsystems, released 2003

[7] Sippel, M.; Klevanski, J.; Atanassov, U.: Search for Technically Viable Options to Improve RLV by Variable Wings, IAC-04-V.8.07, 2004

[8] Jenkins, D. R.: Space Shuttle: The History of the National Space Transportation System, The First 100 Missions, 2010

[9] H. Waldmann, M. Sippel: Adaptation Requirements of the EJ200 as a Dry Hydrogen Fly Back Engine in a Reusable Launcher Stage, ISABE-2005-1121, September 2005

[10] M. Sippel, A. Herbertz: Propulsion Systems Definition for a Liquid Fly-back Booster, 2nd EUCASS, July 2007

[11] M. Sippel, J. Klevanski, J. Kauffmann: Innovative Method for Return to the Launch Site of Reusable Winged Stages, IAF-01-V.3.08, 2001

[12] S. Antonenko, S. Belavskiy: The mid-air retrieval technology for returning of the reusable LV's booster, 2nd EUCASS, 1.03.08, July 1-6, 2007

[13] M. Sippel, J. Klevanski: Progresses in Simulating the Advanced In-Air-Capturing Method, 5th International Conference on Launcher Technology, Missions, Control and Avionics, S15.2, Madrid, November 2003

[14] S. Cain, S. Krause, J. Binger: Entwicklung einer automatischen Koppeleinheit für das Einfangen einer wiederverwendbaren Trägerstufe im In-Air-Capturing, DLRK, München, 2017

[15] S. Krause, S. Cain: Deliverable D2.3: Scaled Experiment Scenario Description, D2.3 Report FALCon, November 2019

[16] S. Stappert, J. Wilken, L. Bussler, M. Sippel, A Systematic Comparison of Reusable First Stage Return Options, 8th European Conference for Aeronautics and Space, Madrid, 1st – 4th July 2019

[17] J.Wilken, S. Stappert, L. Bussler, M. Sippel, E. Dumont, "Future European Reusable Booster Stages: Evaluation of VTHL and VTVL Return Methods", 69th IAC, Bremen 2018

[18] D.Koelle: Handbook of Cost Engineering and Design of Space Transportation Systems – TransCost 8.2 Model Description, Rev. 4,

[19] G. J. D. Calabuig, Conceptual Cost Estimation for Recovery and Refurbishment Operations of Reusable Launch Vehicles, SART TN-006/2019, DLR, 2019

[20] R. H. Liebeck, D. A. Andrastek, J. Chau, R. Girvin, R. Lyon, B. K. Rwdon, P. W. Scott and R. A. Wright, "Advanced Subsonic Airplane Deisgn & Economic Studies," NASA, 1995.

[21] M. T. Vernacchia and K. J. Mathesius, Strategies for Reuse of Launch Vehicle First Stages, 69th International Astronautical Congress 2018, 1st – 5th October 2018, Bremen, Germany

[22] Sippel, M.; Stappert, S.; Bussler, L.; Messe, C.: Powerful & Flexible Future Launchers in 2- or 3-stage Configuration, IAC-19-D2.4.8, 70th International Astronautical Congress 2019, 21st – 25th October 2019, Washington DC, USA

[23] M. Sippel, J. Wilken, Preliminary Component Definition of Reusable Staged-Combustion Rocket Engine, Space Propulsion 2018, Seville, May 2018

[24] Sippel, M.; Klevanski, J.; Atanassov, U.: Search for Technically Viable Options to Improve RLV by Variable Wings, IAC-04-V.8.07, 2004

[25] Daimler-Benz Aerospace, "Life Cycle Cost Estimations for FESTIP Concepts," 1997

[26] Sunayna, S., Towing Aircraft A340-600 study for the In-Air-Capturing of the SpaceLiner Booster, SART TN 019-2020, DLR Bremen

[27] https://www.theverge.com/2020/4/8/21213917/rocket-lab-rocket-electron-helicopters-reusable-mid-air-catch as accessed on 16/10/2020

9 Annex

9.1 Mass and Re-entry Comparison Data

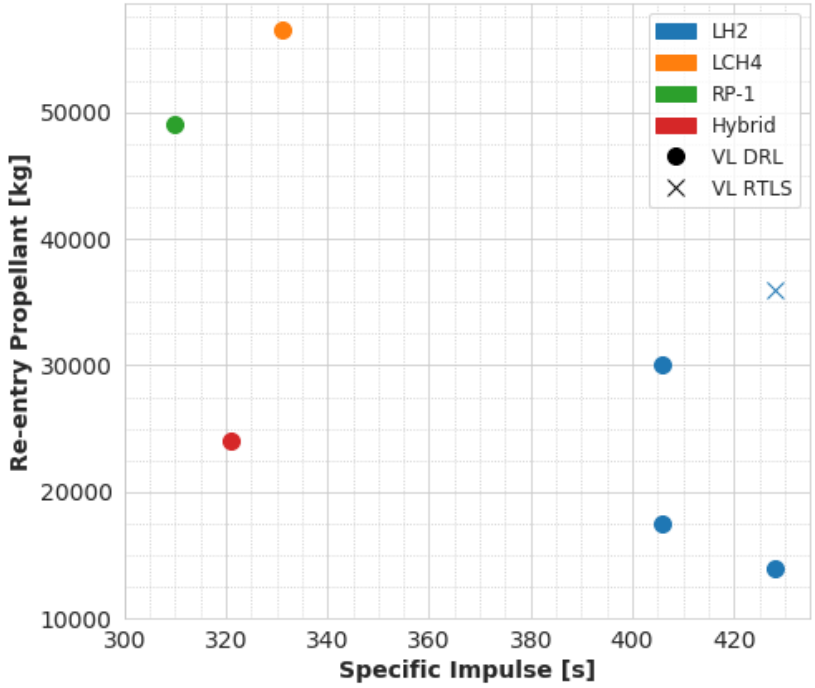

Figure 9-1: Re-entry propellant versus specific impulse of the VL stages

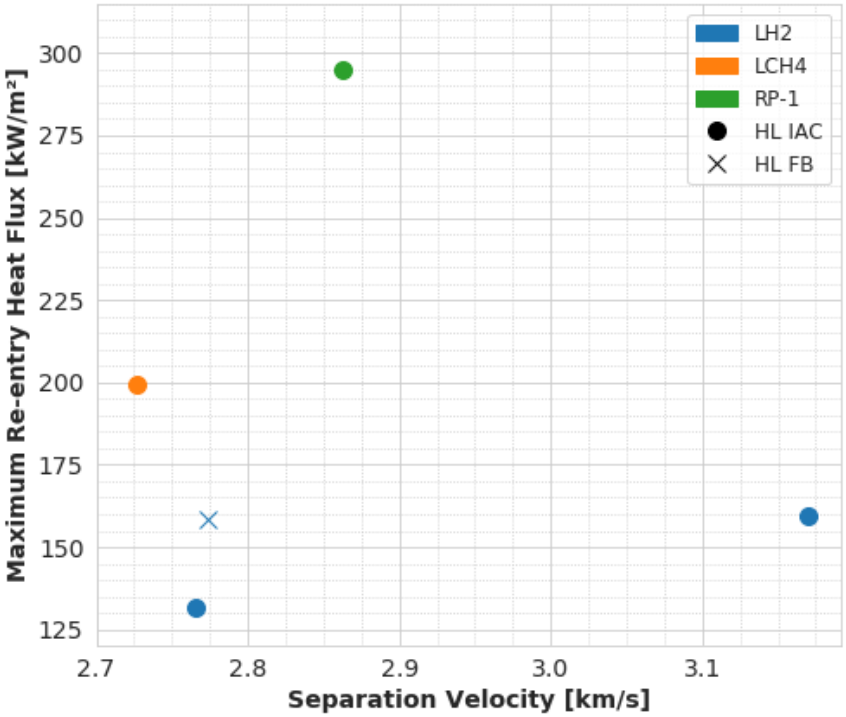

Figure 9-2: Maximum re-entry stagnation point heatflux over separation velocity of the winged HL stages